State of Libya

Ministry of Higher Education and Scientific Research

Alsmarya University

College of Science / Department of Chemistry

Master's thesis titled

Synthesis, DFT Studies Incorporating the Chelating Mixed Ligands (PP`) & (NN`) with Chromium (0), Molybdenum (0) Carbonyl, and Anticancer Application.

Submitted by

Raja Soliman Sowan

A THESIS SUBMITTED IN PARTIAL FULFILLMENT OF THE REQUIREMENTS

FOR THE DEGREE OF MASTER OF SCIENCE

Under Supervision:

Prof. Salem El-Tuhami Ashoor Dr. Khalifa Abdulsalam Alfallous

Academic year: (2023 - 2024)

بِسۡمِ ٱللَّهِ ٱلرَّحۡمَٰنِ ٱلرَّحِيمِ

﴿يَٰٓأَيُّهَا ٱلَّذِينَ ءَامَنُوٓاْ إِذَا قِيلَ لَكُمۡ تَفَسَّحُواْ فِي ٱلۡمَجَٰلِسِ فَٱفۡسَحُواْ يَفۡسَحِ ٱللَّهُ لَكُمۡۖ وَإِذَا قِيلَ ٱنشُزُواْ فَٱنشُزُواْ يَرۡفَعِ ٱللَّهُ ٱلَّذِينَ ءَامَنُواْ مِنكُمۡ وَٱلَّذِينَ أُوتُواْ ٱلۡعِلۡمَ دَرَجَٰتٖۚ وَٱللَّهُ بِمَا تَعۡمَلُونَ خَبِيرٞ ١١﴾

الآية ١١ من سورة المجادلة.

الشكر.

قال الله تعالى في كتابه الكريم: ﴿وَمَن يَشْكُرْ فَإِنَّمَا يَشْكُرُ لِنَفْسِهِ﴾ الآية ١٢ من سورة لقمان.

في البداية لا بدّ لي من أن أتوجه اولاً بالشكر لله عزّ وجلّ الذي وفقني للوصول الى هذه المرحلة العلمية العالية لنيل درجة الماجستير، كما انني أتوجه بالشكر والامتنان لكل من: والدي ووالدتي وزوجي الذين كانوا السند الاول لي في الوصول الى ما وصلت اليه وعائلتي أجمع ولكل من دعمي وساندني.

كمـــــا أتوجه بالشـــكر والامتنان لكل مـــن: **الأســـتاذ الدكتور: سالم التهامي عاشور والدكتور: خليفة عبد السلام الفلوس،** فقد كان لإشرافهما ومنحهما الكثير من الوقت لي اليد الأولى في خروج هذه الرسالة العلمية بالشكل الذي ظهرت عليه، كما كان لتوجيهاتهما ونصائحهما دور أساسي في إتمام دراستي العلمية.

كما أتوجه بالشكر الجزيل لكل من: **الدكتور: بكر جاسم الدوري من دولة العراق، وكذلك الدكتور: إسماعيل طابان (جامعة مصراتة)، والدكتورة: أمل بالقاسم إبراهيم (جامعة الزاوية)، والأستاذة: حنان شواط (جامعة مصراتة)، والأستاذة: سعاد المدني (جامعة مصراتة) والدكتور: محمد أحمد احمودة (الجامعة الأسمرية الإسلامية)،** ولكل من دعم وساعد على إنجاز الدراسة من زملاء او غيرهم من اشخاص مختلفين. بالإضافة للشكر الكبير لكلية العلوم (جامعة مصراتة) ولقسم الكيمياء بكلية العلوم الجامعة الأسمرية الإسلامية ولإدارة كلية العلوم بالجامعة الأسمرية الإسلامية ولكل الكادر التعليمي لما قدموه لنا من جهود في سبيل خروج الرسالة بأدق النتائج واكثرها فعالية ولمساعدتهم بشتى الطرق في كل الأمور التي من شأنها أن توفر لنا فضاءً مريحاً للدراسة وطلب العلم في نظام. وعلى كل ما قدموه لنا من أجل إتمام هذه المرحلة الدراسية.

List of abbreviations.

MCF-7: This is one of the breast cancer cell lines.

(PDB ID: 1ZXM): Human Topo IIa ATPase/AMP-PNP.

BINAP: 2,2′-bis(diphenylphosphino)-1,1′-binaphthyl.

8-HQ: 8-hydroxyquinoline.

2-AP: 2-amino pyridine.

bipy: 2,2'-bipyridin.

IC50: (half-maximal inhibitory concentration).

DFT: Density functional theory.

SRB: Sulphorhodamine-B.

O.D: The optical density.

TCA: Trichloroacetic Acid.

THF: Tetrahydrofuran.

DMSO: Dimethyl sulfoxide.

MLCT: Metal-to-ligand charge transfer.

S: Energy.

RMSD: The root-mean-square deviation.

HeLa cell: The line is derived from cervical cancer cells.

A549 cell: This is a pulmonary epithelial cell line.

MTT: (3-(4,5-dimethylthiazol-2-yl)-2,5-diphenyltetrazolium bromide).

HEPG-2: Is a human hepatoma.

COVID-19: is the virus SARS-CoV-2.

ARPES: Angle-resolved photoemission spectroscopy.

HT-29: Is a human colorectal adenocarcinoma cell line with epithelial morphology.

HCT116: Is a human colorectal carcinoma cell line initiated from an adult male.

LIST OF CONTENTS.

LIST TABLE.

LIST FIGURES

LIST SCHEMES.

Abstract.

A series of complexes, including $[Cr(CO)_2(BINAP)(bipy)]$ (G1), $[Mo(CO)_2(BINAP)(bipy)]$ (G2), $[Cr(CO)_2(BINAP)(2\text{-}Ap)]$ (G3), $[Mo(CO)_2$-(BINAP)(2-AP)] (G4), $[Cr(CO)_2(BINAP)(8\text{-}HQ)]$ (G5) and $[Mo(CO)_2(BINAP)(8\text{-}HQ)]$ (G6) by reaction of $[M(CO)_6]$ where (M= Cr(0) or Mo(0)) with 2,2′-bis(diphenylphosphino)-1,1′-binaphthyl (BINAP) (L1) as a primary ligand and secondary ligands such as 2,2'-bipyridin (bipy) (L2), 2-amino pyridine (2-Ap) (L3) and 8-hydroxyquinoline (8-HQ) (L4), have been synthesized via the microwave instrument, through the solvent-free green chemistry route. The complexes were characterized by UV-Vis, ^{1}HNMR, IR, mass spectroscopy, and elemental analysis, and finally, the biological activity of the complexes was screened in vitro against the MCF-7 human breast cancer cell line. The values of IC_{50} were found for the complexes where all of the complexes exhibited an inhibitory effect against the breast cancer cell line, Complex G1 was determined to be the most effective against the MCF-7 cell line (IC_{50} = 138 μM) due to its lower value. Molecular docking studies were performed to investigate the binding of the synthesized complexes with breast cancer MCF-7 (PDB ID: 1ZXM).

المـلخـص.

تم تصنيع سلسلة من المعقدات [$Cr(CO)_2$(BINAP)(bipy)] (G1) [$Mo(CO)_2$(BINAP)(bipy)] (G2) ,[$Cr(CO)_2$(BINAP)(2-AP)] (G3) , [$Mo(CO)_2$(BINAP)(2-Ap)] (G4) , [$Cr(CO)_2$(BINAP)(8-HQ)] (G5) , [$Mo(CO)_2$(BINAP)(8-HQ)] (G6) عن طريق تفاعل [$M(CO)_6$] حيث (M= Cr(0) Mo(0)) مع الليجاند الأساسي 2,2' -bis(diphenylphosphino)-1,1′-binaphthyl (BINAP) (L1) وليجاندات ثانوية مثل 2,2'-bipyridin و 2-amino pyridine و8-hydroxyquinoline. من خلال مسار الكيمياء الخضراء الخالية من المذيبات، تم تصنيع المعقدات في جهاز الميكروويف. شخصت المعقدات بـجهاز طيف المرئي و^{1}HNMR وIR والطيف الكتلي (mass) والتحليل الأولي للعناصر (CHN). تم فحص النشاط البيولوجي للمعقدات في المختبر ضد خلايا سرطان الثدي البشري من النوع MCF-7. أظهرت قيم IC_{50} لجميع المجمعات تأثيرًا مثبطًا ضد خلايا سرطان الثدي من النوع MCF-7، حيث وجدٌ أن المركب G1 الأكثر فاعلية ضد خط خلية MCF-7 (IC_{50} = 138 µm). كما أجريُت دراسات كمبيوترية لدراسة الطاقة الكلية للجزيئات بعد ارتباطها مع السرطان من النوع MCF-7 (PDB: ID: 1ZXM)، وذلك لغرض التحقيق من مدى ارتباط هذه المعقدات المحضرة بسرطان الثدي MCF-7.

Chapter One

Introduction

Introduction.

The synthesis of novel homoleptic transition metal carbonyl complexes has risen anew after lying dormant for over a decade. carbonyl complexes are part of this century-long research even about 130 years after the discovery of $Ni(CO)_4$, new 'milestones' of homoleptic carbonyl complexes are still to be revealed today [1, 2]. For a long time, numerous compounds containing metal and carbon monoxide have been prepared and known as organometallic compounds that contain at least one bond between carbon and metal. The transition metal complexes of carbon monoxide contain metal-carbon bonds known as metal carbonyls. One of the most important π-acceptor ligands is carbon monoxide an unsaturated ligand because of the C−O multiple bonds. carbon monoxide can stabilize the zero formal oxidation state of metals in carbonyl complexes, because of its π-acidity. It is also soft because it can accept metal dπ electrons by back bonding. Named carbonyls because the carbon atoms donate electrons to the metal as a lone pair of electrons are available on both carbon and oxygen atoms of the carbon monoxide ligand. The general formula of metal carbonyls is $M_x(CO)_y$, which are most of the time nonpolar and electrically neutral compounds and demonstrate the physical properties of organic compounds. The chemistry of metal carbonyls considerable has interest for several decades

mainly due to the structural aspects and reactivity of these compounds concerning several classes of organic ligands where metal carbonyls serve as precursors for the preparation of other organometallic complexes [3-10].

One of the main causes of the ongoing increase in interest in organometallics is the growing number of possible catalytic applications. Although most main-group organometallics are stoichiometric reagents, catalysts are the most useful form of many of their transition metal analogs. Another fundamental tenet of green chemistry is catalysis, which helps prevent waste from being formed [11, 12]. Due to the presence of strong inter-atomic bonding which results in their having high melting points and good mechanical properties, variable oxidation states, catalytic activity, and their complexes are paramagnetic. also, their ions are usually colored and they form a wide variety of complexes so they are transition elements the most industrially important metals [13].

Accessing the finest tuning of a catalytic reaction pathway requires in organometallic chemistry and especially in the catalysis area, a detailed knowledge of the steric and electronic influence of the ligands bound to the metal center. Phosphines are regarded as one of the most important classes of ligands in the field of inorganic chemistry. Recently in organic chemistry, the use of phosphines as one of the reagents/catalysts

has received much attention from scientists. This makes it the ability to act both as bases and as nucleophiles due to the presence of a lone pair of electrons on the phosphorus atom. Tertiary phosphines are an important class of ligands, due for that the R group(s) their electronic and steric properties can be altered systematically and predictably over a very wide range, where can the phosphorus have a high nucleophilic reactivity, strong bonds with carbon, nitrogen, oxygen, or sulfur the Usually, the M-L bond between a ligand and a metal is depicted by the Dewar-Chatt-Duncanson model involving two opposite interactions, a σ-donor and a π-acceptor effect of the ligand. these compounds show an extraordinary reactivity derived from the combined presence of multiple M–P bonding and the lone pair of electrons presence of on the phosphorus, which can be easily donated to the transition metal (σ bond), enabling the phosphorus atom to achieve tetrahedral (sp^3) configuration and a low-lying P-centered LUMO.

It also has vacant d orbitals of proper size and symmetry to accept the electrons from the filled orbitals of the transition metal (Booth 1964) to form the π bond as shown in (Figure 1). This chemical diversity makes compounds act as valuable synthons for the preparation of diverse organophosphorus derivatives or novel metal complexes [14-17].

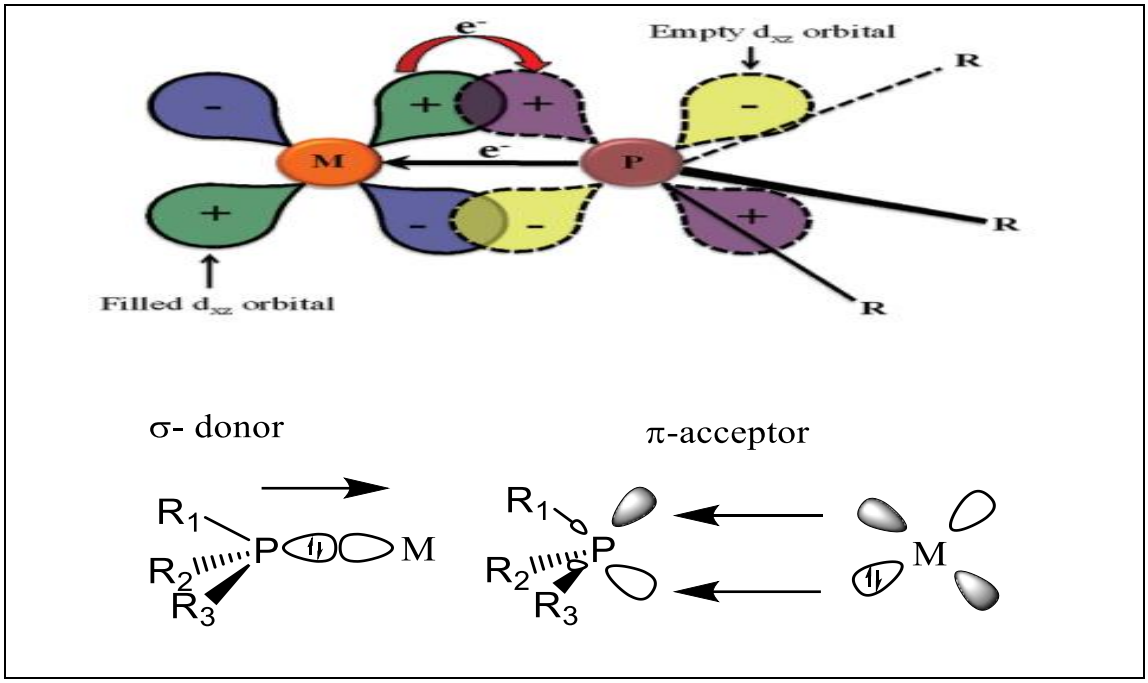

Figure 1. Metal-phosphorus bond formation.

Complexes of the type $[M(CO)_4(o\text{-}Ph_2PC_6H_4–CH=NR)]$ have been synthesized and characterized, as reported by Gregorio Sanchez and colleagues. (M=Mo, W; R=Me, Et, iPr, tBu, NH–Me), made by reacting directly with the precursors cis-$[M(CO)_4(pip)_2]$ and iminophosphine ligands (Scheme 1) [18].

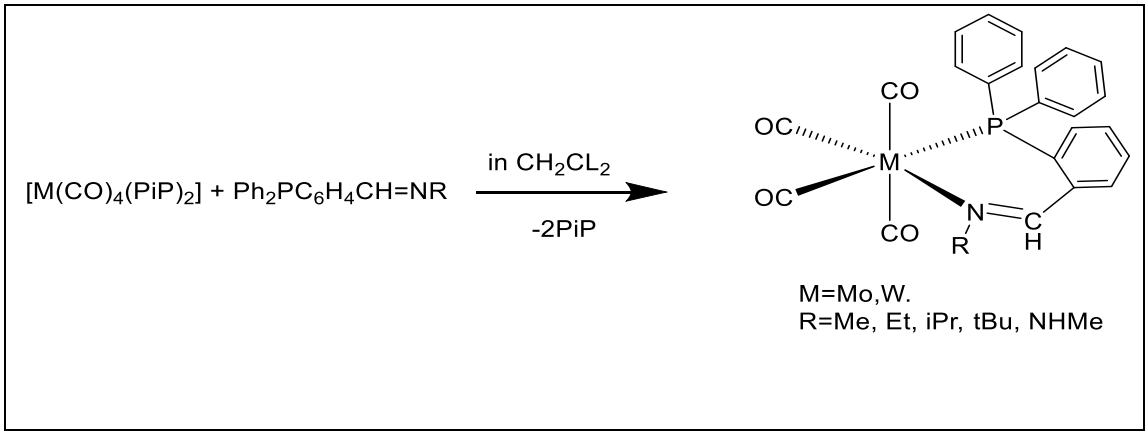

Scheme 1. Synthesis of $[M(CO)_4(o\text{-}Ph_2PC_6H_4–CH=NR)]$ where (M=Mo, W; R=Me, Et, ^{i}Pr, ^{t}Bu, NH–Me).

Transition metal complexes, containing multidentate ligands with electronically different functionalities, due to their versatile coordination chemistry and diverse reactivity. Among them diphosphines which a marked influence on catalyst reactivity and selectivity [19-23]. As can diphosphines coordinate in a monodentate, chelating, or bridging manner with interconversion between these often resulting from slight changes in the ligand backbone or in co-ligands bound to the metal center [24-27], defined Jeffrey and Rauchfuss in 1979 the hybrid ligands which comprise strongly and weakly bound moieties, as hemilabile ones were used molecules with phosphorus donors as strongly bound anchors among a variety of potentially bifunctional ligands, for the preparation of numerous late transition metal compounds. has been in particular focused on the ligands combining soft (P atom) and hard donors (N or O atoms P–N) [28-34].

The synthesis, reactivity, and structure of ortho-metallated tertiary phosphines and arsines of the form $[2\text{-}R_2EC_6H_4]^-$ (E = P, As; R = various substituents) are reviewed in an article by Fabian Mohr et al. A brief overview of the possible synthetic pathways is given, and some general structural and spectroscopic considerations are discussed. These kinds of ortho-metallated complexes are studied in the subsequent sections, which

are organized according to the d-block series triads. The literature has addressed the end of 2004 [35].

The design and synthesis of chiral bisphosphine ligands is an important area of research toward developing highly enantioselective transition metal-catalyzed asymmetric reactions. One of the most useful chiral phosphine ligands is 2,2′ bis(diphenylphosphine)-1,1′-binaphthyl (BINAP), which exhibits high enation selectivity in several types of asymmetric reactions including ruthenium-catalyzed hydrogenation and rhodium-catalyzed addition and its related reactions [36-38].

Substitution in the 3,3'-positions of the BINAP backbone provides the greatest opportunity for both steric and electronic perturbation of catalyst properties. J. Matthew Hopkins introduced this dissertation details the synthesis and applications of a series of novel 3,3'-substituted Binap ligands [39]. The article analyzes Eric Framery and co-workers' recent results obtained in the fields of catalysis using transition metal complexes grafted on organic or inorganic materials. based on only two different ligands of particular interest: the bis(oxazoline) (BOX) and BINAP ligands, that are probably among the most used ligands. BINAP is probably the most used ligand in asymmetric catalysis both in industrial and academic laboratories [40]**.** Wenbin Lin and co-workers report here the design of BINAP-based metal-organic frameworks and their post-

synthetic metalation with Rh complexes to afford highly active and enantioselective single-site solid catalysts for the asymmetric cyclization reactions of 1,6-enynes [41]**.** A range of copper-based photocatalysts of the type $Cu(NN)(BINAP)BF_4$ with π-extended diimine ligands were synthesized by Shawn K. Collin and colleagues (Scheme 2). Next, the activity of the BINAP-derived complexes against triple-negative breast cancer cell lines was assessed. Controls showed that the action was caused by copper complexes rather than their ligands. $Cu(dppz)_2BF_4$, a homoleptic compound, showed encouraging action. [42].

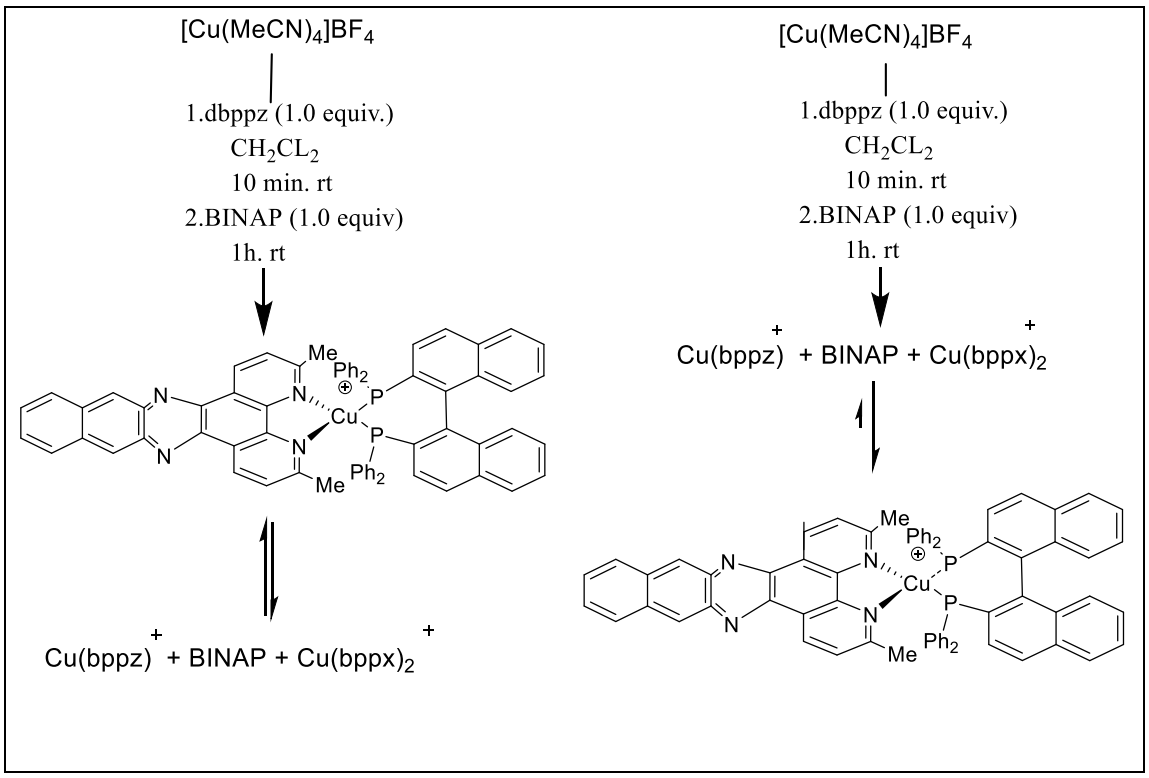

Scheme 2. Synthesis of heteroleptic copper-based complexes using BINAP.

A BINAP-Cu system supported by hydrotalcite is developed by Dawei Wang et al., and it turns out to be a very effective catalyst for the atom-efficient and environmentally friendly borrowing hydrogen process as well as dehydrogenative cyclization. additionally, it has a high air stability and at least five solvent-free recycling cycles. 1H-benzo[d]-1-benzyl-2-aryl for the first time, alcohols could be converted into imidazole derivatives in a single step using water as the solvent. However, the synthesis of functionalized amines, ketones, and 1-benzyl-2-aryl-1H benzo[d]-imidazole derivatives with high yields in water or solvent-free conditions was made much more environmentally friendly and effective by using the BINAP-Cu complex (figure 2) [43].

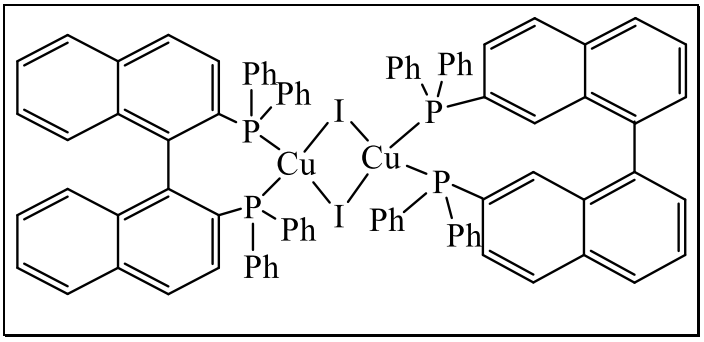

Figure 2. Structure of [Cu(BINAP)I]$_2$.

Masaru Tamura and Hisashi Fujihara reported "demonstrated the synthesis of the chiral BINAP-Au and BINAP-Pd and a new type of catalytic asymmetric induction by the chiral BINAP-Pd. chiral BINAP-Pd is a new and efficient catalyst for the asymmetric hydrosilylation of olefin

under mild conditions. they have found a significant difference in the catalytic activity between BINAP-Pd nanoparticles and the BINAP-Pd complex. This finding indicates a new aspect in the field of asymmetric reactions catalyzed by chiral phosphine-stabilized metal nanoparticles and transition metal-phosphine complexes" [44].

Zhe Liu and co-workers "synthesized a series of half-sandwich Ir^{III} pentamethylcyclopentadienyl and Ru^{II} arene complexes containing P^P-chelating ligands of the type $[(Cp^x/arene)M(P^P)Cl]PF_6$, where M = Ir, Cp^x is pentamethylcyclopentadienyl (Cp*), or 1-biphenyl-2,3,4,5-tetramethyl cyclopentadienyl (Cp^{xbiPh}); M = Ru, arene is 3-phenylpropan-1-ol (bz-PA), 4-phenylbutan-1-ol (bz-BA), or p-cymene (p-cym), and P^P is 2,2-bis(diphenylphosphine)-1,10-binaphthyl (BINAP) (Scheme 3), and have been fully characterized, three of them by X-ray crystallography, and their potential as anticancer agents explored. All five complexes showed potent anticancer activity toward HeLa and A549 cancer cells" [45].

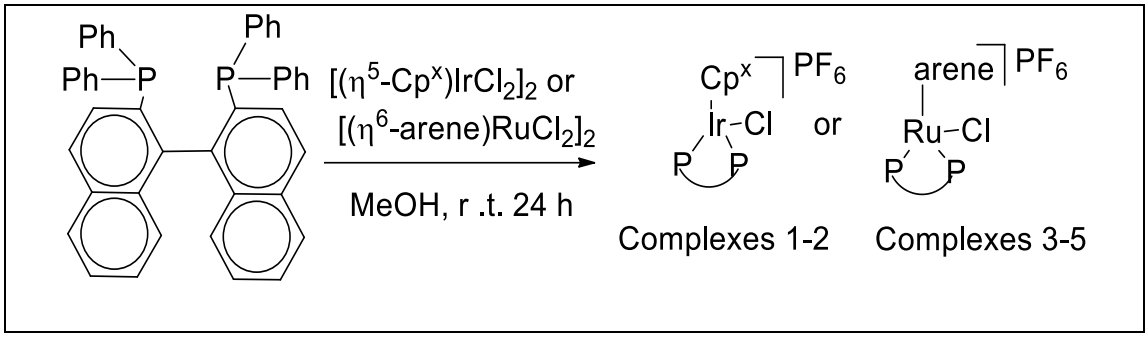

Scheme 3. Synthesis of Respective Half-Sandwich Ir^{III} and Ru^{II} Complexes.

Arnd Vogler and co-workers "have reported the preparation and the r.t. luminescence of the complexes $[Cu(BINAP)_2]^+$ and $[Cu(BINAP)I]_2$ with binap = 2,2 bis(diphenylphosphino)-1,10-binaphthyl. in analogy to previous preparations of complexes of the type $[Cu(P–P)_2]^+$ and $[Cu(P–P)I]_2$ with P–P = bidentate bis-aryl-phosphine, have been synthesizing $[Cu(BINAP)_2]PF_6$ and $[Cu(BINAP)I]_2$" [46].

One type of heterocyclic ligand is 2,2'-bipyridine, which is a ligand that chelates bidentate and is made up of a bond between two pyridine rings in the α-position of the nitrogen. As a chelating donor ligand for bridging ligands, 2,2′-biypyridine, or bipy, is frequently utilized due to its strong redox stability and relative ease of functionalization. In addition to its cytotoxicity and genotoxicity, mixed ligands that are employed as antineoplastic medicines comprise 2,2-bipyridine and other bidentate ligands. These compounds have also been shown to be bactericidal and bacteriostatic versus specific types of bacteria. [47-51]. The ligand's

stability is due to the π-acceptor complementing its σ-donation, which enables metal complexes with stronger antibacterial activity to be arranged in a well-defined spatial pattern [52-56].

In coordination chemistry, A synergistic effect for new applications in the biological system has been brought about by the harmonization of the metal-organic framework via the incorporation of metal ions into organic ligands, primarily, when heteroatoms such as nitrogen and oxygen with lone pair of electrons are involved. in the study of Egbele, R.O.a. et al have "synthesized and characterized some mixed ligands metal complexes by the use of mixed 2,2-bipyridine and penicillin procaine, with Cu and Mn transition metal chloride" (Scheme 4) [57].

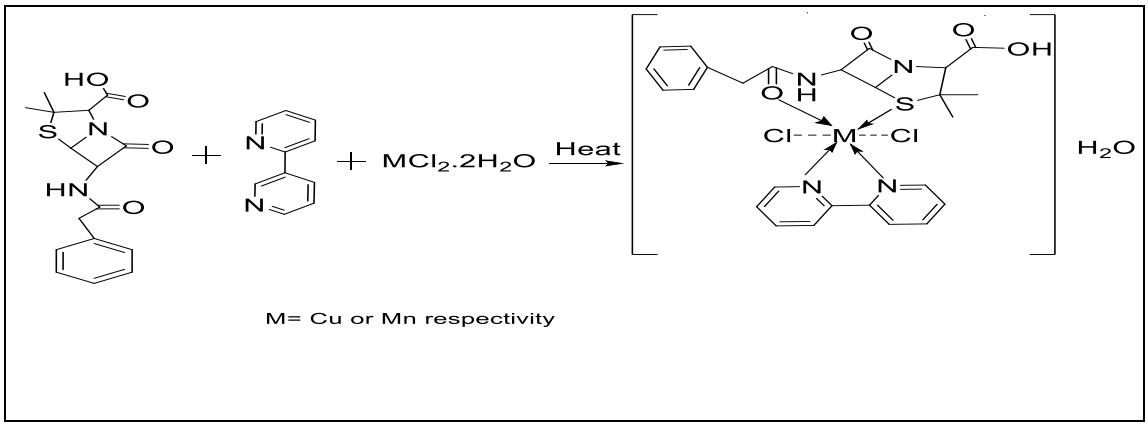

Scheme 4. Reaction scheme for mixed ligand (Penicillin G and 2,2-Bipyridine) metal (II) complex of Cu and Mn complexes respectively.

David A. Vicic. *et al*. "they [prepared Three new complexes [(dtbpy)Ni(CF_3)$_2$] (1), [(dtbpy)Ni(CF_2CF_3)$_2$] (2), and [(dtbpy)Ni(CH_3)$_2$] (3) (dtbpy = 4,4′-di-tert-butyl-2,2′-bipyridine). and they observed

Remarkable differences in the structure, electronics, reactivity, and absorption of visible light for the alkyl versus perfluoroalkyl complexes, which are detailed in their report" [58]. Synthesized stated Three novel 1,10-phenanthroline and 2,2'-bipyridine mixed-ligand complexes of $[Co(bipy)(phen)_2](NO_3)_2.2H_2O$, $[Cu(bipy)(phen)H_2O)_2]Cl_2.2H_2O$, and $[Zn(bipy)_2(phen)]Cl_2.6H_2O$ by M.O. Agwara et al. The compounds were identified using elemental, infrared, and visual spectroscopy examinations [59].

Cristiano Zonta and co-workers "have synthesized Novel cobalt, nickel, and iron complexes based on the pentadentate 8-hydroxyquinoline-di(2-picolyl)amine ligand and thoroughly characterized" [60].

Marguerite Piti et al. "They have synthesized Fourteen different ligands with two covalently linked 8-hydroxyquinoline motifs that favor metal complexion. where included this bis-chelator's different bridges at the C2 positions and different substituents to modulate their physicochemical properties. metal complexes can be formed by a ratio of one ligand per metal ion with Cu II and Zn II, two metal ions involved in the formation of amyloid aggregates of the toxic, Ab-peptides in Alzheimer's disease" [61].

Hydroxyquinoline (8-HQ) (figure 3) and its Compounds exhibit a wide range of biological activities, including antimicrobial, anticancer,

and antifungal effects. Mohammad S. Mubarak and co-workers' review focuses "on the recent advances in the synthesis of 8-HQ derivatives with different pharmacological properties, including anticancer, antiviral, and antibacterial activities" [62].

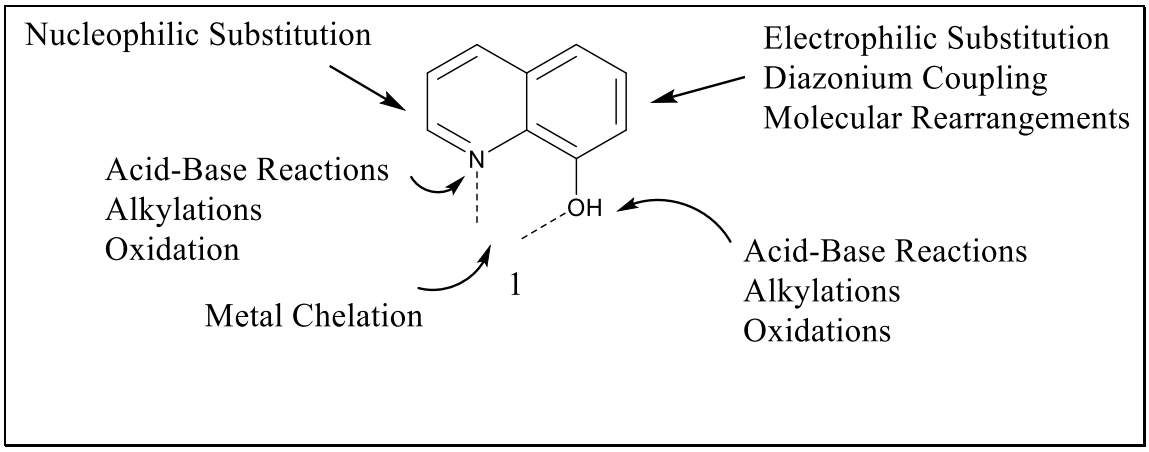

Figure 3. Reaction sites of 8-hydroxyquinoline 1.

Two examples of nitrogenous ligands have been employed widely in base metal catalysis they are Imino-pyridine and amino-pyridine ligands, with the benefit of readily tunable N -aryl or N -alkyl substituents [63].

Ahmed A. Soliman and co-workers explain an interaction "of $[M(CO)_6]$ M = Cr, Mo or W with 2-[2-(methyl aminoethyl)] pyridine (maepy) using direct sunlight irradiation (a green chemistry route of synthesis) in THF. The reactions resulted in the formation of the oxo complex $[Cr_2(O)_4(maepy)_2]$ (1) (Scheme 5) and the tetracarbonyl complexes $[Mo(CO)_4(maepy)]$ (2) (Scheme 6) and $[W(CO)_4(maepy)]$ (3).

(Scheme 7) explains the Proposed mechanism for the formation of Cr oxocomplex" [64].

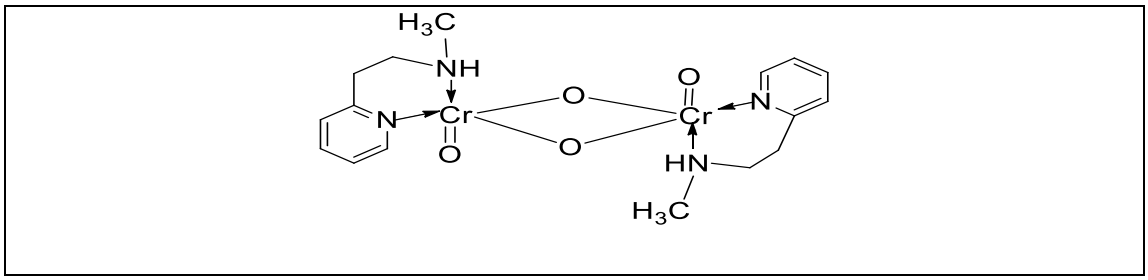

Scheme 5. The proposed structure of $[Cr_2(O)_4(maepy)_2]$.

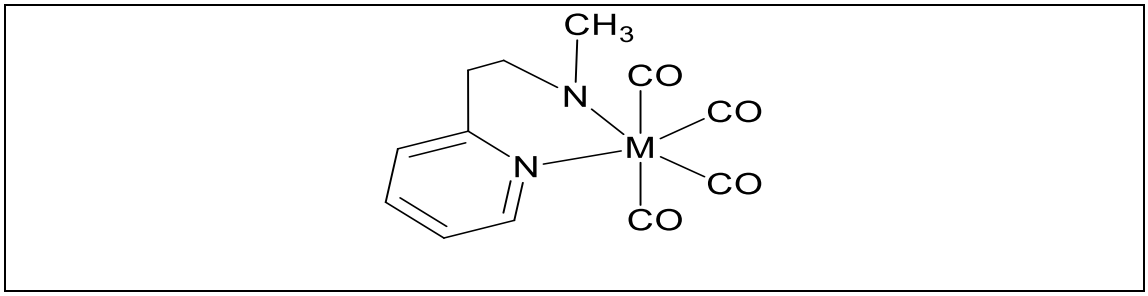

Scheme 6. The proposed structure for $[M(CO)_4(maepy)]$ where M=Mo or W

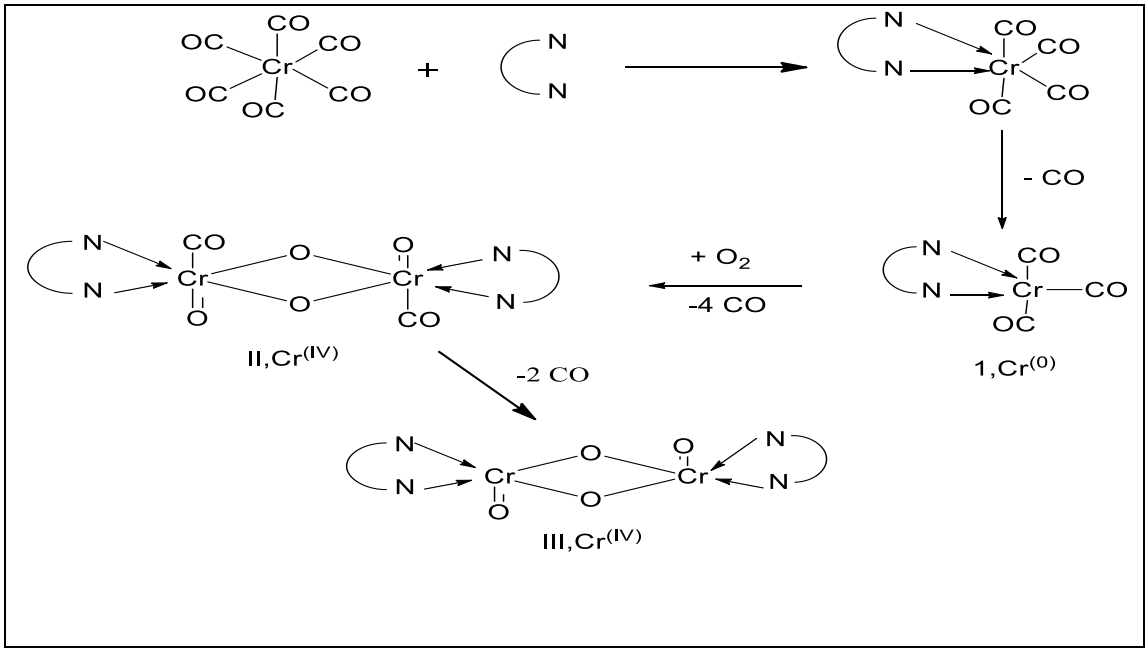

Scheme 7. Proposed mechanism for the formation of Cr oxo complex.

Amah Colette Benedicta Yuoh et al. Have synthesized "a novel one-dimensional coordination polymer bis(2-aminopyridine)-μ-bis(dicyan-amido) cobaltate (II) and characterized by elemental analyses and infrared and ultraviolet-visible spectroscopies and the structure has been determined by single crystal X-ray diffraction. The complex is moderately active, according to antimicrobial screening against eight pathogenic microorganisms (four bacteria and four fungi) obtained from people" [65].

Chengfeng Zhu and co-workers in their article explained "Two new Cr(III) complexes based on 2-substituted 8-hydroxyquinoline ligands, namely $[Cr(L_1)_3]$ (1), (HL1=(E)-2-[2-(4-nitro-phenyl)-vinyl]-8-hydroxy-quinoline) and $[Cr(L_2)_3]$ (2),(HL_2=(E)-2-[2-(4-chloro-phenyl)vinyl]-8-hydroxy-quinoline) (Scheme 8), were prepared by a facile hydrothermal method and characterized thoroughly by single crystal X-ray diffraction, powder X-ray diffraction, FTIR, TGA, ESI-MS, UV-Visible absorption spectra, and fluorescence emission spectra" [66].

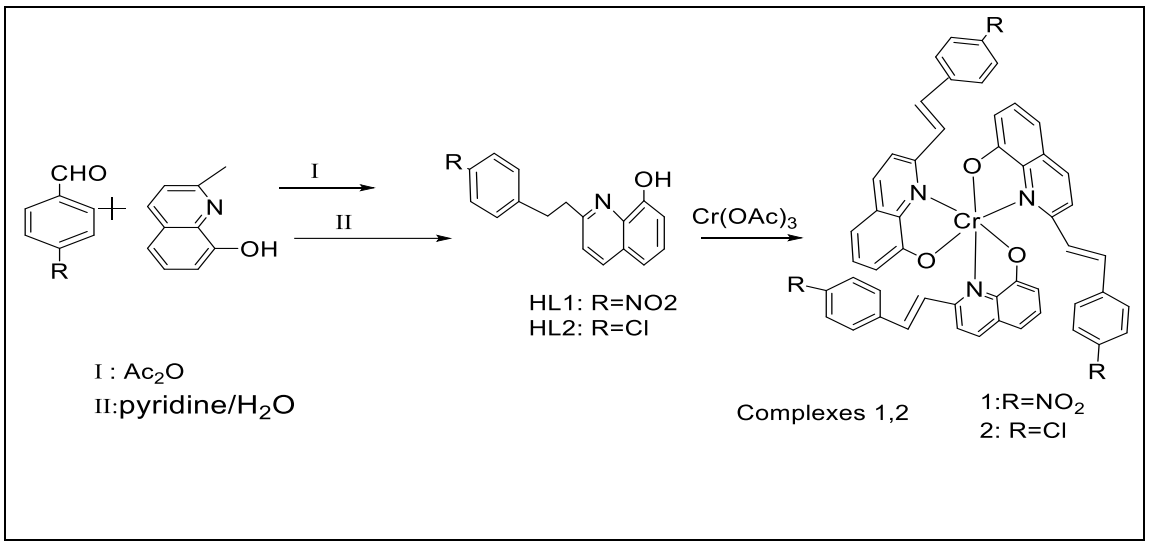

Scheme 8. Synthesis of two Cr(III) complexes $[Cr(L1)_3]$ (1), (HL1=(E)-2-[2-(4-nitro-phenyl)-vinyl]-8-hydroxy-quinoline) and $[Cr(L_2)_{3]}$ (2),(HL2=(E)-2-[2-(4-chloro-phenyl)vinyl]-8-hydroxy-quinoline).

Green and co-workers have shown Reaction times are shortened and yields are increased over previously reported syntheses when a series of compounds of the form $ML(CO)_4$ (M = Cr, Mo, W; L = en, bipy, dppm, dppe) are synthesized with the help of microwaves. Reaction times are shortened by 5 to more than 500 times [67]. More than 20 group 6 organometallic compounds have been synthesized, according to research by Michael Ardon et al. In a traditional microwave oven, hexacarbonyls most notably $Mo(CO)_6$ react easily with a variety of mono- and bidentate amines as well as phosphines to produce tetracarbonyl complexes in good to outstanding yields (Scheme 9) [68].

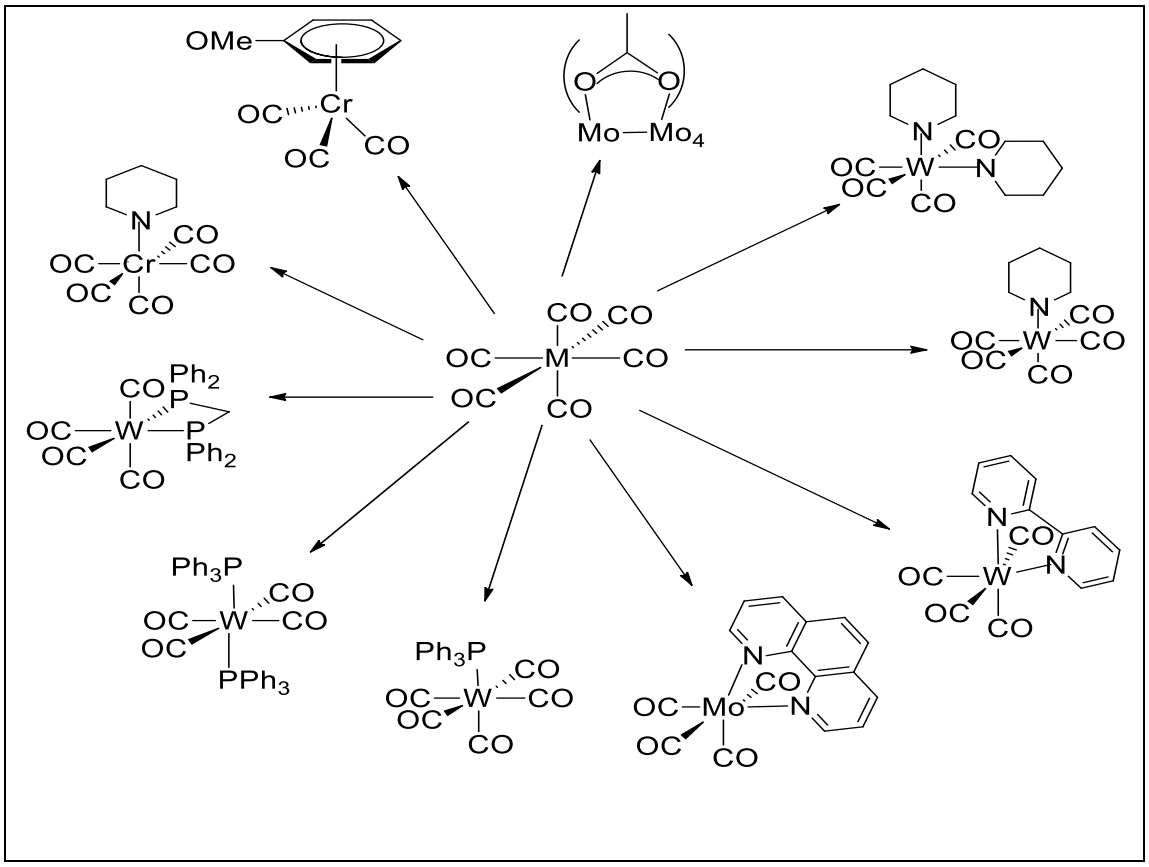

Scheme 9. Microwave accelerated reactions of $Cr(CO)_6$, $Mo(CO)_6$, $W(CO)_6$.

Owing to the chelate effect, "Metal complexes show remarkable stability compared to their ligands and metals alone. where the structural study of mixed-ligand metal complexes can provide information on how biological systems attain their stability and specificity" [69, 70]. Also, it can exploit the unique properties of metal ions for the design of new drugs by medicinal inorganic chemistry. where transition metal complexes are important in catalysis, materials synthesis, and photochemistry [71].

Transition metals are under scrutiny as potential anticancer agents because transition metals can coordinate with electron-rich biomolecules such as DNA. This can lead to the deformation of DNA and ultimately to cell death [72]. Prepared novel molybdenum tetracarbonyl and molybdenum allyl dicarbonyl complexes and studied the modulation of their biological activity by variation of the ligands and conjugation to carrier peptides theses the general aim of work Hendrik Pfeiffer in a model procedure molybdenum hexacarbonyl was reacted with 1,10-phenanthroline in a toluene/diglyme mixture in a CEM microwave reactor under aerobic conditions in a sealed vial (Scheme 10) [73].

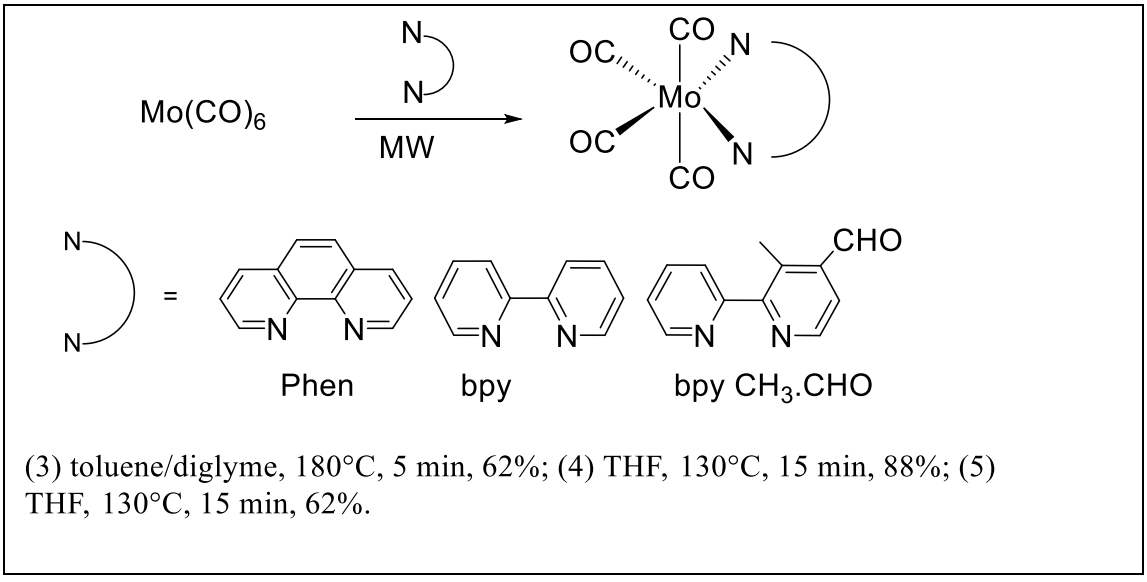

(3) toluene/diglyme, 180°C, 5 min, 62%; (4) THF, 130°C, 15 min, 88%; (5) THF, 130°C, 15 min, 62%.

Scheme 10. Microwave-assisted synthesis of [Mo(CO)$_4$(α-diimine)] complexes.

Ayodele T. Odularu and co-workers reported through their review "of the molybdenum compound intervention to control cancer disease.

The main contributions of molybdenum compounds as anticancer agents could be observed in their nanofibrous support with suitable physicochemical properties, combination therapy, and biosensors (biomarkers)" [74].

The reactions of $[M(CO)_6]$, M = Cr, Mo, and W with 2,6-diaminopyridine (dap) in ethanol were reported by Ahmed A. Soliman and coworkers. The synthesis approaches of sunlight and microwave irradiation were used, and the results were compared with the conventional thermal reflux method. The synthesis of binuclear oxo complexes with the general formulae $[M_2(O)_4(dap)_2]$ was the outcome of all routes. Elements analysis, infrared spectroscopy, ^{1}HNMR, mass spectrometry, and magnetic measurement were used to characterize the produced complexes. dap and its complexes have been tested for their biological action as antifungal and antibacterial reagents [75].

Guido D. Frey and co-workers have studied "the relative stability of cis- and trans-isomers of bis(NHC)tetracarbonyl complexes of group 6 metals, as they synthesized the corresponding complexes with triazolin- and tetrazolinylidene ligands. By the reaction of the free carbene (L = 1,3,4-triphenyl-4,5-dihy-dro-1H-1,2,4-triazolin-5-ylidene) first synthesized by Enders – with the hexacarbonyl of Cr, Mo, and W the corresponding $M(L)(CO)_5$ complexes are generated. Depending on an

excess of carbene the cis-$(L)_2Mo(CO)_4$ complex was obtained. The latter can be photolytically converted to the trans-$(L)_2Mo(CO)_4$ complex. The corresponding complexes with the 1,4-dimethyltetrazolin-5-ylidene ligand (L'), $Cr(L')(CO)_5$, cis-$(L')_2Cr(CO)_4$ and trans-$(L')_2Cr(CO)_4$ can be obtained by reaction of hexacarbonyl-l-trihydroxy-dichromate with dimethyl-tetrazolium salt. In the cis-$(L')_2Cr(CO)_4$ complex, one carbonyl ligand can be replaced by donor ligands such as pyridine or phenyl isocyanide to form sym-mer-tricarbonyl complexes" (Scheme 11) [76].

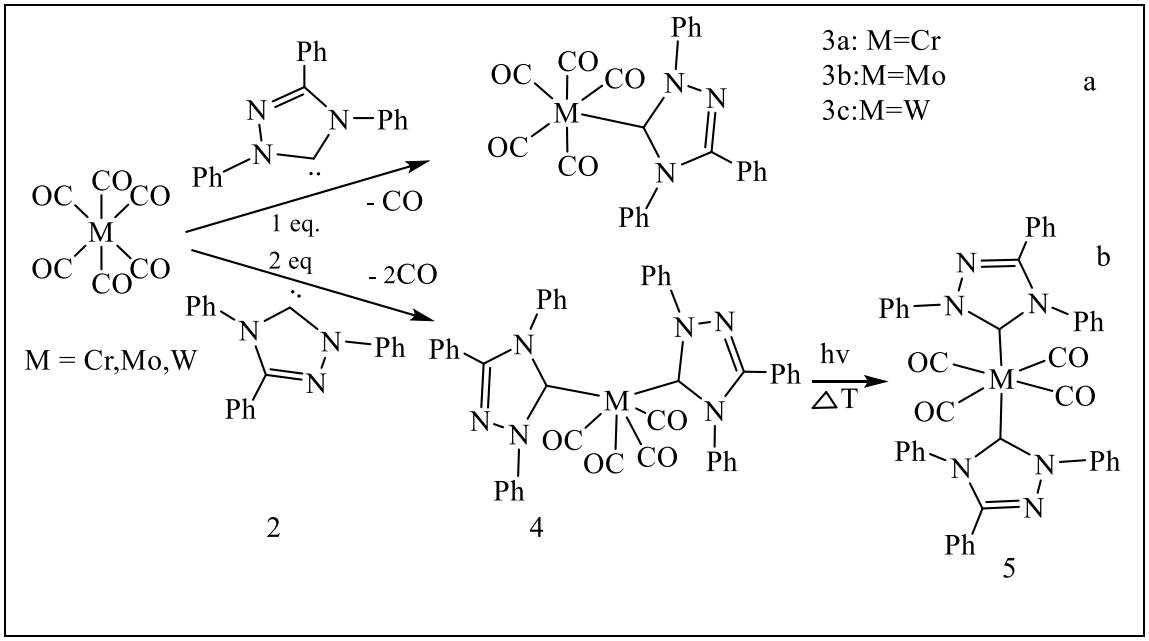

Scheme 11. Synthesis of triazolinylidene-substituted tetra- and pentacarbonyl complexes.

The nitrogen-containing ring systems of interest in medicine are applicable in compounds such as vitamins, herbicides, anti-fungal agents, anti-bacterial agents, and anti-cancer agents. The importance of N-

heterocycles necessitates the development of techniques to boost their synthesis efficiencies and investigate how alterations affect their biological usefulness. Microwave-assisted organic synthesis (MAOS) has been used by medicinal chemists to create complicated heterocyclic compounds more easily. An overview of MAOS and its significance in the recent and urgent developments for the synthesis of small- and medium-sized nitrogen-containing heterocycles, such as lactams, 1,2,3-triazoles, imidazoles, pyrazoles, pyrazolines, and pyrroles, is provided in Maged Henary and co-workers review. These compounds are important scaffolds for medicinal uses [77].

Microwave irradiation has demonstrated its value as a quicker process and a different approach to difficult conversions. Even the phrase "microwave synthesis: chemistry at the speed of light" was used metaphorically by Hayes. Among the 12 principles of green chemistry, the desire to utilize “safer solvents” and to “design for energy efficiency are two key principles of relevance to synthetic chemists" [78-80].

Beneficial characteristics of metal complexes that enable the collection construction of an ensemble of recognition elements and have a broad range of photophysical properties. Particularly, a growing area of research has been the investigation of transition metal complexes that specifically bind DNA. Jacqueline K. Barton and co-workers "review

recent experiments in their laboratory aimed at the design and study of octahedral metal complexes that bind DNA noncovalently and target reactions to specific sites. Emphasis is placed both on the variety of methods employed to confer site-specificity and upon the many applications for these complexes. Particular attention is given to the family of complexes recently designed that target single base mismatches in duplex DNA through metallo-insertion.

The earliest work focused on the DNA-binding of octahedral metal with centers tris(phenanthroline) complexes of ruthenium, chromium, zinc, nickel, and cobalt" [81].

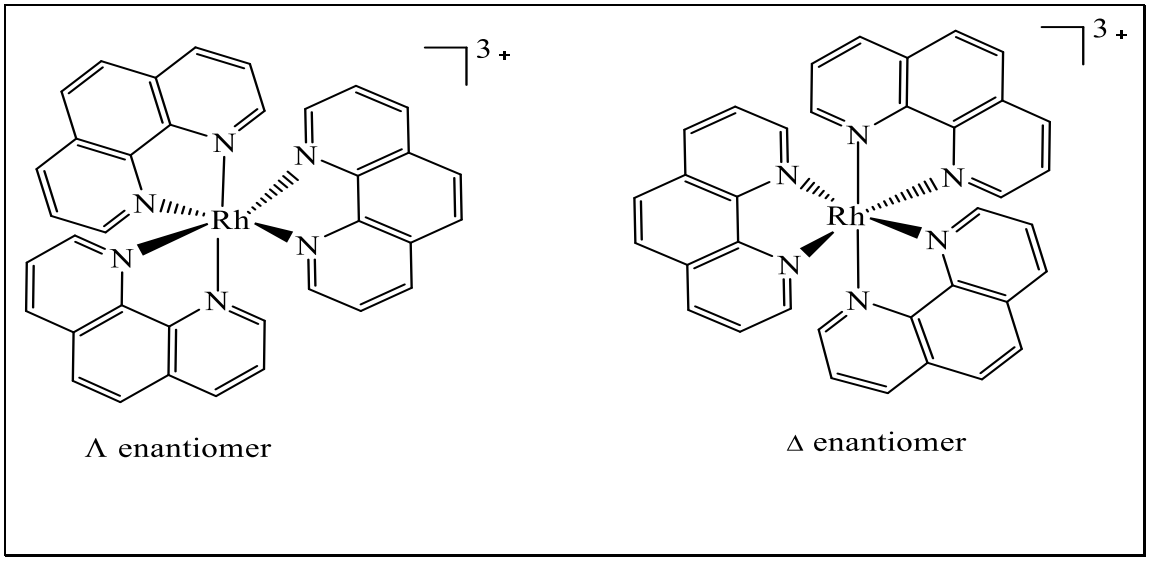

Figure.4 Λ- and Δ-enantiomers of $[Rh(phen)_3]^{+3}$.

As metallodrugs, gold complexes have been studied for their potential as antitumoral agents. Gold-phosphine compounds, in particular, appeared very promising since the use of the antiarthritic auranofin drug

(thiolate-Au-PEt_3 complex) was presented. Thus, Laura Rodríguez and João Carlos Lima have investigated many auranofin analogs, for this reason, the main number of phosphine-gold complexes developed with this goal contain thiolate ligands. Phosphine-gold-halides and tetrahedral bis(phosphine)gold(I) are two more complexes that have been explored. Phosphine-gold-alkynyl compounds have also demonstrated highly intriguing biological activities very recently, even though very few papers have been published on them [82].

Dennis W. Bennett et al. explain by single crystal X-ray diffraction "The crystal and molecular structure of trans-$Cr(CO)_4(PPh_3)_2$ has been determined. they predict that the “gas phase” cis conformer is more stable than the trans conformer for all three metals by density functional calculations on cis-$M(CO)_4(PPh_3)_2$ vs. trans-$M(CO)_4(PPh_3)_2$, M = Cr, Mo, and W" [83].

In medicinal inorganic chemistry the search for novel metal complexes with therapeutic activity, in particular against cancer and infectious diseases, is an active and important area of research. In recent years organometallic compounds have gained considerable importance, In addition to the well-studied platinum- and ruthenium-based coordination complexes. also, some metal carbonyl compounds

exhibited remarkable antitumor activity, this increased interest steadily [84-90].

Shiaw Xian Lee et al. reacted group 6 metal carbonyls with "a new ligand 1 (1,10-phenanthrolin-5-amine, N-(2-fluorenylmethylene)) were synthesized to form UV activable photoCORMs with the formulation of $M(1)(CO)_4$ (M = Cr, Mo, and W, which correspond to 2, 3, and 4, respectively) (Scheme 12). All synthesized compounds were characterized by FT-IR, ^{1}HNMR, ^{13}C NMR, CHN elemental analysis, and single crystal X-ray diffraction. as exhibited compounds 1–4 potent cytotoxicity against human colorectal cancer cell lines (HT-29 and HCT 116) and 2–4 displayed strong photo-induced cytotoxicity against the same cell lines with remarkedly high selectivity" [91].

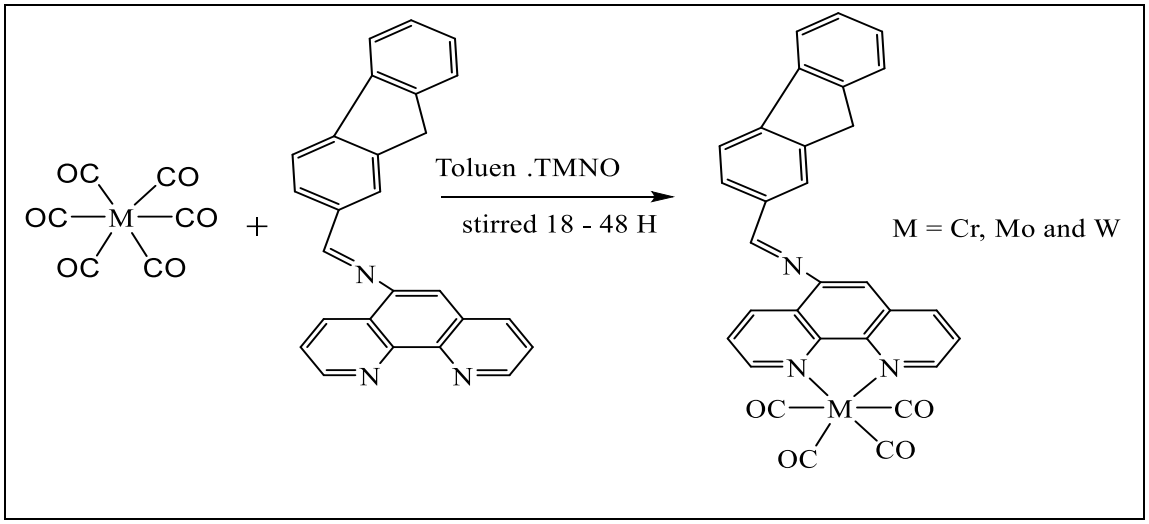

Scheme 12. Schematic representation and proposed structure for 2–4.

Laila H. Abdel-Rahman and co-workers performed The MTT technique in their study to assess the in vitro "cytotoxicity of the two ligands and their Mn(II), Fe(III), and Cr(III) complexes on the Hep-G2 human liver carcinoma cell line and the MCF-7 human breast cancer cell line" [92].

Shimaa Hosny and co-workers showed that "the primary objective of their study was to describe the cytotoxicity on HEPG-2 cells and to study the COVID-19 activities of the novel H_2L ligand and its Cr and Cu nano-complexes. The results showed the Cr nano complex, exhibited strong antitumor activity with IC_{50} value (3.349 μg/ml) after heating" [93].

Ayodele T. Odularu and co-workers showed in their review "to report the molybdenum compound intervention to control cancer disease. could be observed main contributions of molybdenum compounds as anticancer agents in their nanofibrous support with suitable physicochemical properties, combination therapy, and biosensors (biomarkers)" [94].

Density functional theory has been the dominant method for the quantum mechanical simulation of periodic systems for the past 30 years and its efficiency was acknowledged by the attribution of the Nobel Prize in Chemistry in 1998 to one of its authors, Walter Kohn. Density

functional theory (DFT) computations are quickly becoming the "standard tool" for solving a variety of materials modeling issues in chemistry, materials science, physics, and several engineering disciplines. Quantum chemists have also embraced it in recent years, and it is now extensively utilized for the simulation of molecular energy surfaces. DFT is a phenomenally successful approach to finding solutions to the fundamental equation that describes the quantum behavior of atoms and molecules, the Schrödinger equation, in settings of practical value. The atomic number of each constituent atom and some preliminary structural information is the only input data used by DFT, which is based on quantum theory and does not employ any empirical or changeable parameters. The structural or dynamical properties (lattice structure, charge density, magnetization, phonon spectrum, etc.) of a broad range of solids have been effectively determined using DFT. whereas optical properties, Predictive calculations of transport properties, materials characterization via vibrational spectroscopy, computational materials discovery, Predictive calculations of the superconducting critical temperature, and many-body effects in ARPES are examples of calculations based on DFT Predictive, DFT is very popular because of transferability, simplicity, reliability, software, robust platform [95-98].

Chapter two

Experimental and Method

Experimental and Method

2.1 Reagents and Materials.

All solvents were purchased from Goss Chemicals. Molybdenum (0) hexacarbonyl [$Mo(CO)_6$] 98%, Chromium(0) hexacarbonyl [$Cr(CO)_6$] 98%, Tungsten(0) hexacarbonyl [$W(CO)_6$] 98% and BINAP were purchased from Sigma-Aldrich. The Co-Ligands such (bipyridine, 2-amino pyridine, 8-hydroxyquinoline) were purchased from Sigma-Aldrich.

2.2 Spectroscopic Techniques.

The Ultraviolet-Visible spectra (UV-Vis) were acquired at Misurata University on Cary 60 UV-Visible spectrophotometer (Agilent Technologies) in the range of 200 to 800 nm and operating with Excel software. Diamond FT-IR- Spectrometer Frontier was acquired at Misurata University on FT – IR Spectrometer Frontier (Perkin Elmer) in the range 4000 to 600 cm^{-1} and results of the infrared spectrum were recorded jpg formatted.

Elemental analyses were carried out by Gas Chromatography/Mass Spectrometry (GC/MS) under model pf 689N network (Agilent Technologies), in the range of 40 to 650 m/s.

^{1}HNMR spectra of all complexes were acquired on a Bruker Spectro spin AG 400DPX and operating at 400 MHZ. Chemical shifts are

reported in ppm and referenced to the solvent peaks. Coupling constants are quoted in Hertz (HZ).

Elemental analyses were carried out by Mikroanalytisches Labor Pascher of Remagen-Bandorf, Germany. Mass Spectrometry, ^{1}HNMR spectra, and elemental analysis were obtained from the regional Center for Mycology and Biotechnology (Al-Azhar University). Microwave instrument was used for all prepared complexes with a power of 2000W and (220Ev from Hommer company).

2.3 Determination of potential cytotoxicity of novel Chromium-molybdenum complexes with BINAP ligand:

2.3.1 Principle:

The sensitivity of the MCF-7 to Cr(0), and Mo(0) complexes was determined by sulphorhodamine-B (SRB) assay, which provides a sensitive index of cellular protein content. SRB is a bright pink aminoxanthene dye with two sulphonic groups that stains protein by binding to the amino groups of intracellular protein under mildly acidic conditions [99].

2.3.2 Reagents and buffers:

Acetic acid: 1% concentration was used for dissolving the unbound SRB dye. SRB: 0.4% SRB dissolved in 1% acetic acid was used as

protein dye in the cytotoxicity assay. TCA: A stock solution of TCA (50%) was prepared and stored at 4C° in the refrigerator. Fifty µl of the stock was added to 200 µl RPMI-1640 medium/well to yield a final concentration of 10% for protein precipitation. Tris base: It was used for SRB dye solubility at a concentration of 10 mM and pH of 10.5 (adjusted by 2 M HCl).

2.4 Theoretical calculations.

2.4.1. Docking studies

Crystal structural determinations of human breast cancer cell line MCF-7 (PDB code 1ZXM) used in the current study and its binding interaction with complexes (G1-G6), were investigated using Molecular Operating Environment (MOE) 2015.10.

Output files were visualized under both Discovery Studio 2021 Client and (MOE) 2015.10, on personal computers. Finally, were converted to tagged images finally formatted as jpg images in 'Paint Shop Pro'. Thermal ellipsoids are set at 50% unless otherwise stated.

2.5 Experimental.

2.5.1 Synthesis of the ligand BINAP.

Among the methods of synthesis of BINAP, Barry M. Trost and coworkers have prepared 2,2'-bis(diphenylphosphino)-l,l'-binaphthyl(BINAP), as outlined in (Scheme 13) [100].

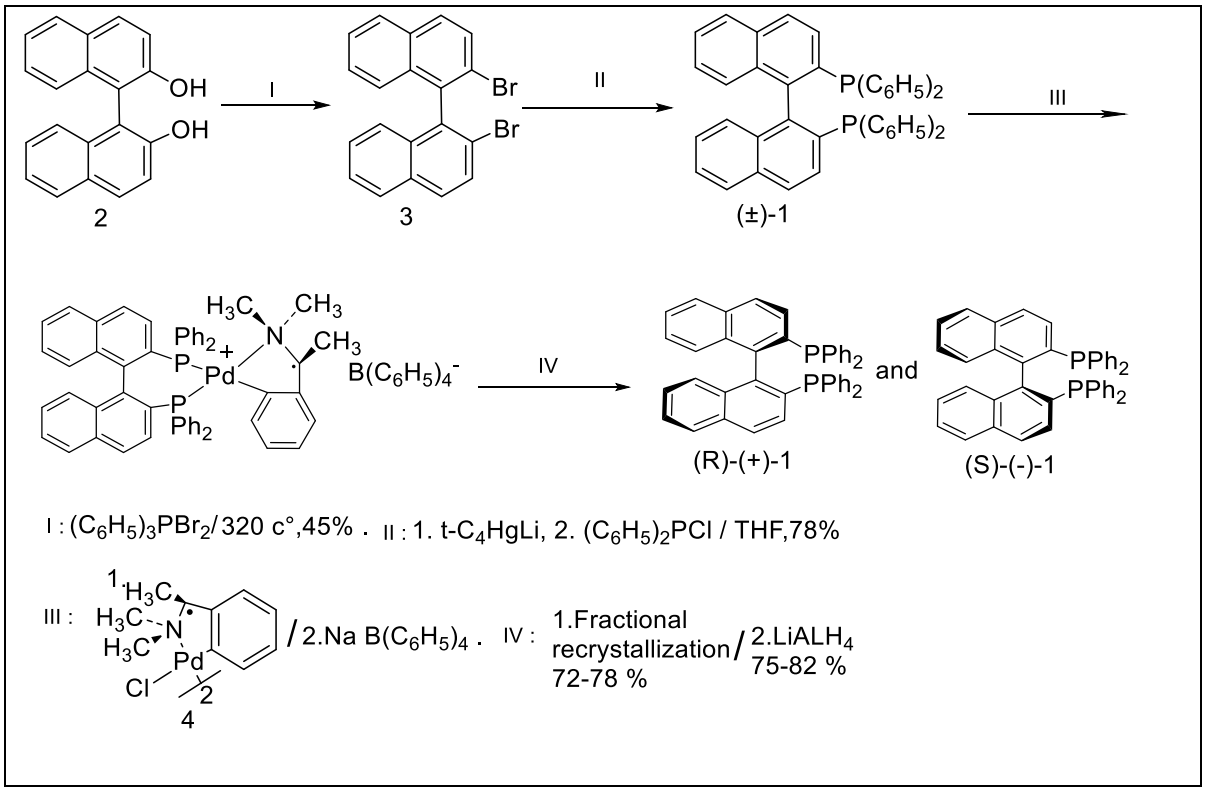

Scheme 13. Synthesis of (R), (S) 2,2'-Bis(dipheny1phosphino)-1,l'-binaphthyl (BINAP).2.5.2 **Synthesis of the complexes.**

2.5.2 Synthesis of the complexes.

2.5.3 Synthesis of complex [$Cr(CO)_2$(BINAP)(bipy)] (G1).

The Complex (G1) was synthesized by mixing and grinding of [$Cr(CO)_6$] (0.15 g, 0.679 mmol) with two ligands, 2,2′-bis(diphenylphosphino)-1,1′-binaphthyl (BINAP) (0.424 g, 0.680 mmol) and (0.106 g, 0.679 mmol) 2,2´-bipyridin (bipy) with a molar ratio 1:1, the materials were placed in a small tube in the microwave for 10 minutes. Then washed light yellow solid of the product using THF several times (Scheme 14). The weight of the product was (0.3182 g) (52.68%) and the melting point for this complex is approximately (253 C˚).

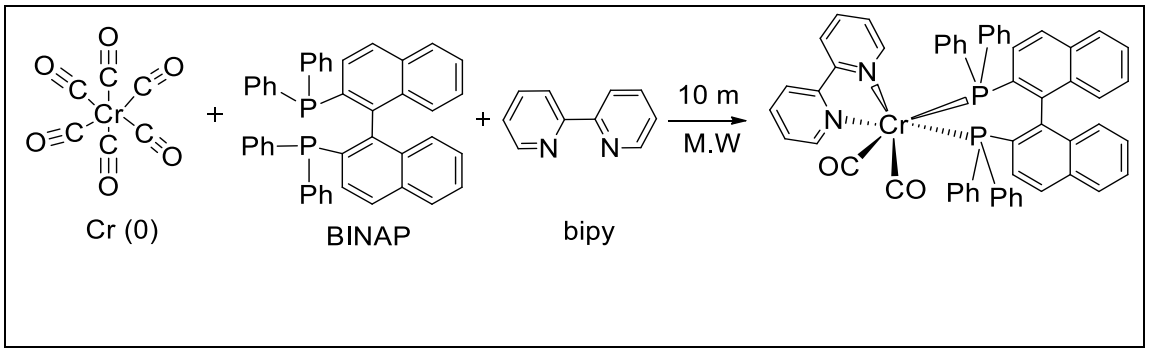

Scheme 14. Synthesis of [$Cr(CO)_2$(BINAP)(bipy)].

2.5.4 Synthesis of [$Cr(CO)_2$(BINAP)(2-Ap)] (G3).

Complex (G3) was synthesized by mixing and grinding of [$Cr(CO)_6$] (0.15 g, 0. 679 mmol) with two ligands, (0.424 g, 0.680 mmol) 2,2′-bis(diphenylphosphino)-1,1′-binaphthyl (BINAP) and (0.0641 g, 0.680 mmol) 2-amino pyridine with a molar ratio 1:1, then the materials are put

in a small tube in the microwave for 8 minutes until the color of the reactants turned into a light grey color, Then we wash the solid product with some drops of THF and leave it to dry (Scheme 15). The weight of the product was (0.3515 g) (62.7%) and the melting point for this complex is approximately (253 C°).

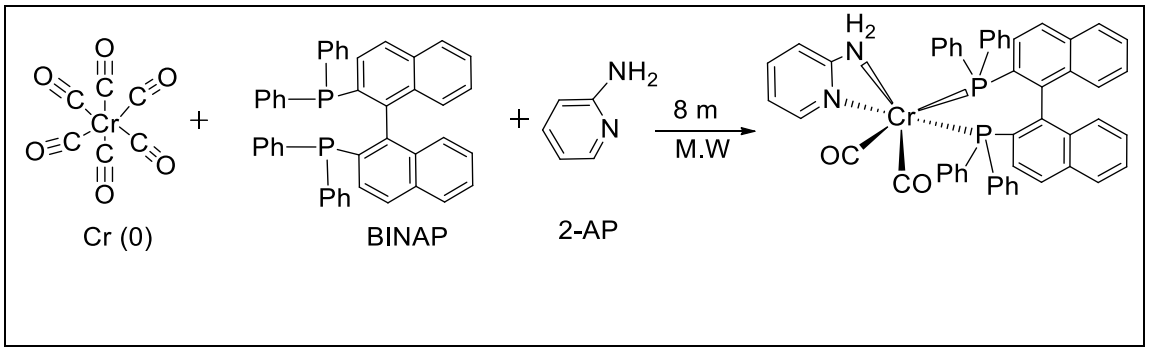

Scheme 15. Synthesis of [Cr(CO)$_2$(BINAP)(2-AP)].

2.5.5 Synthesis of [Cr(CO)$_2$(BINAP)(8-HQ)] (G5).

Complex (G5) was synthesized by mixing [Cr(CO)$_6$] (0.15 g, 0. 679 mmol) with two ligands, (0.424 g, 0.680 mmol) 2,2′-bis(diphenyl-phosphino)-1,1′-binaphthyl (BINAP) and (0.098 g, 0.675 mmol) 8-hydroxyquinoline, then we grind the materials well together put in and them in in a small tube in the microwave for 8 minutes until the color of the reactants turned into a light grey color, Then we wash the solid product with some drops of THF and leave it to dry (Scheme 16). The weight of the product was (0.4095 g) (68.8%) and the melting point for this complex is approximately (244 C°).

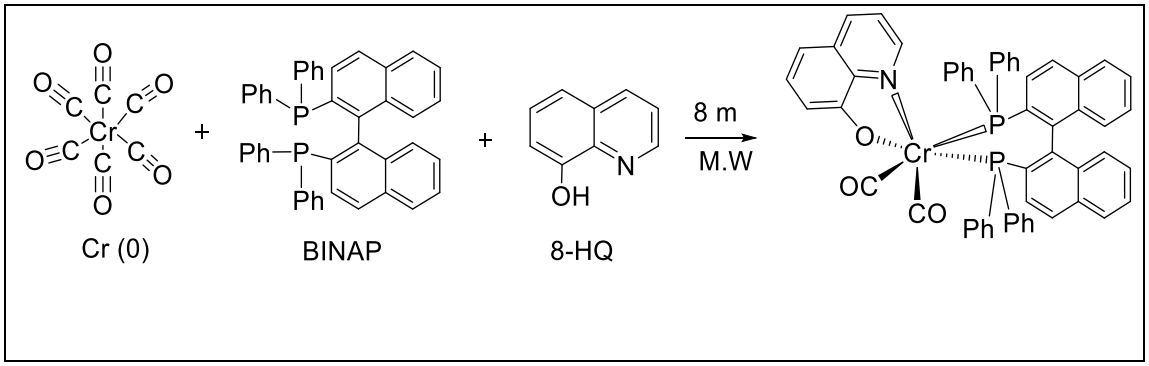

Scheme 16. Synthesis of [Cr(CO)$_2$(BINAP)(8-HQ)].

2.5.6 Synthesis of [Mo(CO)$_2$(BINAP)(bipy)] (G2).

The complex (G2) was synthesized by mixing [Mo(CO)$_6$] (0.15 g, 0.568 mmol) with two ligands (0.353 g, 0.567 mmol) 2,2′ bis(diphenyl-phosphino)-1,1′-binaphthyl (BINAP) and (0.088 g, 0.564 mmol) 2,2´-bipyridin (bipy), with a molar ratio 1:1, then grind of materials and placed in a small tube in the microwave for 5 minutes until the color of the reactants turned into an orange color. wash the product with drops of THF on the orange solid and leave it to dry (Scheme 17). The weight of the product was (0.3491 g) (66.0%) and the melting point for this complex is approximately (246 C◦).

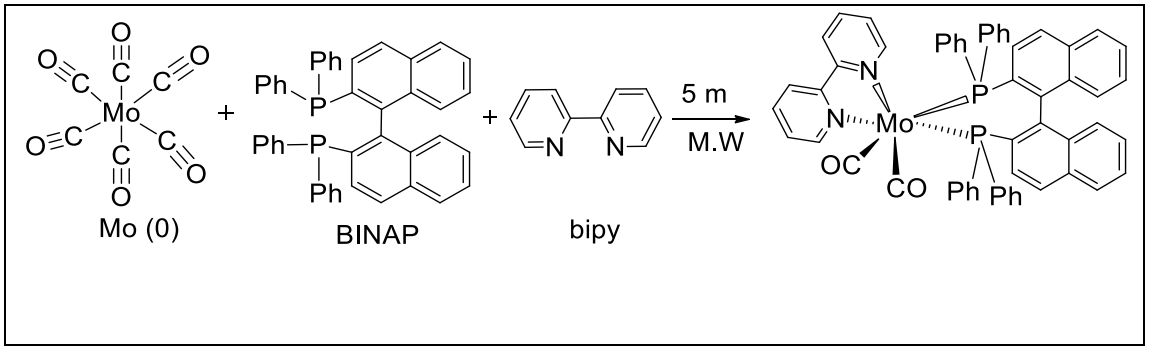

Scheme 17. Synthesis of [Mo(CO)$_2$(BINAP)(bipy).

2.5.7 Synthesis of [Mo(CO)$_2$(BINAP)(2-AP)] (G4).

The complex was synthesized (G4) by mixing and grinding of [Mo(CO)$_6$] (0.15 g, 0. 568 mmol) with two ligands, (0.353g, 0.567 mmol) 2,2′-bis(diphenylphosphino)-1,1′-binaphthyl (BINAP) and (0.0534g, 0.567 mmol) 2-amino pyridine with a molar ratio 1:1, then the materials is put in a small tube in the microwave for 4 minutes until the color of the reactants turned into a light brown color, Then we wash the solid product with some drops of THF and leave it to dry (Scheme 18). The weight of the product was (0.3637 g) (73.59%) and the melting point for this complex is approximately (244 C˚).

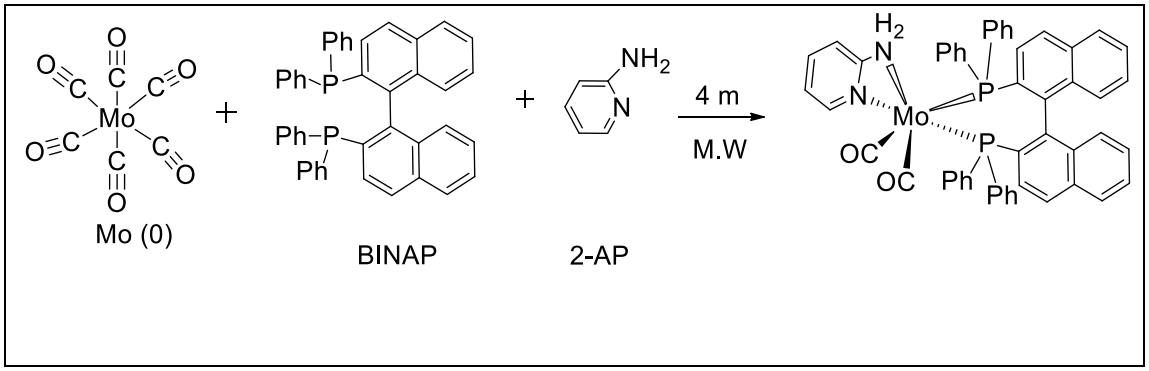

Scheme 18. Synthesis of [Mo(CO)$_2$(BINAP)(2-Ap)].

2.5.8 Synthesis of [Mo(CO)$_2$(BINAP) (8-HQ)] (G6).

The complex was synthesized (G6) by mixing and grinding of [Mo(CO)$_6$] (0.15 g, 0. 568 mmol) with two ligands, (0.353 g, 0.567 mmol) 2,2′-bis(diphenylphosphino)-1,1′-binaphthyl (BINAP) and (0.0824 g, 0.567 mmol) 8-hydroxyquinoline with a molar ratio 1:1, then

put the materials in a small tube in the microwave for 2 minutes until the color of the reactants turned into a black color, we wash the orange solid product with drops of THF and leave it to dry (Scheme 19). The weight of the product was (0.3965 g) (75.84%) and the melting point for this complex is approximately (245 C˚).

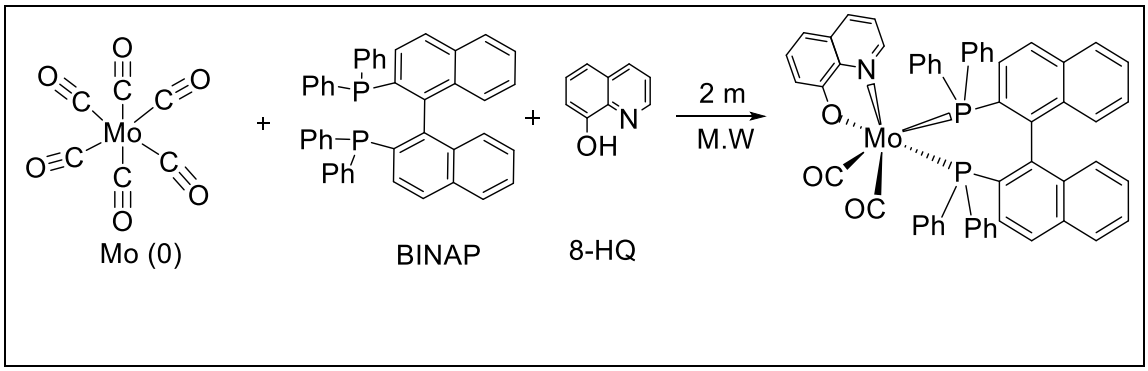

Scheme 19. Synthesis of [Mo(CO)$_2$(BINAP)(8-HQ)].

2.6 Anticancer Application.

2.6.1 Procedure:

1. Cells were used when 70% confluence was reached in T75 flasks. The adherent cell line was harvested with 0.025% trypsin. Viability was determined by trypan blue exclusion using the inverted microscope.

2. Cells were seeded in 96-well plate microtiter plates at a concentration of 3×10^3 cells/well in fresh medium and left to attach to the plates for 24 hours.

3. After 24 hours, cells were incubated with four concentrations of Cr(0), and Mo(0) complexes (62.500, 125, 250, 500 µg/ml) for the

MCF-7 cell line. Wells were completed to 200 µl volume/well using fresh medium and incubation was continued for 48 hours. Control cells were treated with a vehicle alone. For each drug concentration, 4 wells were used, and the experiment was repeated 3 times each.

4. Following treatment, the cells were fixed with 50 µl cold 50% TCA for 1 hour at 4C°. Wells were then washed once with distilled water and stained for 30 minutes at room temperature with 50 µl of 0.4% SRB dissolved in 1% acetic acid.

5. The wells were then washed once with 1% acetic acid the plates were air dried and the dye was solubilized with 10 mM of tris base (pH 10.5, 100 µl/well) for 5 minutes on a shaker (Orbital shaker OS 20, Boeco, Germany).

6. The optical density (O.D.) of each well was measured spectrophotometrically at 570 nm with a microplate reader (Tecan Sunrise™, Germany). The mean values for each drug concentration were calculated.

2.6.2 Calculation:

The percentage of cell survival was calculated as follows: Survival fraction= O.D. (treated cells)/ O.D. (control cells). The concentrations of Cr(0) and Mo (0)complexes with BINAP ligand required to produce 50% inhibition of cell growth (IC_{50} values) were calculated using dose-response curve-fitting models (GraphPad Prizm software, version 5).

Chapter Three

Results and Discussion

Results and Discussion.

3.1 Chromium (0) Complexes:

Electronic absorption spectra of the chromium complexes were measured in the range of 200 to 800 nm in THF solvent. Chromium complexes have been diagnosed and several bands at different wavelengths have been observed of which (π-π*) transition, another type of transition is called Charge transfer (CT) and is found in the spectrum of complexes which are usually observed in the ultraviolet region of the spectrum, although in some cases they appear in the visible region. Consequently, they frequently overlap or mask transitions of the d-d type [101]. Somewhat unexpectedly, the Contribution to the correlation energy comes from the charge-transfer double replacement ($3d(t_2g) \rightarrow 2\pi^*(t_2g)$) ($6\sigma(eg) \rightarrow 3d(eg)$). where the electrons in the 6σ CO orbitals move toward chromium and the electrons in the Cr 3d (t_2g) orbital move toward the 2π* orbital of CO [102]. The absorption peaks around (233 nm) in [$Cr(CO)_2$(BINAP)(bipy)] (G1) can be assigned to the ($\pi \rightarrow \pi^*$) transition, the other band at 394 nm, which was assigned to $Cr(d\pi) \rightarrow$ bipy(π*) the metal-to-ligand charge-transfer transition (Figure 5). In agreement with to their experimental observations in the previously studied absorptions at 300-400 nm involve Ru → bipy MLCT transitions [103]. Two distinct bands at max = (226 nm) in [$Cr(CO)_2$(BINAP)(2-

AP)] (G3) and as broad band at 437-535 nm are attributable to π→π* and transition of Cr(dπ) → 2-AP(π*) respectively (Figure 6). The $[Cr(CO)_2(BINAP)(8\text{-}HQ)]$ (G5) shows absorption bands displayed bands at (226 nm) and a broad band observed at 390 nm, which may be assigned to π→π* transition, and transition Cr(dπ) → 8-HQ(π*) charge-transfer (CT), respectively (Figure 7). The transient absorption spectra of the G1, G3, and G5 may be attributed at (600 nm, 769 nm, and 757 nm) for Cr(0)-to-BINAP charge transfer state (MLCT) MLCT of BINAP, as stated in a complex diagnosis $[Pt(BINAP)_2]$ [104].

Physical properties, maximum absorption wavelength (λ), and molecular weight data of chromium complexes are presented in (Table 1), where molecular weight data confirms the proposed formula.

Table 1. Physical properties and Maximum absorption wavelength (λ) of chromium complexes.

Complex	Mol.Wt g/mol	Color	m.p C°	λ max (nm)
$[Cr(CO)_2(BINAP)(bipy)]$ G1	885.91	Light yellow	253	233
$[Cr(CO)_2(BINAP)(2\text{-}AP)]$ G3	823.91	Light grey	253	226
$[Cr(CO)_2(BINAP)(8\text{-}hq)]$ G5	873.9	Light grey	244	226

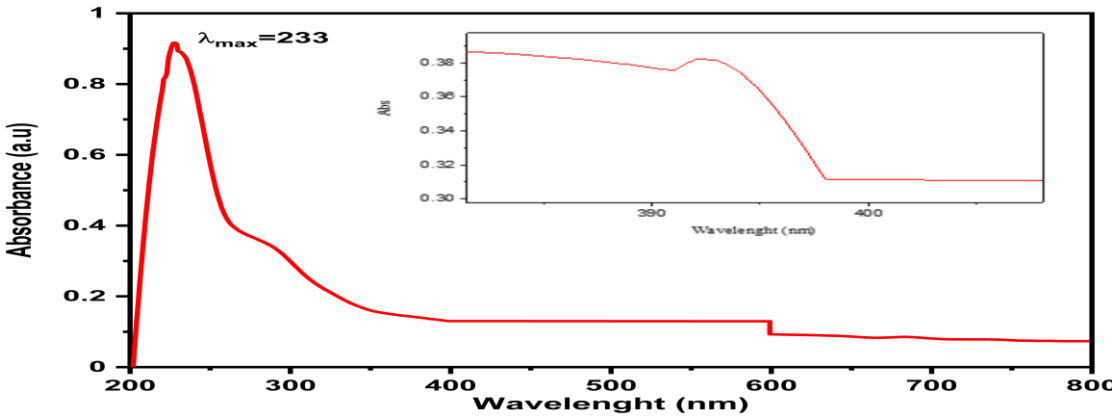

Figure 5. Electronic transitions of [Cr(CO)$_2$(BINAP)(bipy)].

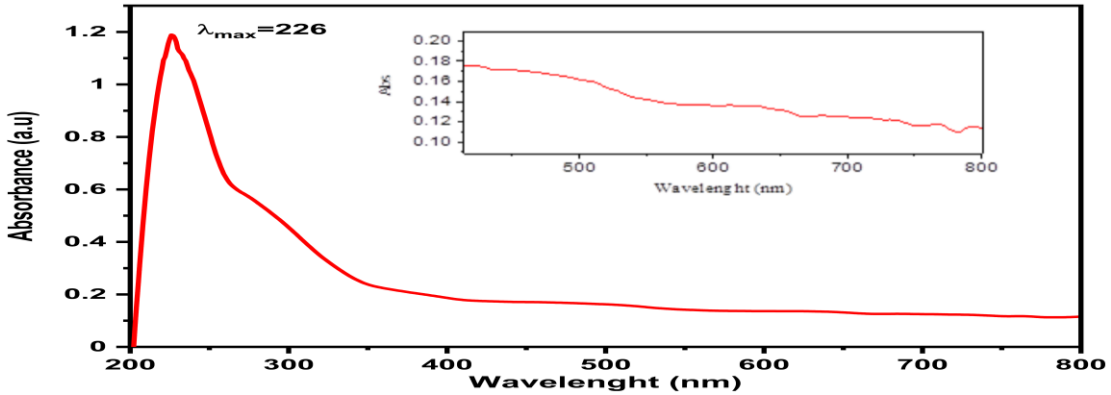

Figure 6. Electronic transitions of [Cr(CO)$_2$(BINAP)(2-AP)].

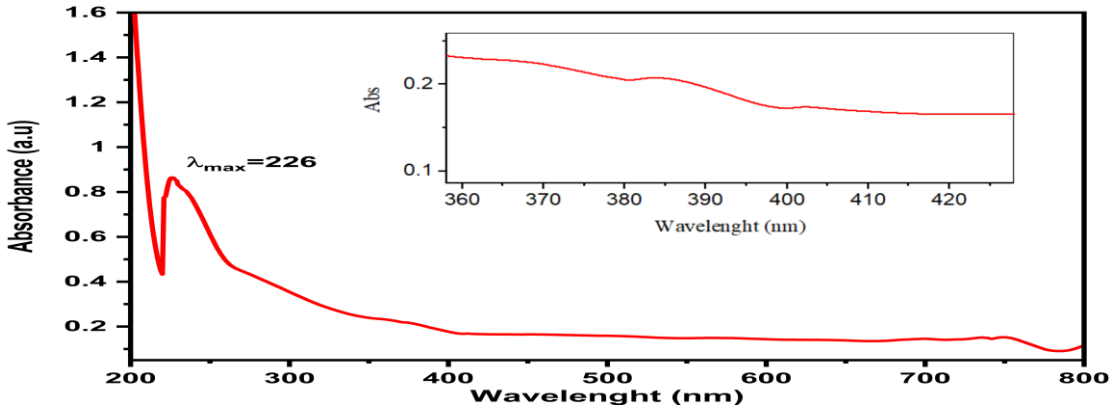

Figure 7. Electronic transitions of [Cr(CO)$_2$(BINAP)(8-HQ)].

The characterization of metal carbonyls vibrational spectroscopy is an important method. It is a well-known fact that the C-O vibration (νCO)

for the free carbonyl group (CO gas) absorbs at (2143 cm^{-1}). However, this C–O absorption shifts downward (sometimes upward) to cover a very wide range of wavenumber as the carbonyl ligand gets attached to a metal center. This is due that the energies of the νCO band for the metal carbonyls directly correlate with the strength of the carbon-oxygen bond, and are inversely correlated with the strength of the π-backbonding between the metal and the carbon [105], the normal range of the observed of ν(CO) at (1820–2150 cm^{-1}) [16].

From the data IR spectra of the chromium complex (G1), it can be seen that the bands of (1951 &1940 cm^{-1}) were assigned to υ(C=O) as two M(CO)-bands are found according to a cis-configuration.

The characteristic stretching bands in free ligand 2,2'-bipyridine at (3055 cm^{-1})(s), (1577 cm^{-1})(s), (1449 cm^{-1})(s) and (1246 cm^{-1})(s) assigned for νC-H, νC=N, νC=C, and νC-N [52]. After complexation the band of νC=N at (1584 cm^{-1}) for pyridine rings. This band was shifted and changed in complexes to higher frequencies because of coordination with metal ions via the nitrogen atom [106]. The C–N stretching vibration is always mixed with other bands and is usually assigned in the region (1266–1382 cm^{-1}) [107, 108]. The absorption band at (1311 cm^{-1}) for νC-N. The bands shown at (1480 cm^{-1}) were assigned to the ν(C=C) stretching mode in the ligands in bipy. The hetero aromatic organic

compounds commonly exhibit multiple week bands in the region (3000–3100 cm^{-1}) due to C–H stretching vibrations [109-111], the bands have been assigned at (3049, 2999, 3012 cm^{-1}) to C–H ring stretching vibrations [112]. The important IR absorption bands for the chromium complex [$Cr(CO)_2$(BINAP)(2-AP)] (G3), it can be seen that the bands of (1951&1968 cm^{-1}) were assigned to υ(C=O). Two M(CO)-bands are found according to a cis-configuration. The characteristic stretching bands at (1584 cm^{-1}), (1311 cm^{-1}), (1480 cm^{-1}) assigned for ν(C=N), ν(C–N) , ν(C=C) respectively . The bands have been assigned at (3049, 2999, 3012 cm^{-1}) to νC–H ring stretching vibrations. The important IR absorption bands for the chromium complex [$Cr(CO)_2$(BINAP)(8-HQ)] (G5) It can be seen that the bands of (1894&1955 cm^{-1}) were assigned to υ(C=O). Two M(CO)-bands are found according to a cis-configuration. The characteristic stretching bands at (1584 cm^{-1}), (1311 cm^{-1}), (1479 cm^{-1}) assigned for ν(C=N), ν(C–N), ν(C=C) respectively. The bands have been assigned at (3049, 2999, 3012 cm^{-1}) to ν(C–H) ring stretching vibrations. the band is observed at (1215 cm^{-1}) due to ν(C-O) of ligand 8-HQ, which indicates the coordination of the phenolic oxygen atom was also confirmed of metal complex formation by the redshift range (1207– 1231 cm^{-1}) [113]. The bands related to Cr-O and Cr-N vibrations are exhibited within region (552–497 cm^{-1}) [114]. FTIR spectra have that are shown in Table 2.

Table 2. Characteristic FT-IR bands of the Chromium Complexes.

Complex	Assignments	Experimental(cm^{-1})	Calculation(cm^{-1})
$[Cr(CO)_2(BINAP)(bipy)]$ (G1)	ν(CO)	1951& 1940 cm^{-1}	1770& 1742 cm^{-1}
	νC=N	1584cm-1	1588cm^{-1}
	νC=C	1480cm^{-1}	1489cm^{-1}
	νC-N	1311cm^{-1}	1313 cm^{-1}
	νC-H	3068, 2999cm^{-1}	3276 cm^{-1}
$[Cr(CO)_2(BINAP)(2\text{-}AP)]$ (G3)	ν(CO)	1951& 1968cm^{-1}	1876&1703cm^{-1}
	νC=N	1584cm-1	1616 cm^{-1}
	νC=C	1480cm^{-1}	1479 cm^{-1}
	νC-N	1311cm^{-1}	1319 cm^{-1}
	νC-H	3049,2998cm^{-1}	2447& 3128cm^{-1}
$[Cr(CO)_2(BINAP)(8\text{-}HQ)]$ (G5)	ν(CO)	1894& 1874cm^{-1}	1911&1734 cm^{-1}
	νC=N	1584cm^{-1}	1594 cm^{-1}
	νC=C	1479cm^{-1}	1476 cm^{-1}
	νC-N	1311cm^{-1}	1309 cm^{-1}
	νC-O	1215cm^{-1}	1201 cm^{-1}
	νC-H	3049, 2998cm^{-1}	3342,2776 cm^{-1}

The mass spectra of all the complexes showed a variety of fragmentation patterns, and the results were found to be in good agreement with the molecular formulae of the compounds. According to the mass spectra of the complex $[Cr(CO)_2(BINAP)(bipy)]$ which displayed a molecular ion peak at $[M]^+$ m/z= 885.99 which is in agreement with the molecular formula of $[Cr(CO)_2(BINAP)(bipy)]^+$. The spectrum of EI-MS also showed an ion peak at m/z =702.88 which is a characteristic of the loss of a 2CO and bipy rings of $[Cr\text{-}C_{44}H_{32}N_2]^+$. And the fragments observed at m/z= 411.16 (99.72%). The base peak fragment was observed at 252.04 (100%) (Figure 8).

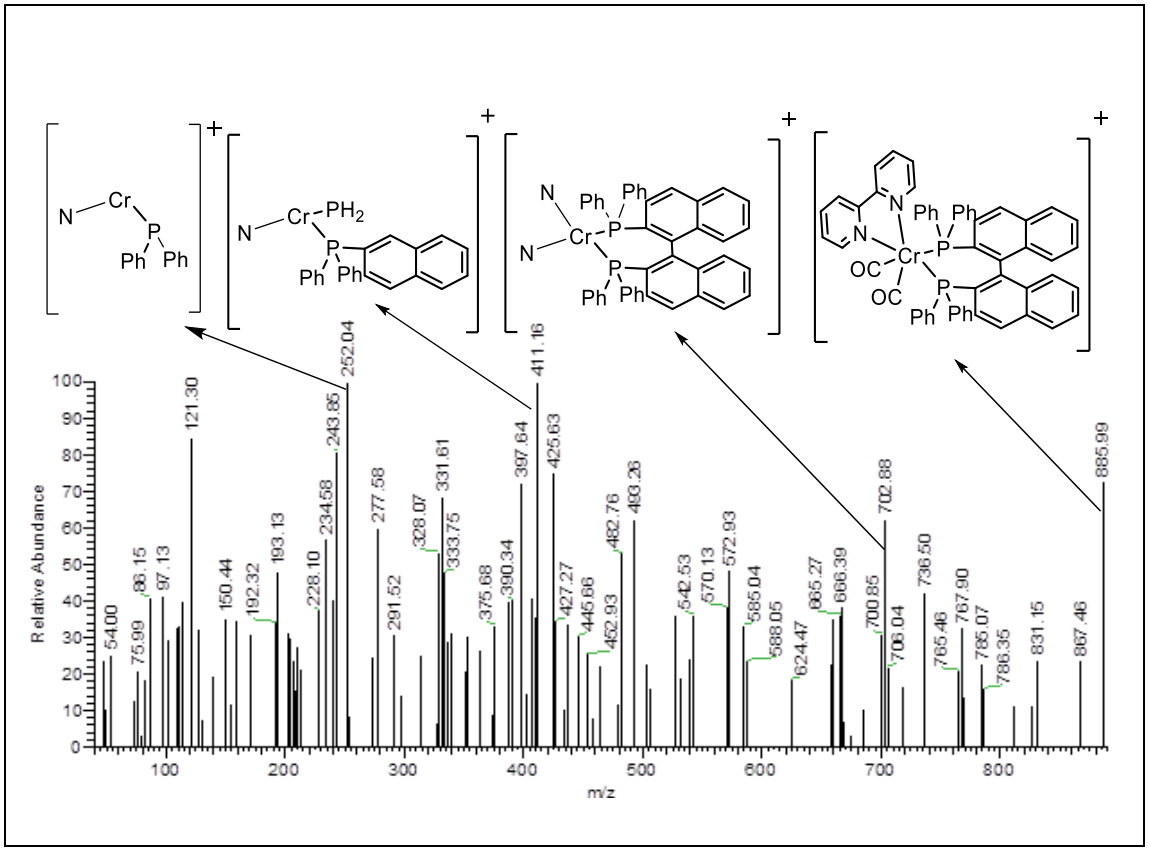

Figure 8. Mass spectrum and fragments of [Cr(CO)$_2$(BINAP)(bipy)].

The EI-MS of complex [Cr(CO)$_2$(BINAP)(2-AP)] showed molecular ion peak $[M]^+$ at m/z=823.08 (72.42%) which is in agreement with the molecular formula of $[Cr(CO)_2(BINAP)(2\text{-}AP)]^+$. The spectrum of EI-MS also showed an ion peak at m/z = 519.41 (69.44%), which is a characteristic of the loss of 2CO and 2-AP and 2 phenyl rings [Cr-$C_{32}H_{22}P_2$] $^+$. Also, the fragments observed at m/z= 519.41 (69.44%), 364.73 (58.21%). The base peak observed at m/z 50.53 (100%) (Figure 9).

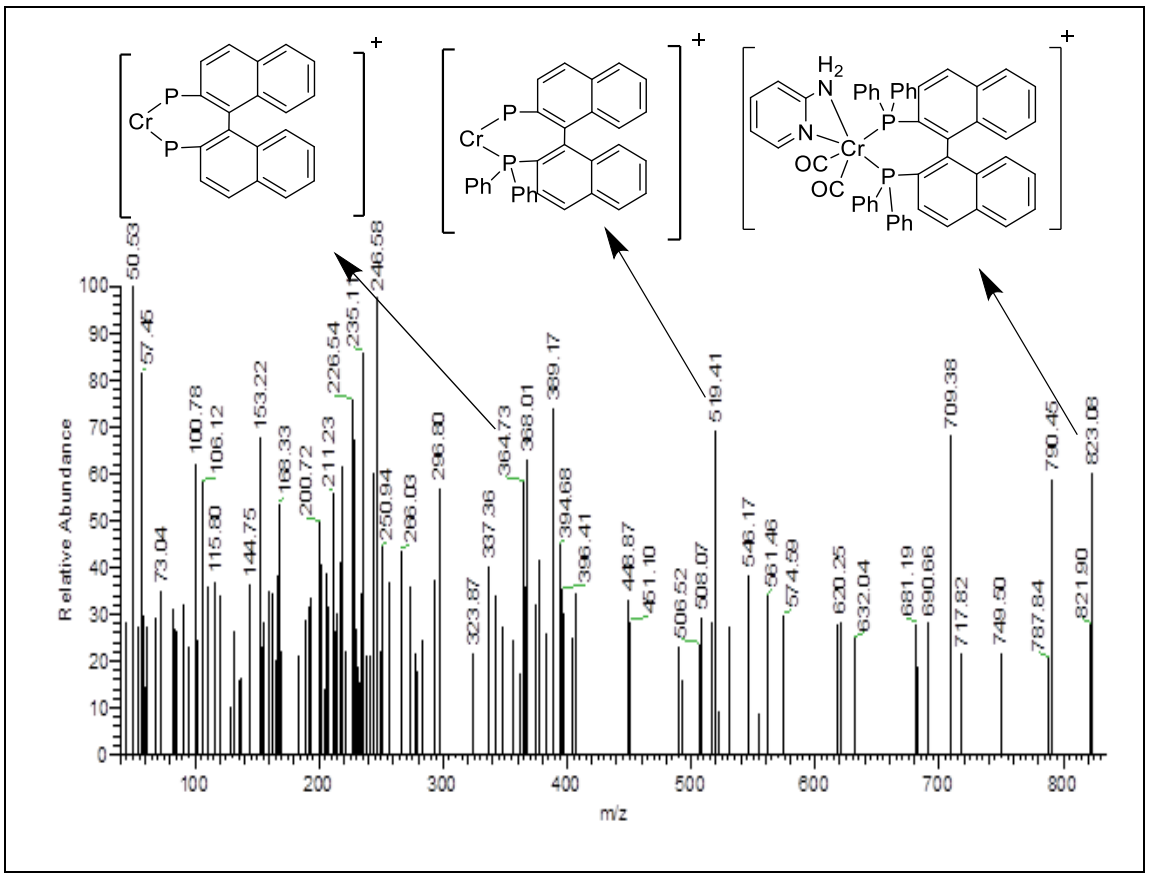

Figure 9. Mass spectrum and fragments of [Cr(CO)$_2$(BINAP)(2-AP)].

The EI-MS of complex [Cr(CO)$_2$(BINAP)(8-HQ)] showed the parent ion peak at $[M]^+$ m/z= 873.92 (26.96%) which is in agreement with the molecular formula of $[Cr(CO)_2(BINAP)(8\text{-}HQ)]^+$. The spectrum of EI-MS also showed an ion peak at m/z = 674.95 (95.09%) which is a characteristic of the loss of a 2CO and 8-hq moiety $[Cr\text{-}C_{44}H_{32}P_2]^+$. Also, the fragments were observed at 399.95 (79.09%). The base peak fragment was observed at 107.36 (100%) (Figure 10).

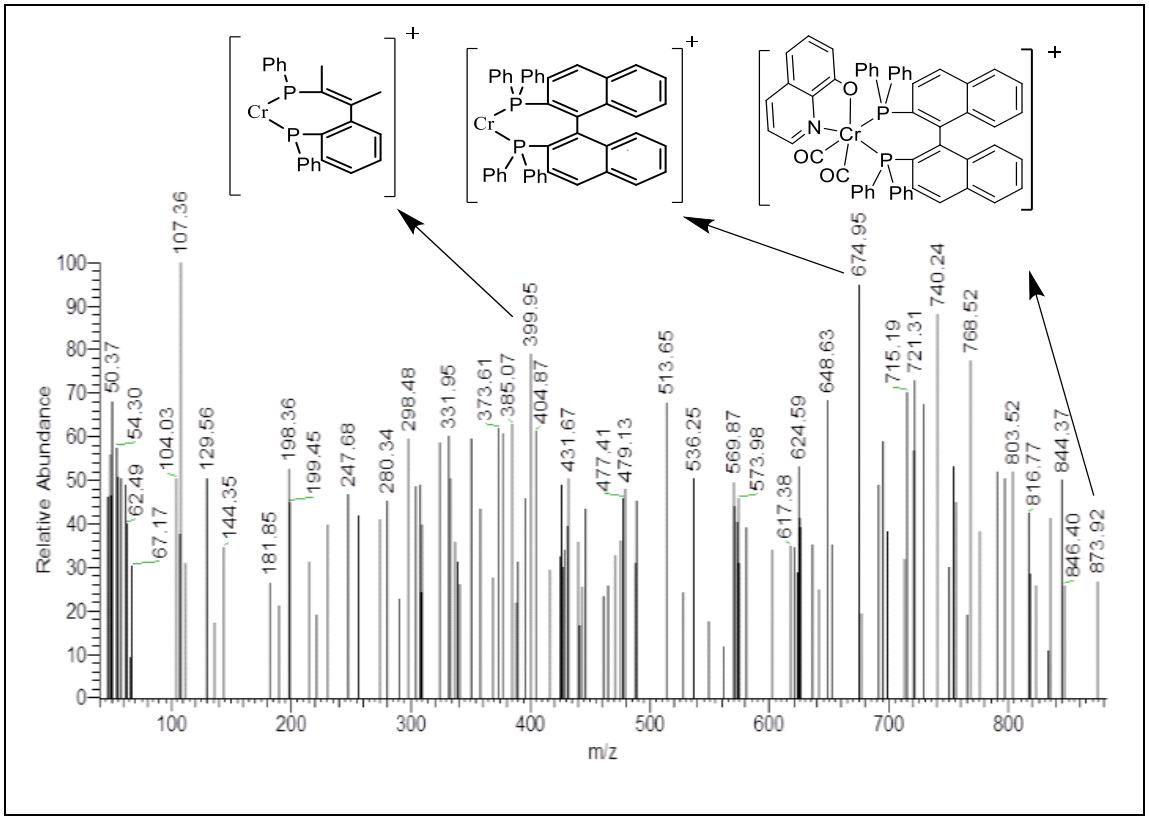

Figure 10. Mass spectrum and fragments of [Cr(CO)$_2$(BINAP)(8-HQ)].

The ^{1}HNMR spectra of the Cr(0) complexes were recorded in DMSO-d^6 (400 MHz, 25 C°) as a solvent and showed signals at (2.50 ppm) [115]. The Complexes contain a BINAP ligand in which the aromatic Hydrogen atoms coordinated to some extent overlap with those of the aromatic Hydrogen atoms of bipy, 2-AP, and 8-HQ ligands. in the complexes containing the BINAP ligand Appearance of broad aromatic proton resonance between 6 and 7 ppm reveals its existence. This signal is associated with restricted rotation of the P-axial phenyl (or p-tolyl) groups as previously suggested in ^{1}HNMR studies [116-118]. Figure 11 displays the ^{1}HNMR spectra of the G1, the broad multiple observed in the

range (δ 6.69–7.44) ppm is assigned to the phenyl protons of BINAP ligand (32H, m, aromatic, CH), also the range (δ 7.92-8.02) assigned to the protons of the bipy rings (4H). The ^{1}HNMR spectrum of G3 showed a set of multiples at (δ 6.71 –7.34) ppm due to the ring's phenyl of BINAP (32H, CH) and (δ 7.89-7.98) due to pyridyl protons (4H, CH) (Figure 12). In the spectrum of G5 the multiple signals in the region (δ 6.70-7.40) ppm may be assigned to aromatic protons of ligand BINAP (32H, CH), also (δ 7.89-8.00) assigned to protons of 8-HQ rings (6H, CH) (Figure 13). ^{1}HNMR for 8-hydroxyquinoline was previously studied in [119, 120]. Also, the signal observed at 3.17 and 3.30 ppm could be assigned to the THF which was used to recrystallize the complexes.

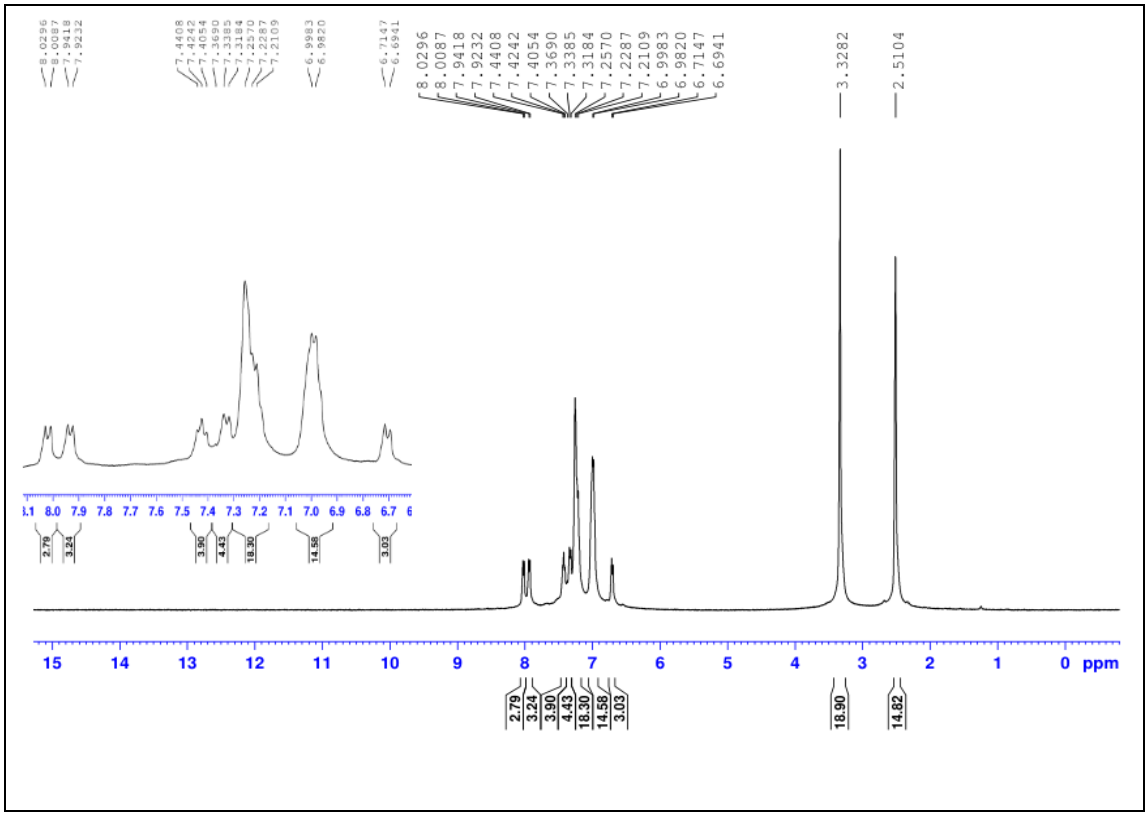

Figure 11. ^{1}HNMR Spectrum of [Cr(CO)$_2$(BINAP)(bipy)] G1.

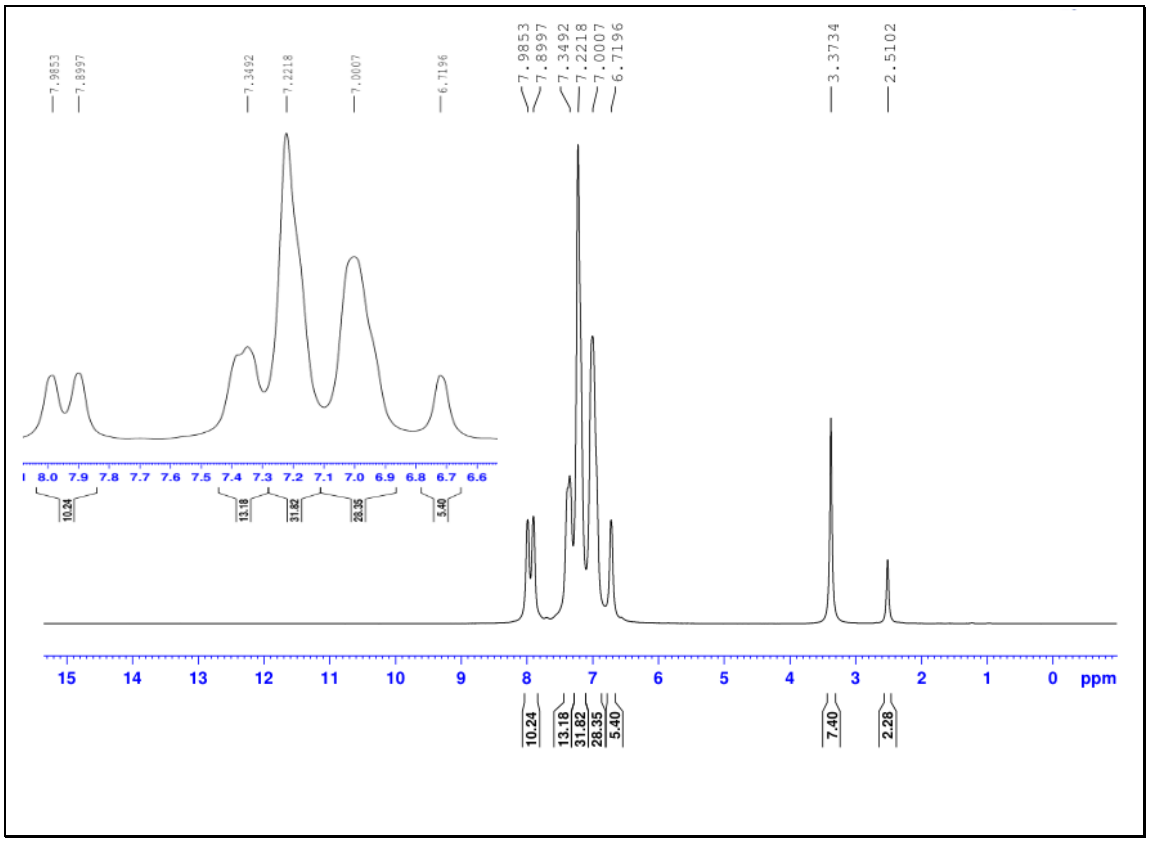

Figure 12. ^{1}HNMR Spectrum of [Cr(CO)$_2$(BINAP)(2-AP)] G3.

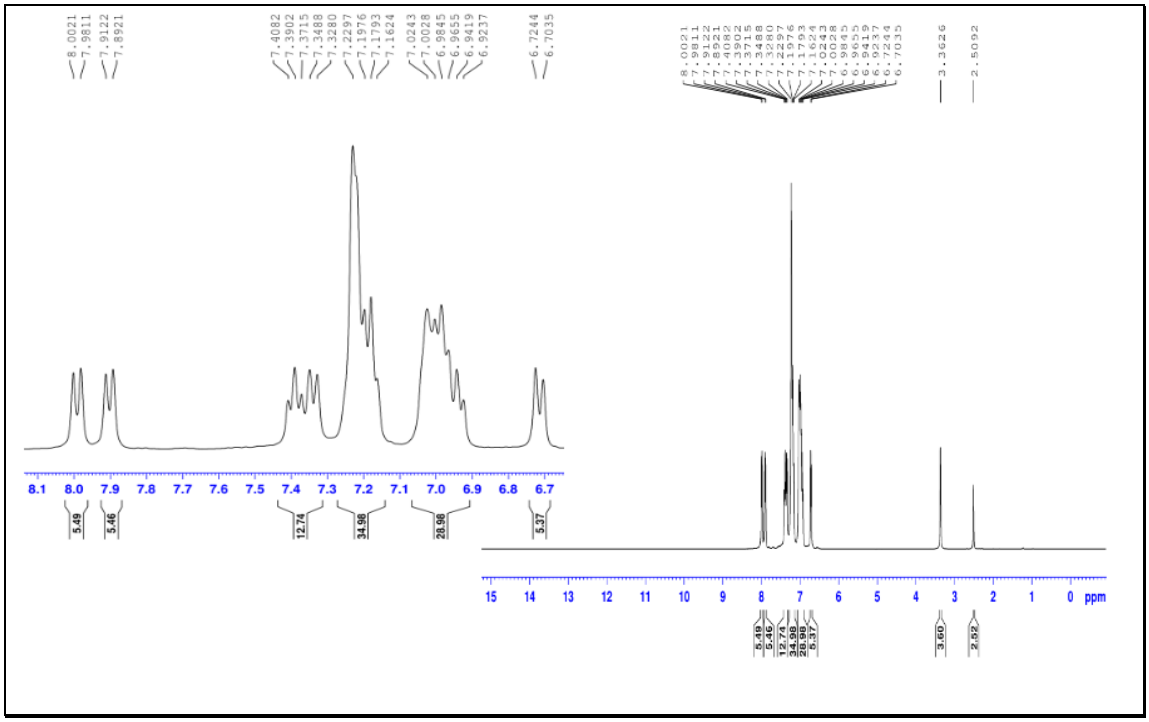

Figure 13. ^{1}HNMR Spectrum of [Cr(CO)$_2$(BINAP)(8-HQ)] G5.

Elemental analysis of the prepared complexes showed agreement between the theoretical values and the process, as shown in Table 3.

Table 3. Elemental analysis data for the chromium complexes (CHN).

Compounds	Elemental analysis					
	Calculations			Found		
	C%	H%	N%	C%	H%	N%
G1	75.85	4.51	3.16	75.61	4.68	3.42
G3	74.27	4.61	3.39	74.52	4.89	3.53
G5	75.52	4.34	1.60	75.38	4.56	1.83

Through structural estimates of DFT, the structure of G1 was studied by X-ray diffraction (figure 14), where the X-ray crystal structure calculations confirmed the constitution of the G1 complex. The coordination about the central metal atom is a distorted octahedron, as consists of a central Cr atom surrounded by six coordination centers two C(CO), two N(bipy), and two P(BINAP) piano-stool fashion bonding .

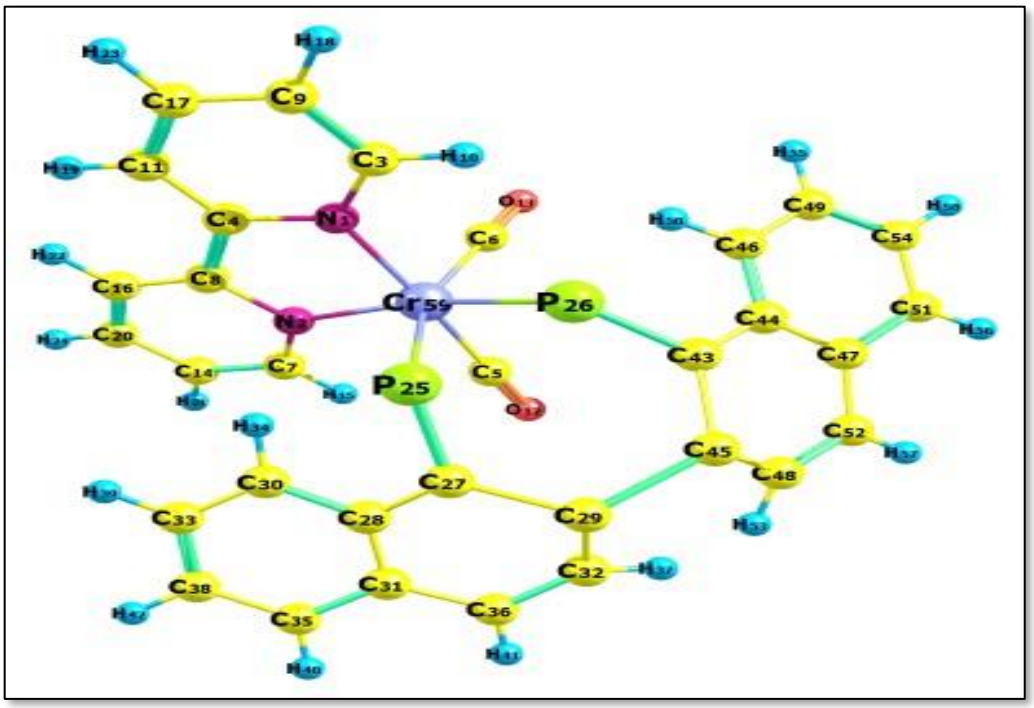

Figure 14**: Molecular structure of [Cr(CO)$_2$(BINAP)(bipy)] (G1).**

As expected, structural analysis of G1 determined the chromium center being coordinated in a strongly distorted octahedral configuration with the two nitrogen of bipyridine, two phosphors of phosphene, and two carbon of carbonyl donors chelating around the chromium center. This is best illustrated by the six angles at Chromium involving N_1-Cr-N_2, N_1-Cr-C_6, N_2-Cr-P_{25}, P_{25}-Cr-C5, C5-Cr-C6 bond angles of 48.923, 45.422, 36.824, 40.204, 48.719° and the bite angle P_{25}-Cr-P_{26}, where a large deviation from ideal octahedral geometry is observed for the N_2–Cr–P_{25} angle, for which a contraction from 90 to 36.824° occurs. The bond length values for The Cr–C_5(CO), Cr-C_6(CO), Cr–N_1(bipy), Cr–N_2(bipy), Cr-P_{25} (BINAP), and Cr-p_{26} (BINAP) are 2.058, 2.054,

2.01814, 2.03376, 2.28180, and 2.27870 Å respectively. Selected bond distances and angles are presented in Table 4 based on the computational results of the gas phase.

Table 4. Selected bond lengths and angles in [$Cr(CO)_2$ (BINAP) (bipy)].

Complex G1				Reference [83, 121-123]			
Bond	length(Å)	Fragment	Angles	Bond	length(Å)	Fragment	Angles
Cr-N_1	2.01814	N_1-Cr-N_2	48.923	Cr-N_1	2.159	N_1-Cr-N_2	75.15
Cr-N_2	2.03376	N_1-Cr-C_6	45.422	Cr-N_2	2.157	N_5-Cr-C_{28}	94.81
Cr-P_{25}	2.28180	N_2-Cr-P_{25}	36.824	M-P1	2.176	N_2-Cr-P_{25}	
Cr-p_{26}	2.27870	P_{25}-Cr-C_5	40.204	M-P2	2.172	C1-M-P	97.0
Cr-C_5	2.05809	P_{25}-Cr-P_{26}	58.368	Cr-C1	1.872	P_1-M-P_2	97.37
Cr-C_6	2.05498	C_5-Cr-C_6	48.719	Cr-C4	1.852	C_1-Cr-C_4	84.1

3.2. Molybdenum (0) Complexes.

Electronic absorption spectra of the molybdenum complexes were measured in range the of 200 to 800 nm in THF solvent. Molybdenum complexes have been diagnosed and several bands at different wavelengths have been observed. in $[Mo(CO)_2(BINAP)(bipy)]$ (G2) the absorption peaks around (227) nm can be assigned to the ($\pi \rightarrow \pi^*$) transition, the electronic spectra of the complex showed new bands in the 485 nm due to Mo(dπ)→bipy(π*) (Figure 15). The G4 $[Mo(CO)_2BINAP(2\text{-}AP)]$ shows absorption bands displayed bands at (228) nm and band observed at 476, which may be assigned to $\pi \rightarrow \pi^*$ transition and transition Mo(dπ)→2-AP(π*) in G4 absorption bands at (226 nm), can be assigned to the ($\pi \rightarrow \pi^*$) transition, and weak band in range 473 nm due to Mo(dπ)→8-HQ(π*) (Figure 17). The longer wavelength band could be attributed to metal-to-ligand (MLCT) charge transfer transitions. The transient absorption spectra of the G2, G4, and G6 may be attributed at (676 nm, 678 nm, 690 nm) for Mo(0)-to-BINAP charge transfer state (MLCT) MLCT of BINAP, as stated in a complex diagnosis $[Pt(BINAP)_2]$ [104].

Physical properties, maximum absorption wavelength (λ), and molecular weight data of molybdenum complexes are presented in (Table 5), where molecular weight data confirms the proposed formula.

Table 5. Physical properties and Maximum absorption wavelength (λ) of molybdenum complexes.

Complex	Mol. Wt g/mol	Color	m.p C°	λ max (nm)
$[Mo(CO)_2(BINAP)(bipy)]$ G2	929.86	orange	246	227
$[Mo(CO)_2(BINAP)(2\text{-}AP)]$ G4	867.87	Light brown	244	228
$[Mo(CO)_2(BINAP)(8\text{-}hq)]$ G6	917.85	black	245	226

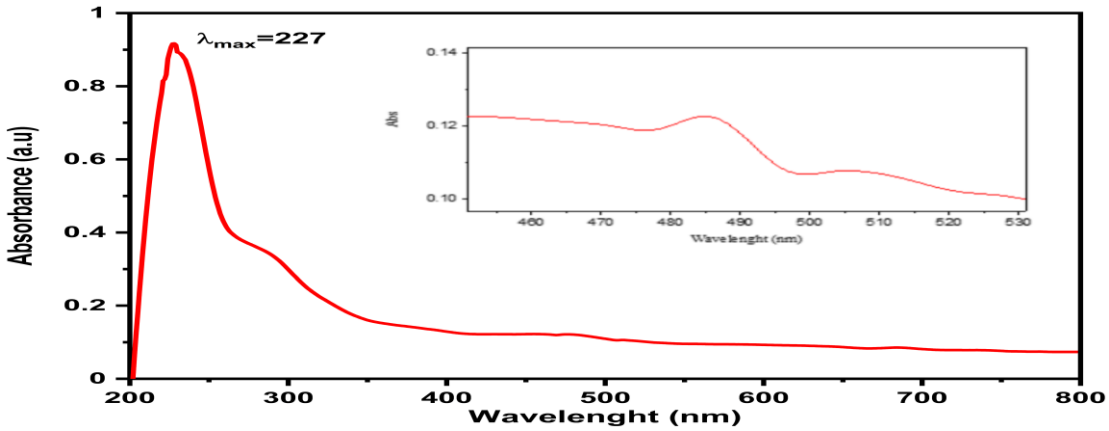

Figure 15. Electronic transitions of $[Mo(CO)_2(BINAP)(bipy)]$.

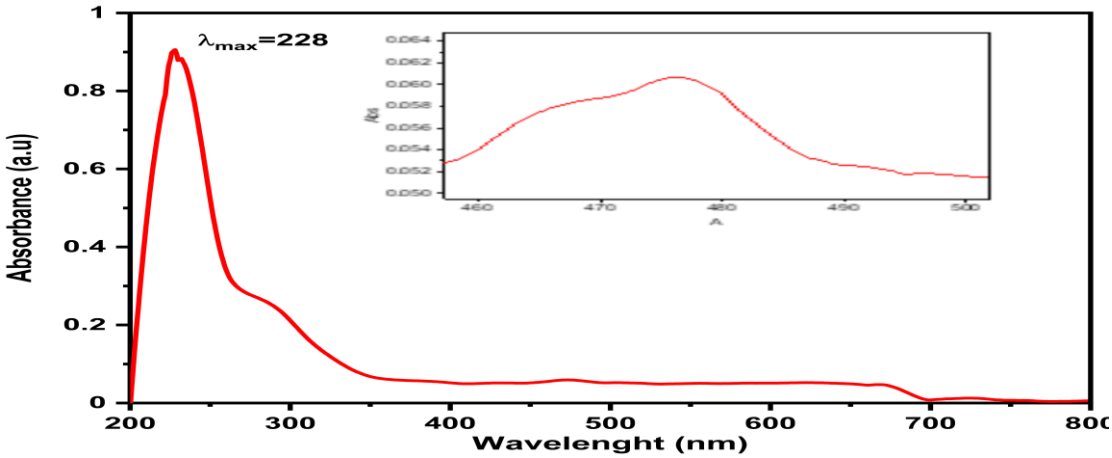

Figure 16. Electronic transitions of [Mo(CO)$_2$(BINAP)(2-AP)].

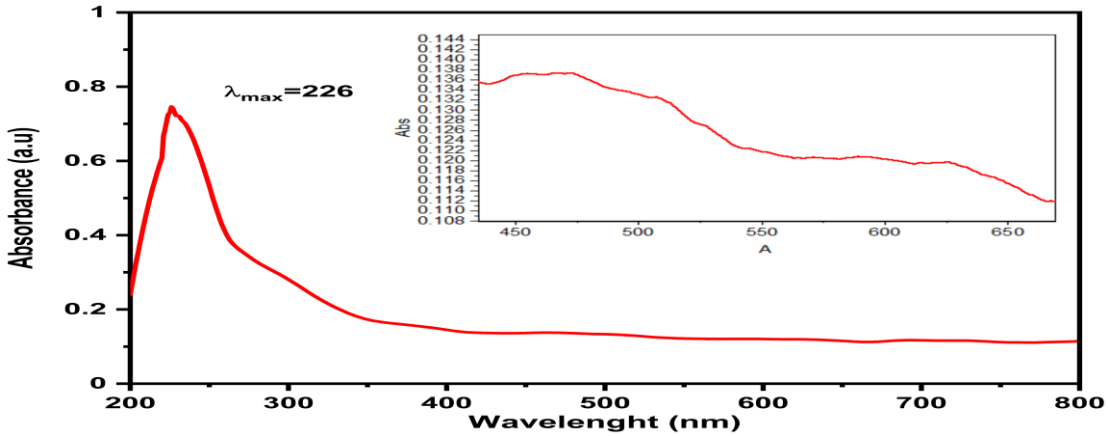

Figure 17. Electronic transitions of [Mo(CO)$_2$(BINAP)(8-HQ)].

From the data of IR spectra of the molybdenum complex [Mo(CO)$_2$(BINAP)(bipy)] (G2), it can be seen that the bands at (1893 &1828 cm^{-1}) were assigned to υ(C=O). As two M(CO)-bands are found according to a cis-configuration. The characteristic stretching band at (1584 cm^{-1}) is attributed to ν(C=N) when in coordination with the metal ion. the bands show at (1480 cm^{-1}) and (1311 cm^{-1}) were assigned to the ν(C=C) and ν(C-N) stretching mode respectively in the ligand bipy. The hetero aromatic organic compounds commonly exhibit multiple-week

bands in the region (3000–3100 cm^{-1}) due to C–H stretching vibrations. the bands have been assigned at (3049, 2999, 3012 cm^{-1}) to C–H ring stretching vibrations. The important IR absorption bands for the Molybdenum complex [$Mo(CO)_2$(BINAP)(2-AP)] (G4) It can be seen that the bands of (1893 &1904 cm^{-1}) were assigned to υ(C=O). Two M(CO)-bands are found according to a cis-configuration. The characteristic stretching bands at (1584 cm^{-1}), (1311cm^{-1}), (1480 cm^{-1}) assigned for ν(C=N), ν(C–N), ν(C=C) respectively . The bands have been assigned at (3049, 2999, 3012 cm^{-1}) to C–H ring stretching vibrations. The important IR absorption bands for the chromium complex [$Mo(CO)_2$(BINAP)(8-HQ)] (G6) It can be seen that the bands of (1892 &1914 cm^{-1}) were assigned to υ(C=O). Two M(CO)-bands are found according to a cis-configuration. The characteristic stretching bands at (1584 cm^{-1}), (1311cm^{-1}), (1479 cm^{-1}) assigned for ν(C=N), ν(C–N), ν(C=C) respectively. The bands have been assigned at (3049, 2999, 3012 cm^{-1}) to C–H ring stretching vibrations. the band is observed at (1207 cm^{-1}) due to ν(C-O) of ligand 8-HQ in G6, which indicates the coordination of the phenolic oxygen atom was also confirmed of metal complex formation by the redshift range (1207–1231 cm^{-1}). the band related to Mo-N vibrations showed at 470 cm^{-1} due to the Mo-N bond [124]. In the low-frequency region, the peaks at 550–590 cm^{-1} due to

Mo–O asymmetric vibrations are present [125]. FTIR spectra have that are shown in Table 6.

Table 6. Characteristic FT-IR bands of Molybdenum Complexes.

Complex	Assignments	Experimental(cm^{-1})	Calculation(cm^{-1})
$[Mo(CO)_2(BINAP)(bipy)]$ G2	ν(CO)	1893 & 1875cm^{-1}	1777& 1750cm^{-1}
	νC=N	1584cm^{-1}	1588cm^{-1}
	νC=C	1480cm^{-1}	1471cm^{-1}
	νC-N	1311cm^{-1}	1308cm^{-1}
	νC-H	3068,2999cm^{-1}	3280cm^{-1}
$[Mo(CO)_2(BINAP)(2\text{-}AP)]$ G4	ν(CO)	1893 & 1904cm^{-1}	1872&1718cm^{-1}
	νC=N	1584cm^{-1}	1616cm^{-1}
	νC=C	1480cm^{-1}	1482cm^{-1}
	νC-N	1311cm^{-1}	1319cm^{-1}
	νC-H	3049& 2998cm^{-1}	3131& 2752 cm^{-1}
$[Mo(CO)_2(BINAP)(8\text{-}HQ)]$ G6	ν(CO)	1892&1914 cm^{-1}	
	νC=N	1584cm^{-1}	
	νC=C	1479cm^{-1}	
	νC-N	1311cm^{-1}	
	νC-O	1207cm^{-1}	
	νC-H	3049, 2998cm^{-1}	

The EI-MS of the complex $[Mo(CO)_2(BINAP)(bipy)]$ showed the parent ion peak $[M]^+$ at m/z =929.09 (21.69%) which is in agreement with the molecular formula of $[Mo(CO)_2(BINAP)(bipy)]^+$. The spectrum of EI-MS also showed an ion peak at m/z= 735.08 (59.00%) which is in agreement with the molecular formula of $[Mo\text{-}C_{44}H_{34}P_2N]^+$. And the fragments observed at m/z= 405.49 (68.10 %). The base peak fragment observed at m/z= 130.78 (100%) (Figure 18).

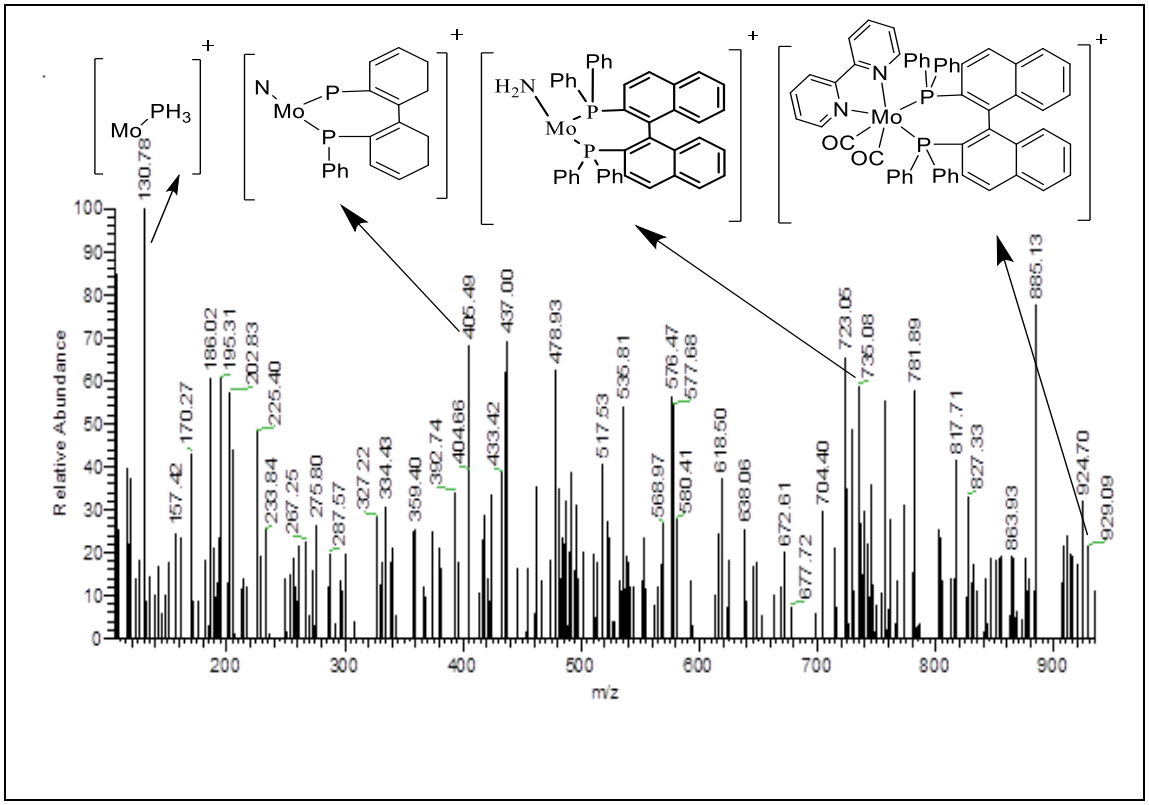

Figure18. Mass spectrum and fragments of $[Mo(CO)_2(BINAP)(bipy)]$.

The EI-MS of complex $[Mo(CO)_2(BINAP)(2\text{-}AP)]$ showed the parent ion peak $[M]^+$ at m/z= 867.59 (34.17%) which is in agreement with the molecular formula of $[Mo(CO)_2(BINAP)(2\text{-}AP)]^+$. The spectrum of EI-MS also showed an ion peak at m/z= 816.63 (97.53%) which is in agreement with the molecular formula of $[Mo\text{-}C_{49}H_{39}N_2P_2]^+$. And the fragments observed at m/z= 310.84 (100%) this is the base peak. The proposed fragmentation pattern of this complex is given in (Figure 19).

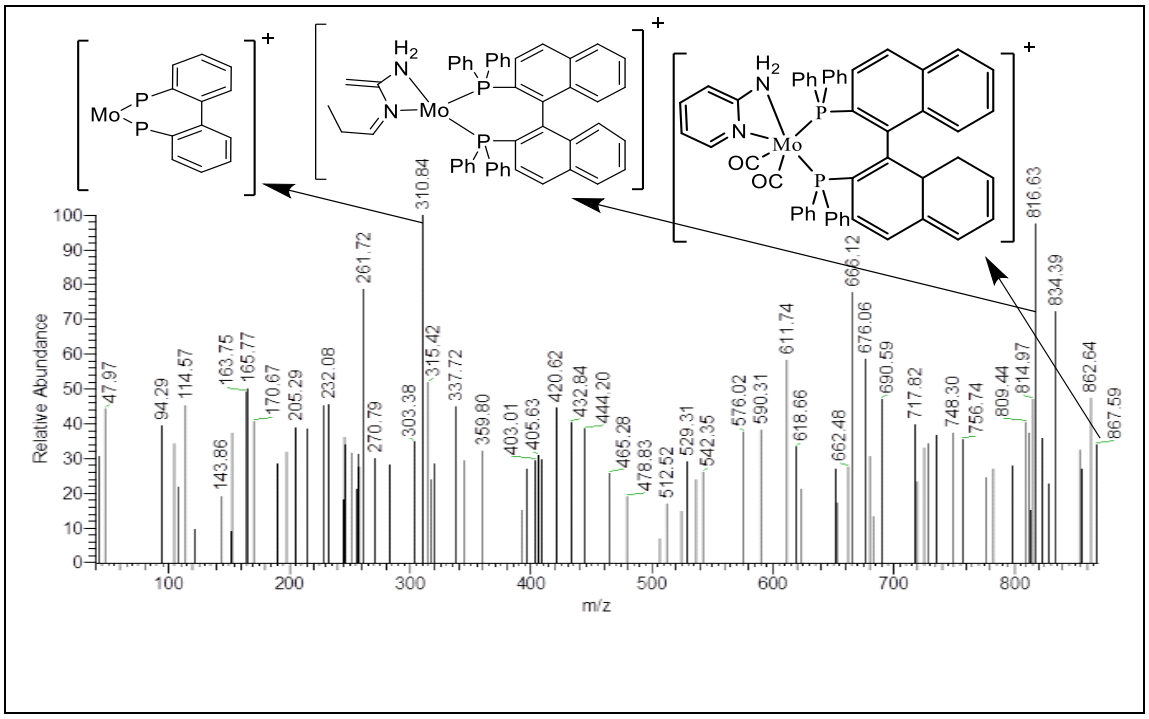

Figure19. Mass spectrum and fragments of [Mo(CO)$_2$(BINAP)(2-AP)].

The EI-MS of complex [Mo(CO)$_2$(BINAP)(8-HQ)] showed the parent ion peak $[M]^+$ at m/z= 917.12 (12.20%) which is in agreement with the molecular formula of $[Mo(CO)_2(BINAP)(8\text{-}HQ)]^+$. The spectrum of EI-MS also showed an ion peak at m/z = 814.14 (55.37%) which is a characteristic of the loss of a CO and phenyl group moiety $[Mo\text{-}C_{30}H_{34}O_2P_2]^+$, also the fragments observed at m/z =574.93 (81.10%). The base peak fragment observed at m/z =226.33 (100%). The proposed fragmentation pattern of this complex is given in (Figure 20).

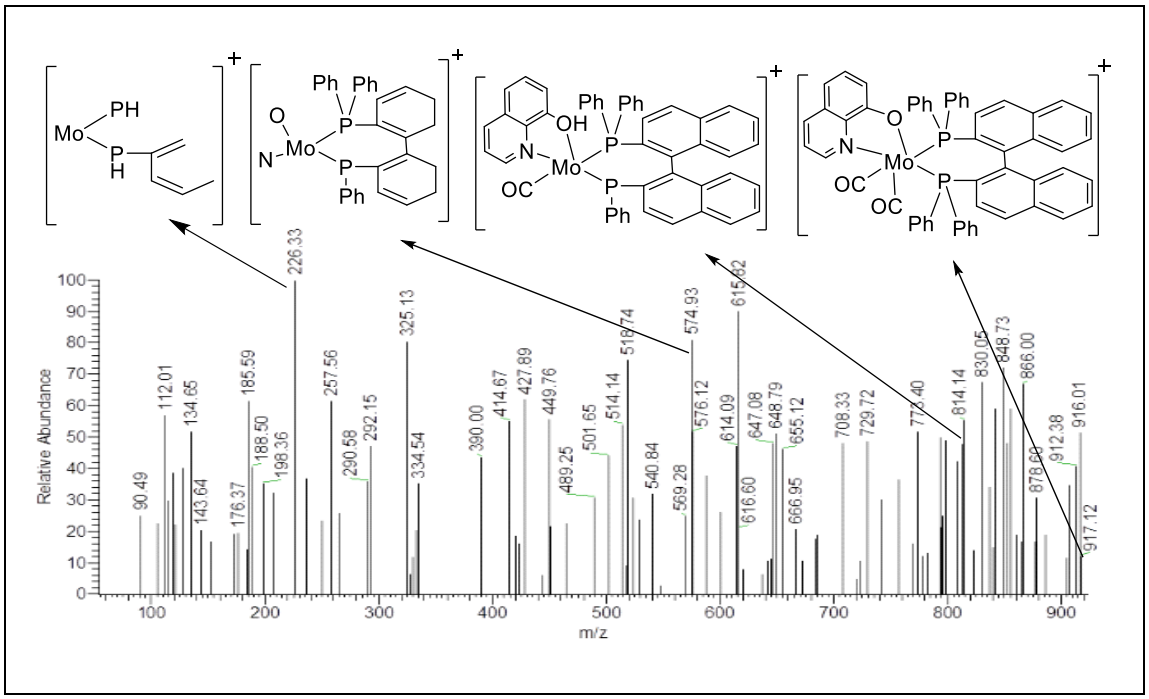

Figure 20. Mass spectrum and fragments of [Mo(CO)$_2$(BINAP)(8-HQ)].

The ^{1}HNMR spectra of Mo(0) complexes were recorded in DMSO-d^6 (DMSO, 400 MHz, 25 C°) as solvent shows signals at (2.50 ppm) [115]. The ^{1}HNMR spectrum of G2 (Figure 21) shows signals bands multiplied at (δ 6.69-7.44) ppm belong to the aromatic rings protons of BINAP (32H.CH) and signals bands at (δ 7.92-8.03) (4H, CH) belong to protons of the bipy rings. (Figure 22) displays the ^{1}HNMR spectra of the G4, the broad multiple observed in the range (δ 6.69-7.42) ppm due to aromatic protons of BINAP (32H, CH) and (δ 7.90-8.01) assigned to pyridyl ring protons (4H, CH). in the spectrum of G6 (Figure 23) the multiple signals in the region (δ 6.69-7.58) ppm assigned to aromatic protons for ligand BINAP (32H, CH) and signals bands at (δ 7.68-8.85) belong to 8-HQ

rings (6H, CH). The appearance of a peak at 9.8 ppm is due to the presence of OH in G6 [126]. We also notice the disappearance of peak proton (H-NH_2) in G4 due to complex formation. the differences in the chemical shift of pyridine H atoms indicate that the N atom of pyridine coordinates with the metal ion [127]. Has also been explained ^{1}HNMR for complexes 2-aminopyridine in [128]. Also, the signal observed at 3.17 and 3.30 ppm could be assigned to the THF which was used to recrystallize the complexes.

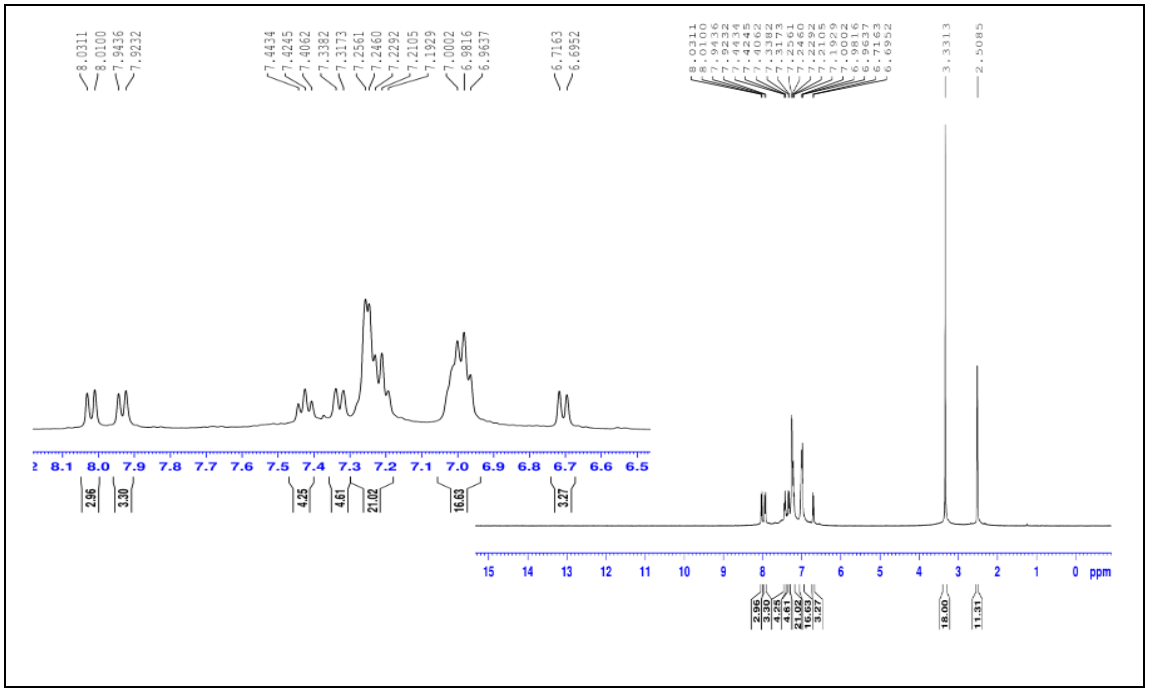

Figure 21. ^{1}HNMR Spectrum of [Mo(CO)$_2$(BINAP)(bipy)] G2.

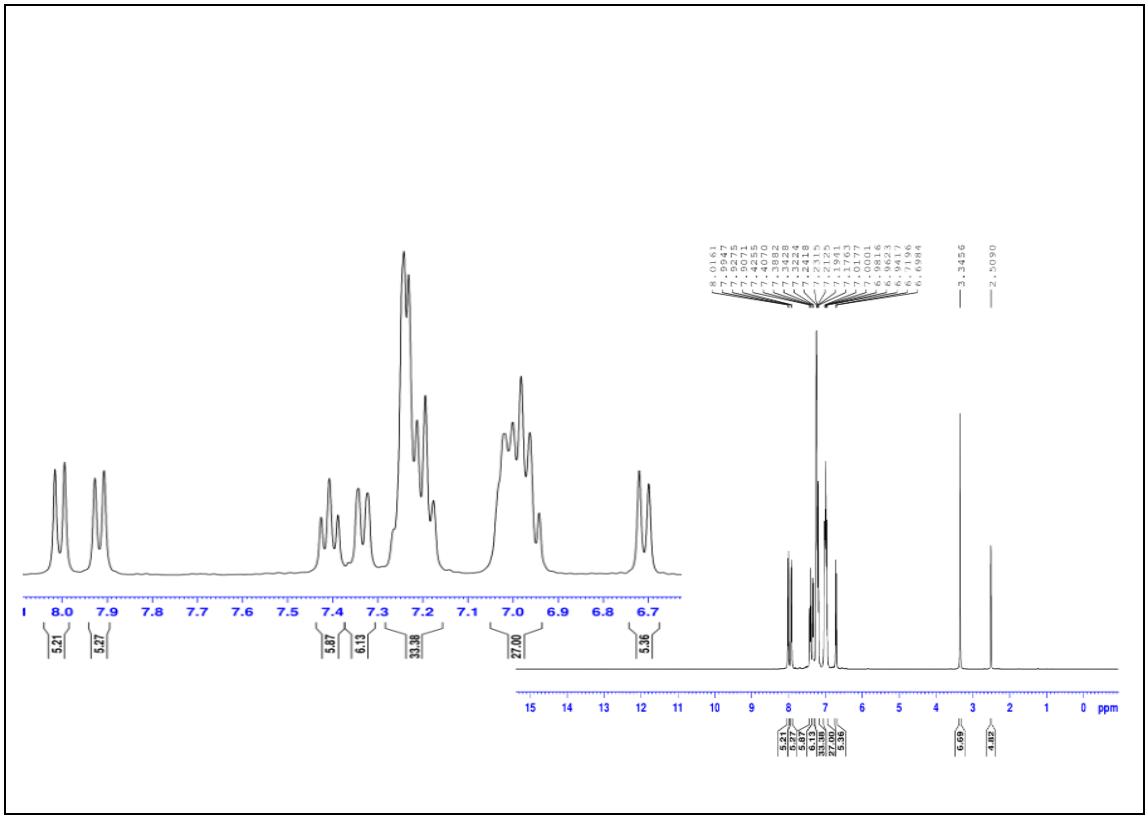

Figure 22. ^{1}HNMR Spectrum of [Mo(CO)$_2$(BINAP)(2-AP)] G4.

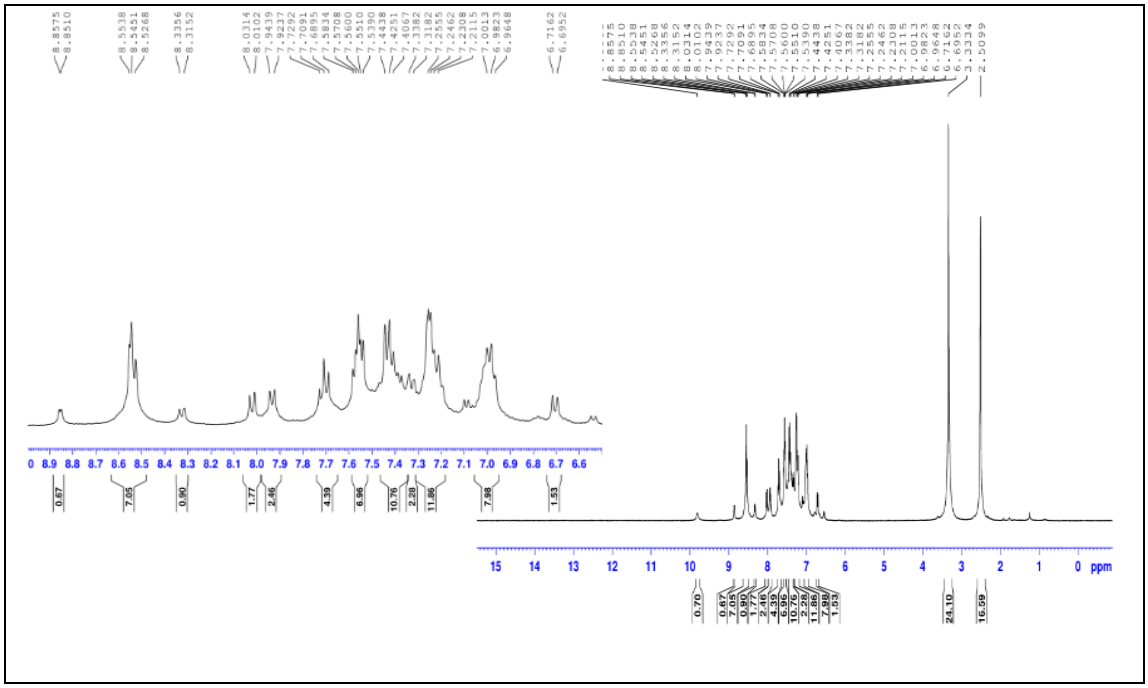

Figure 23. ^{1}HNMR Spectrum of [Mo(CO)$_2$(BINAP)(8-HQ)] G6.

Elemental analysis of the prepared complexes showed agreement between the theoretical values and the process, as shown in Table 7.

Table 7. Elemental analysis data for the molybdenum complexes (CHN).

compounds	Elemental analysis					
	Calculations			Found		
	C%	H%	N%	C%	H%	N%
G2	72.19	4.30	3.01	72.45	4.42	3.29
G4	70.5	4.37	3.22	70.73	4.54	3.46
G6	71.90	4.24	1.52	71.79	4.51	1.74

Through structural estimates of DFT, the structure of G2 was studied by X-ray diffraction (figure 24), where the X-ray crystal structure calculations confirmed the constitution of the G2 complex. The coordination about the central metal atom is a distorted octahedron, as consists of a central Mo atom surrounded by six coordination centers two C(CO), two N(bipy), and two P(BINAP) piano-stool fashion bonding.

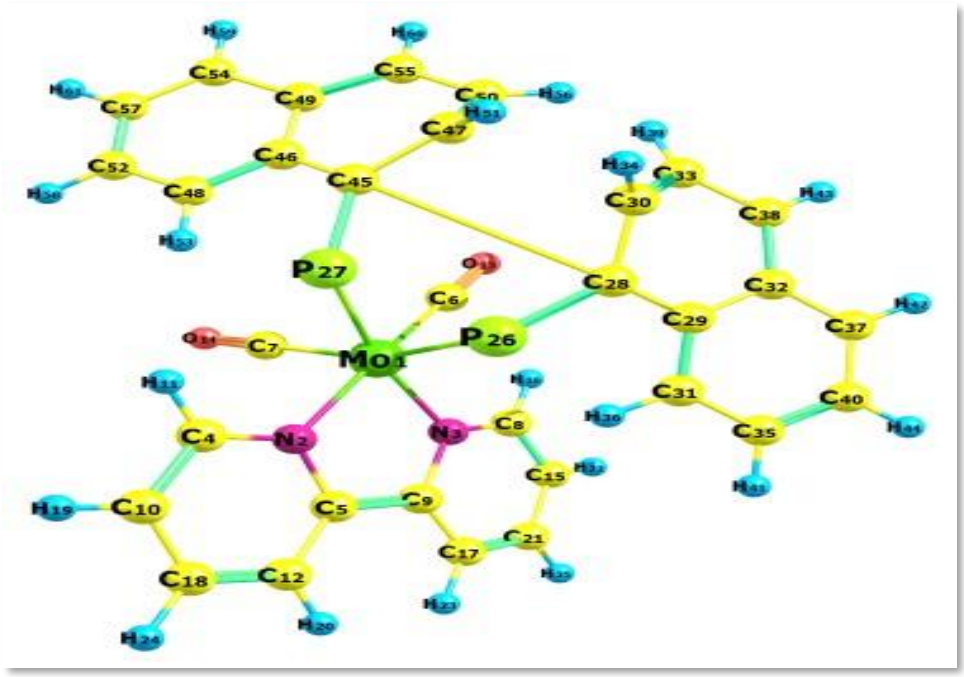

Figure 24: Molecular structure of [Mo(CO)$_2$(BINAP)(bipy)] (G2).

As expected, structural analysis of G2 determined the molybdenum center being coordinated in a strongly distorted octahedral configuration with the two nitrogen of bipyridine, two phosphors of phosphene and two carbon of carbonyl donors chelate around the molybdenum center. This is best illustrated by the Six angles at molybdenum involving N_2-Mo-N_3, N_2-Mo-C_7, N_3-Mo-P_{26}, P_{26}-Mo-C_6, C_6-Mo-C_7 bond angles of 48.421, 45.422, 42.258, 40.204, 48.719° and the bite angle P_{26}-Mo-P_{27}, where a large deviation from ideal octahedral geometry is observed for the P_{26}–Mo–C_6 angle, for which a contraction from 90 to 40.204° occurs. The Mo–C_6 and Mo-C_7 bond lengths of the cis-coordinated carbonyls (2.05809 and 2.05489 A˚) are similar to those found in related compounds [76]. The bond length values for Mo–N_2(bipy), Mo–

N_3(bipy), Mo-P_{26} (BINAP), and Mo-p_{27} (BINAP) are 2.01814,2.03376 ,2.28180 and 2.27870 Å respectively. Selected bond distances and angles are presented in Table 8 based on the computational results of the gas phase.

Table 8. Selected bond lengths and angles in [$Mo(CO)_2$(BINAP) (bipy)].

Complex G2				References. [18, 76, 121, 123]			
Bond	length(Å)	Fragment	Angles	Bond	length(Å)	Fragment	Angles
Mo-N_2	2.01814	N_2-Mo-N_3	48.421	Mo-N	2.279	N_2-Mo-N_3	
Mo-N_3	2.03376	N_2-Mo-C_7	45.422			N_5-Mo-C_{28}	86.27
Mo-P_{26}	2.28180	N_3-Mo-P_{26}	42.258	M-P1	2.176	N-Mo-P	77.78
Mo-p_{27}	2.27870	P_{26}-Mo-C_6	40.204	M-P2	2.172	C1-M-P	97.0
Mo-C_6	2.05809	P_{26}-Mo-P_{27}	58.368	Mo-C_1	2.056	P_1-M-P_2	97.37
Mo-C_7	2.05498	C_6-Mo-C_7	48.719	Mo-C_4	2.023	C1–Mo–C4	166.7

3.3. Anticancer Activity.

3.3.1 In vitro results.

Cytotoxicity of chromium and molybdenum complexes on cancer cell line (MCF-7):

The effect of chromium-molybdenum complexes with BINAP ligand in inhibition of on human breast cancer cell line was studied where these complexes showed a clear effect in inhibiting the growth of the cancer line cell line (MCF-7) outside the body of the organism (in vitro). The results shown in data presented in table (9) and Figure (25) illustrate the effect of four different concentrations Chromium-Molybdenum complexes (G1-G6) (62.5, 125, 250, 500 μM) on surviving fraction of MCF-7 cell line following 48 hours of treatment. complexes(G1-G6) produced a decrease in cell viability of the cell line compared to the non-treated control. The IC_{50} of complexes (G1-G6) on MCF-7 was (138 μM-397 μM).

Table 9. Effect of different concentrations of chromium-molybdenum complexes with BINAP ligand on surviving fraction of MCF-7 cell line following 48 hours of treatment and IC_{50}.

Concentration µm/ml	Surviving fraction MCF-7					
	G1	G2	G3	G4	G5	G6
62.500	0.614	0.952	0.904	0.952	0.919	0.946
125.000	0.506	0.747	0.819	0.870	0.760	0.747
250.000	0.470	0.446	0.639	0.519	0.627	0.518
500.000	0.313	0.398	0.407	0.363	0.387	0.458
IC_{50}	138	226	397	278	380	292

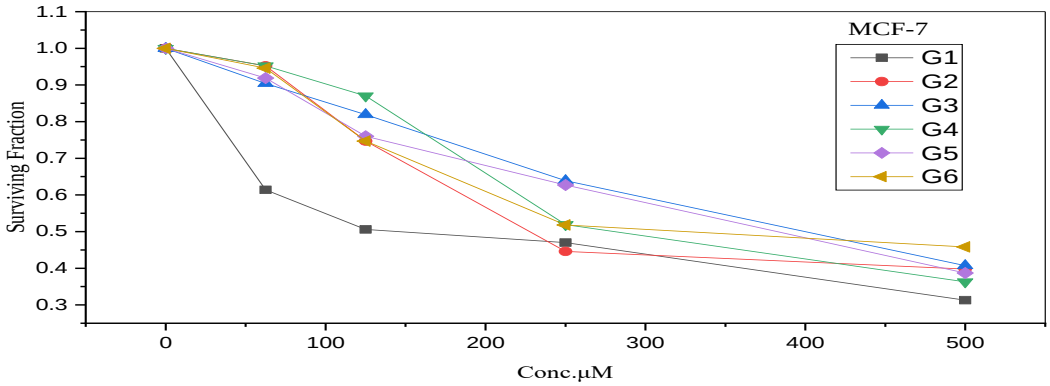

Figure 25. Surviving fraction and IC_{50} of MCF-7 cells treated with chromium-molybdenum with BINAP ligand for 48 hours.

3.3.2. Molecular docking studies.

As a result of molecular docking, data such as the binding site map of the topo MCF-7 protein and chromium-molybdenum complexes binding parameters were calculated. the association strength of protein and chromium-molybdenum complexes is determined based on minimum binding energy and scoring function. To determine target protein specificity on a structural basis, we utilized the active site target binding approach to analyze structural complexes of (PDB ID: 1ZXM) with selected compounds. Finally, these ligands were docked with the potential active site of target molecules, and binding energies were calculated. Briefly, atomic affinity potentials were utilized at each step of the simulation to measure the interaction energy of chromium-molybdenum complexes and protein (PDB ID: 1ZXM). The lowest binding energy cluster reflected the representative binding state in docking results, as in (Table 10) and shown in (Figure 26). The lowest binding energies indicated that target proteins were docked successfully with complexes.

Table 10. Energy values were obtained during docking analysis of compounds as ligand molecules against 1ZXM as target molecules.

Complexes	G1	G2	G3	G4	G5	G6
Rseq	1	1	1	1	1	1
Mseq	1	2	3	4	5	6
S	-4.3098	-5.1858	-5.8951	-4.7787	-5.6447	-6.2247
Rmsd	5.3969	3.4101	5.5349	2.2642	1.9776	5.6016
E-conf	-89.4362	322.1966	135.0602	7.9848	-30.2943	-14.4318
E-place	133.8959	106.4253	94.9034	111.8989	19.7802	76.8224
E-refine	-17.6773	-24.4333	-27.3081	4.5103	-29.7586	-32.2
E-score 2	-4.3098	-5.1858	-5.8951	-4.7787	-5.6447	-6.2247

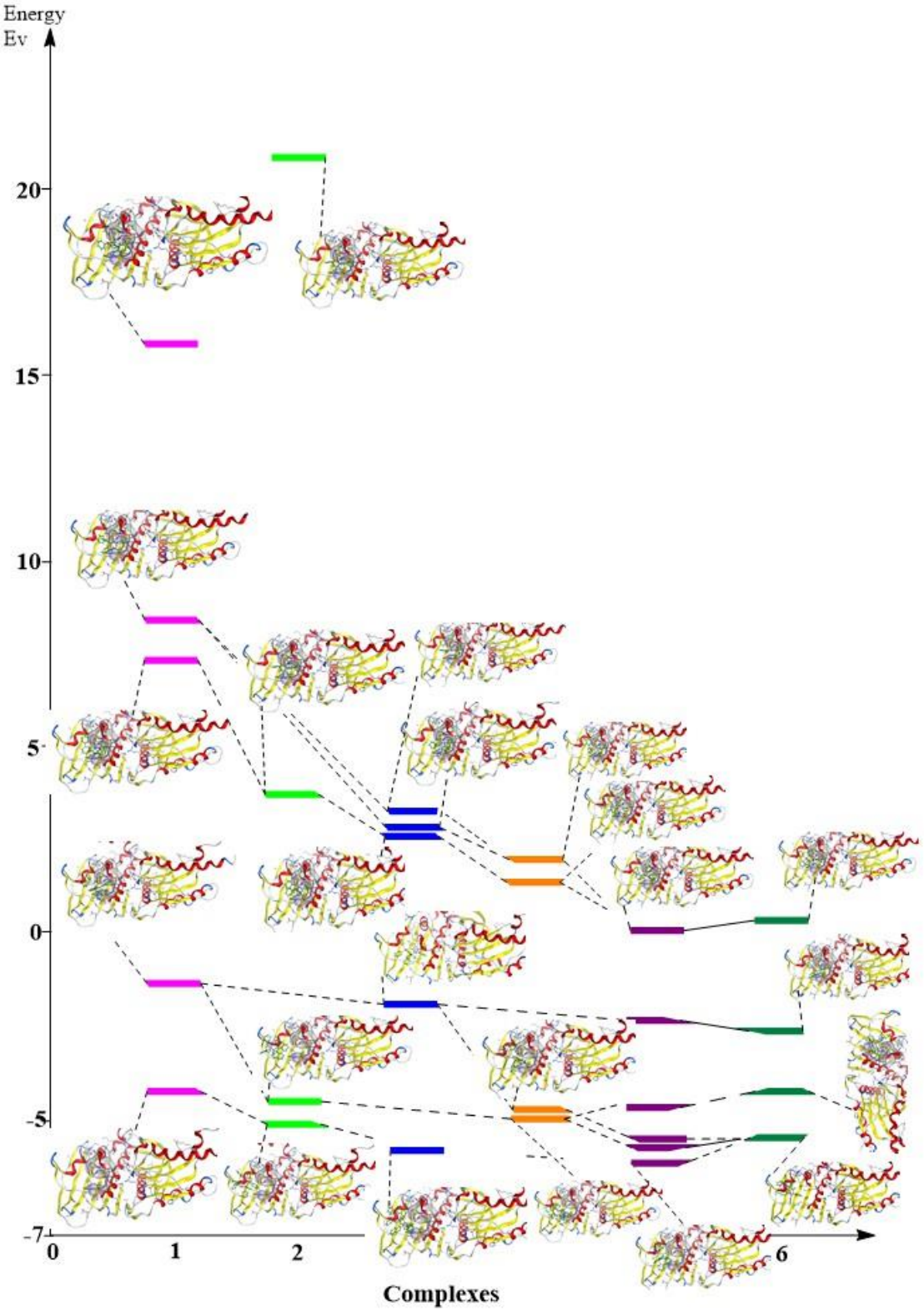

Figure 26. Energy conformation of docked complexes G1 to G6.

Binding pockets are shown as surface.

The most common way to evaluate the correctness of the docking geometry is to measure the Root Mean Square Deviation (RMSD) of the chromium-molybdenum complexes and protein of (PDB ID: 1ZXM) from its reference position in the answer complexes G1 to G6 after the optimal superimposition of the receptor molecules, as shown (figure 27).

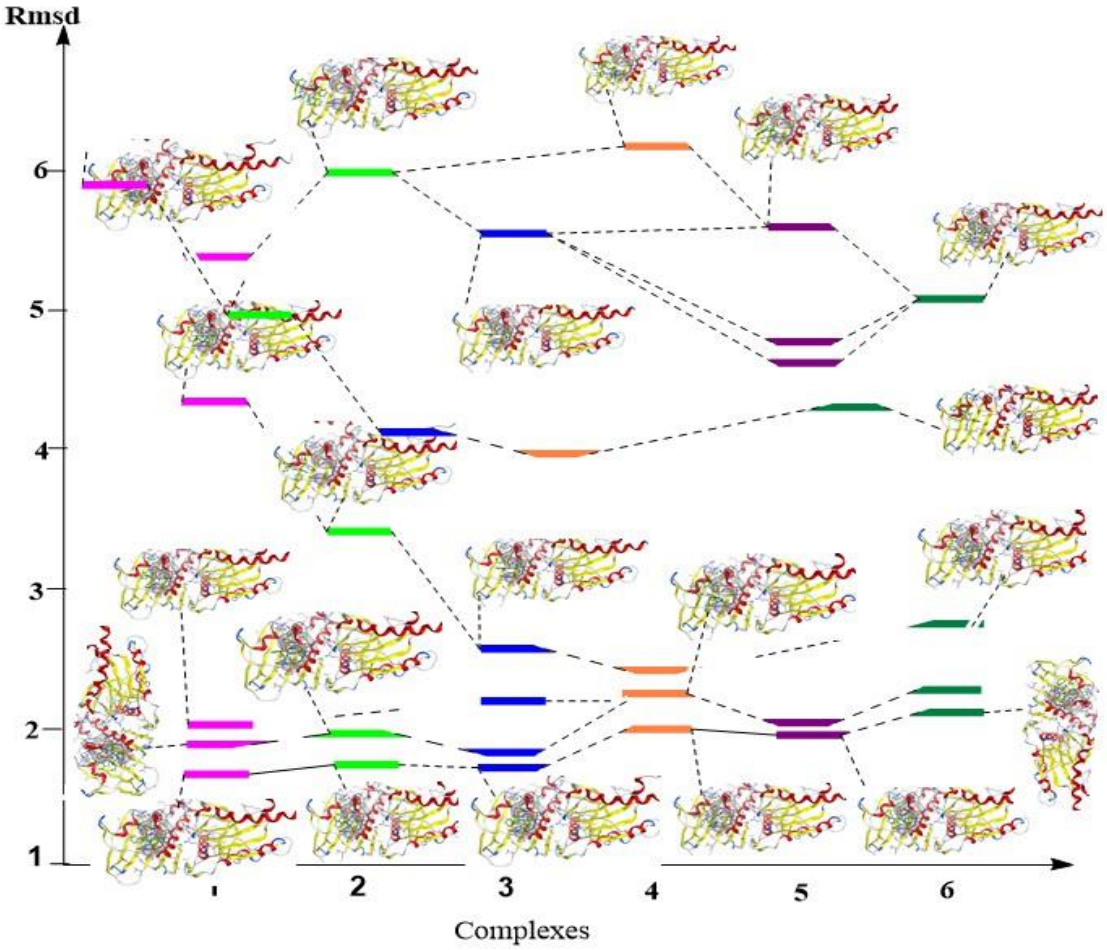

Figure 27. The Root Mean Square Deviation (RMSD) conformation of docked complexes G1 to G6 Binding pockets are shown as surface.

4.0 Conclusion.

In conclusion, six novel complexes for Cr(0) carbonyl and Mo(0) carbonyl were synthesized of four bidentate ligands (BINAP, bipy, 2-AP, 8-HQ) using microwave technology. Various spectroscopic methods were used to suggest the chemical structures of the novel complexes (G1-G6).

It was suggested the six coordination centers of Cr and Mo with two C(CO), two P(BINAP), N, N' (bipy) or N, N' (2-AP) or N, O (8-HQ). UV–vis spectral data, Mass, and CHN values suggest the octahedral structure of all complexes. The distorted octahedral geometry of the novel compounds has been validated and optimized by DFT analysis. FT-IR spectral data revealed that all chromium-molybdenum complexes are in cis-configuration. The in vitro cytotoxicity results of the prepared chromium and molybdenum complexes showed a different inhibitory effect of the complexes when treated with four different concentrations against breast cancer type (MCF-7). IC_{50} values were calculated for the compounds tested on the MCF-7 cell line ranging from (138 to 397μM). The complex G1 (IC_{50}= 138) was the most effective among the prepared complexes. Molecular docking studies were conducted to comprehend the appropriate binding modes of the Cr-Mo complexes evaluated for DNA topo II (PDB ID: 1ZXM) inhibitory activity. The association strength of protein and chromium-molybdenum complexes is determined based on

minimum binding energy and scoring function. Values Energy of docked complexes G1 to G6 are (-4.3098) to (-6.2247) and RMSD values of docked complexes G1 to G6 are (1.9776 - 5.6016). The lowest binding energies indicated that target proteins were docked successfully with complexes.

5.0 References.

[1] L. Mond, C. Langer, and F. J. J. o. t. C. S. Quincke, Transactions, "L.—Action of carbon monoxide on nickel," *Journal of the Chemical Society, Transactions,* vol. 57, pp. 749-753, 1890.

[2] J. Bohnenberger, W. Feuerstein, D. Himmel, M. Daub, F. Breher , and I. J. N. c. Krossing, "Stable salts of the hexacarbonyl chromium (I) cation and its pentacarbonyl-nitrosyl chromium (I) analogue," *nature.com,* vol. 10, no. 1, p. 624, 2019.

[3] B. Gupta, *Basic Organometallic Chemistry: Concepts, Syntheses and Applications*. Universities Press, 2011.

[4] R. H. Crabtree, *The organometallic chemistry of the transition metals*. John Wiley & Sons, 2009.

[5] V. D. Bhatt, "Selected Topics in Co-ordination Chemistry," 2014.

[6] C. W. Bielawski, "Organometallics. Third, Completely Revised and Extended Edition By Christoph Elschenbroich (Philipps-Universität Marburg). Wiley. 2006.," ed: ACS Publications, 2006.

[7] O. Casagrande Jr, K. Tomita, A. Mauro, and D. J. P. Vollet, "Small angle X-ray scattering and IR spectroscopy study of metal carbonyl complexes immobilized on a silica gel surface chemically modified with piperazine," *Polyhedron,* vol. 15, no. 23, pp. 4179-4183, 1996.

[8] P. Datta and C. J. P. Sinha, "Group 6 tetracarbonyl complexes of N-[(2-pyridyl) methyliden]-α (or β-(aminonaphthalene: Spectral characterization, electrochemistry, solvatochromism and photophysical studies," *Polyhedron,* vol. 26, no. 12, pp. 2433-2439, 2007.

[9] P. Datta, D. Sardar, A. P. Mukhopadhyay, E. López-Torres, C. J. Pastor, and C. J. J. o. O. C .Sinha, "Group-6 metal carbonyl complexes of pyridylbenzoxazole and pyridylbenzothiazole:

Synthesis, structure, electrochemistry, photophysical property and DFT calculations," *Organometallic Chemistry*, vol. 696, no. 2, pp. 488-495, 2011.

[10] W. Hieber" ,Metal Carbonyls, Forty Years of Research11Translated from the German by M. McGlinchey, University of Bristol, Bristol, England," in *Advances in Organometallic Chemistry*, vol. 8, F. G. A. Stone and R. West, Eds.: Academic Press, 1970, pp. 1-28.

[11] R. H .Crabtree, The organometallic chemistry of the transition metals, Sixth edition ed. Hoboken, New Jersey: Wiley, 2014. [Online]. Available.

[12] P. Anastas and N. J. C. S. R. Eghbali, "Green chemistry: principles and practice," *Chemical Society Reviews*, vol. 39, no. 1, pp. 301-312, 2010.

[13] H. H. Abbas, "Preparation of significant complexes of selected transition elements with appropriate ligands," *osti.gov*, 2000.

[14] J. G. J. J. R. i. I. C. Raj, "Metal-organophosphine complexes: structure, bonding, and applications," *Reviews in Inorganic Chemistry*, vol. 35, no. 1, pp. 25-56, 2015.

[15] M. E. García, D. García-Vivó, A. Ramos, and M. A. Ruiz, "Phosphinidene-bridged binuclear complexes," *Coordination Chemistry Reviews*, vol. 330, pp. 1-36, 2017.

[16] H. Dossmann, D. Gatineau, H. Clavier, A. Memboeuf, D. Lesage, and Y. J. T. J. o. P. C. A. Gimbert, "Exploring phosphine electronic effects on molybdenum complexes: a combined photoelectron spectroscopy and energy decomposition analysis study," *Physical Chemistry A*, vol. 124, no. 42, pp. 8753-8765, 2020.

[17] R. H. Crabtree, *The organometallic chemistry of the transition metals*, 4th ed ed. Hoboken, N.J.: Wiley-Interscience, 2005.

[18] G. Sánchez, J. L. Serrano, C. M. López, J. n. García, J. Pérez, and G. J. I .C. A. López, "Synthesis of Group 6 metal carbonyl complexes with iminophosphine ligands: crystal structure of [Mo (CO) 4 (o-Ph2PC6H4–CH ・ NMe)]," *Inorganica Chimica Acta.*, vol. 306, no. 2, pp. 168-173, 2000.

[19] F. A. J. P. P. T. S. Cotton, Structural Aspects, and S. Applications, "A. Tridentate Phosphines," *Progress in Inorganic Chemistry*, p. 216, 1992.

[20] M.-N. Birkholz, Z. Freixa, and P. W. J. C. S. R. van Leeuwen, "Bite angle effects of diphosphines in C–C and C–X bond forming cross coupling reactions," *Chemical Society Reviews*, vol. 38, no. 4, pp. 1099-1118, 2009.

[21] J.-P. Genet, T. Ayad, and V. J. C. R. Ratovelomanana-Vidal, "Electron-deficient diphosphines: the impact of DIFLUORPHOS in asymmetric catalysis," *Chem. Rev*, vol. 114, no. 5, pp. 2880-4282, 2014.

[22] S. Jeulin, S. D. de Paule, V. Ratovelomanana-Vidal, J.-P. Genêt, N. Champion, and P. Dellis, "Chiral biphenyl diphosphines for asymmetric catalysis: Stereoelectronic design and industrial perspectives," *J. PNAS*, vol. 101, no. 16, pp. 5804-9957, 2004.

[23] T.-L. Terry and A. S. J. C. c. r. Chan, "Biheteroaromatic diphosphines and their transition metal complexes: synthesis, characterisation and applications in asymmetric catalysis," *Coordination Chemistry Reviews*, vol. 248, no. 21-24, pp. 2151-2164, 2004.

[24] V. Gallo, P. Mastrorilli, C. F. Nobile, P. Braunstein, and U. J. D. T. Englert, "Chelating versus bridging bonding modes of N-substituted bis (diphenylphosphanyl) amine ligands in Pt complexes and Co 2 Pt clusters," *Dalton Transactions.*, no. 19, pp. 2342-2349, 2006.

[25] S. Ghosh, G. Hogarth, N. Hollingsworth, K. B. Holt, I. Richards, M. G. Richmond, B. E. Sanchez, and D. J. D. T. Unwin, "Models of the iron-only hydrogenase: a comparison of chelate and bridge isomers of Fe 2 (CO) 4 {Ph 2 PN (R) PPh 2}(μ-pdt) as proton-reduction catalysts," *Dalton Transactions.,* vol. 42, no. 19, pp. 6775-6792, 2013.

[26] N. Begum, U. K. Das, M. Hassan, G. Hogarth, S. E. Kabir, E. Nordlander, M. A. Rahman, and D. A. J. O. Tocher, "Chelate and Bridge Diphosphine Isomerization: Triosmium and Triruthenium Clusters Containing 1, 1 '-Bis (diphenylphosphino) ferrocene (dppf)," *Organometallics,* vol. 26, no. 25, pp. 6462-6472, 2007.

[27] K. Yang, S. G. Bott, and M. G. J. O. Richmond, "Reversible Chelate-to-Bridge Ligand Exchange in Co2 (CO) 4 (. mu.-PhC. tplbond. CPh)(bma) and Alkyne-Diphosphine Ligand Coupling. Synthesis, Reactivity, and Molecular Structures of Co2 (CO) 4 (. mu.-PhC. tplbond. CPh)(bma), Co2 (CO) 4 (. mu.-PhC. tplbond. CPh){(Z)-Ph2PCH: CHPPh ,{2and Co2 (CO) 4 {. eta. 2,. eta. 2,. eta. 1,. eta. 1-(Z)-Ph2PC (Ph):(Ph) CC: C (PPh2) C (O) OC (O)}," *Organometallics,* vol. 13, no. 10, pp. 3788-3799, 1994.

[28] J. C. Jeffrey and T. B. J. I. C. Rauchfuss, "Metal complexes of hemilabile ligands. Reactivity and structure of dichlorobis (o-(diphenylphosphino) anisole) ruthenium (II)," *Inorganic Chemistry* vol. 18, no. 10, pp. 2658-2666, 1979.

[29] P. Braunstein and F. J. A. C. I. E. Naud, "Hemilability of hybrid ligands and the coordination chemistry of oxazoline-based systems," *Angewandte Chemie International Edition,* vol. 40, no. 4, pp. 680-699, 2001.

[30] Z. Weng, S. Teo, and T. A. J. A. o. c. r. Hor, "Metal unsaturation and ligand hemilability in Suzuki coupling," *Accounts of chemical research,* vol. 4 ,0no. 8, pp. 676-684, 2007.

[31] A. Bader and E. J. C. c. r. Lindner, "Coordination chemistry and catalysis with hemilabile oxygen-phosphorus ligands," *Coordination Chemistry Reviews,* vol. 108, no. 1, pp. 27-110, 1991.

[32] R. Lindner, B. van den Bosch ,M. Lutz, J. N. Reek, and J. I. J. O. van der Vlugt, "Tunable hemilabile ligands for adaptive transition metal complexes," *Organometallics,* vol. 30, no. 3, pp. 499-510, 2011.

[33] D. C. Babbini and V. M. J. O. Iluc, "Iridium PCsp3P-type Complexes with a Hemilabile Anisole Tether," *Organometallics,* vol. 34, no. 13, pp. 3141-3151, 2015.

[34] V. V. J. C. r. Grushin, "Mixed phosphine− phosphine oxide ligands," *Chemical reviews,* vol. 104, no. 3, pp. 1629-1662, 2004.

[35] F. Mohr, S. H. Privér, S. K. Bhargava, and M. A. J. C. c. r. Bennett, "Ortho-metallated transition metal complexes derived from tertiary phosphine and arsine ligands," *Coordination chemistry reviews.*, vol. 250, no. 15-16, pp. 1851-1888, 2006.

[36] a. A. Miyashita, A. Yasuda, H. Takaya, K. Toriumi, T. Ito, T. Souchi, and R. J. J. o. t. A. C. S. Noyori, "Synthesis of 2, 2'-bis (diphenylphosphino)-1, 1'-binaphthyl (BINAP), an atropisomeric chiral bis (triaryl) phosphine, and its use in the rhodium (I)-catalyzed asymmetric hydrogenation of. alpha-.(acylamino) acrylic acids," *the American Chemical Society,* vol. 102, no. 27, pp. 7932-7934, 1980.

[37] R. Noyori, *Asymmetric catalysis in organic synthesis*. Wiley, 1993.

[38] T. Hayashi and K. J. C. R. Yamasaki, "Rhodium-catalyzed asymmetric 1, 4-addition and its related asymmetric reactions," *Chemical reviews,* vol. 103, no. 8, pp. 2829-2844, 2003.

[39] J. M. Hopkins, "The synthesis, resolution, and applications of 3, 3'-substituted binap ligands in asymmetric catalysis," *collectionscanada.gc.ca*, 2007.

[40] E. Framery, B. Andrioletti, and M. J. T. A. Lemaire, "Recent progress in homogeneous supported asymmetric catalysis: example of the BINAP and the BOX ligands," *Tetrahedron: Asymmetry*, vol. 21, no. 9-10, pp. 1110-1124, 2010.

[41] T. Sawano, N. C. Thacker, Z. Lin, A. R. McIsaac, and W. J. J. o. t. A. C. S. Lin, "Robust, chiral, and porous BINAP-based metal–organic frameworks for highly enantioselective cyclization reactions," *American Chemical Society*, vol. 137, no. 38, pp. 12241-12248, 2015.

[42] C. Cruché, S. Gupta, J. Kodanko, and S. K. J. M. Collins, "Heteroleptic Copper (I)-Based Complexes Incorporating BINAP and π-Extended Diimines: Synthesis, Catalysis and Biological Applications," *Molecules*, vol. 27, no. 12, p. 3745, 2022.

[43] Z. Xu, X. Yu, X. Sang, and D. J. G. C. Wang, "BINAP-copper supported by hydrotalcite as an efficient catalyst for the borrowing hydrogen reaction and dehydrogenation cyclization under water or solvent-free conditions," *Green Chemistry*, vol. 20, no. 11, pp. 2571-2577, 2018.

[44] M. Tamura and H. J. J. o. t. A. C. S. Fujihara, "Chiral bisphosphine BINAP-stabilized gold and palladium nanoparticles with small size and their palladium nanoparticle-catalyzed asymmetric reaction," *American Chemical Society*, vol. 125, no. 51, pp. 15742-15743, 2003.

[45] J. Li, M. Tian, Z. Tian, S. Zhang, C. Yan, C. Shao, and Z. J. I. C. Liu, "Half-sandwich iridium (III) and ruthenium (II) complexes containing P^ P-chelating ligands: A new class of potent anticancer agents with unusual redox features," *Inorganic Chemistry*, vol. 57, no. 4, pp. 1705-1716, 2018.

[46] H. Kunkely, V. Pawlowski, and A. J. I. C. C. Vogler, "Copper (I) binap complexes (binap=(2, 2′-bis (diphenylphosphino)-1, 1′-

binaphthyl). Luminescence from IL and LLCT states," *Inorganic Chemistry Communications*, vol. 11, no. 9, pp. 1003-1005, 2008.

[47] H. H. Mihsen and N. K. Shareef, "Synthesis, characterization of mixed-ligand complexes containing 2, 2-Bipyridine and 3-aminopropyltriethoxysilane," in *Journal of Physics: Conference Series*, 2018, vol. 1032, no. 1, p. 012066: IOP Publishing.

[48] P. J. J. C. C. R. Steel, "Aromatic nitrogen heterocycles as bridging ligands; a survey," *Coordination Chemistry Reviews*, vol. 106, pp. 227-265, 1990.

[49] M. Selvaganapathy, N. J. J. o. C. B. Raman, and Therapeutics, "Pharmacological activity of a few transition metal complexes: A short review," *A short review," J. Chemical Biology & Therapeutics*, vol. 1, no. 02, p. 1000108, 2016.

[50] R. Maurya, P. a. Patel, S. J. S. Rajput, r. i. inorganic, and m.-o. chemistry, "Synthesis and characterization of Mixed-Ligand Complexes of Cu (II), Ni (II), Co (II), Zn (II), Sm (III), and U (VI) O2, with a Schiff Base Derived from the Sulfa Drug Sulfamerazine and 2, 2′-Bipyridine," *Synthesis and reactivity in inorganic and metal-organic chemistry*, vol. 33, no. 5, pp. 801-816, 2003.

[51] S. Chandraleka, K. Ramya, G. Chandramohan, D. Dhanasekaran, A. Priyadharshini, and A. J. J. o. S. C. S. Panneerselvam, "Antimicrobial mechanism of copper (II) 1, 10-phenanthroline and 2, 2′-bipyridyl complex on bacterial and fungal pathogens," *Saudi Chemical Society.*, vol. 18, no. 6, pp. 953-962, 2014.

[52] A. Abebe, M. Kendie, and G. T. J. B. R. A. C. Tigineh, "Mono-and binuclear cobalt (II) mixed ligand complexes of 2, 2′-bipyridine and ethylenediamine: synthesis, characterization and biological application," *Biointerface Res Appl Chem*, vol. 12, p. 1962, 2021.

[53] S. Schöne, T. Radoske, J. März, T. Stumpf, and A. J. I. C. Ikeda-Ohno, "Synthesis and characterization of heterometallic iron–uranium complexes with a bidentate N-donor ligand (2, 2′-

bipyridine or 1, 10-phenanthroline)," *Inorganic Chemistry Communications*, vol. 57, no. 21, pp. 13318-13329, 2018.

[54] D. Avcı, S. Altürk, F. Sönmez, Ö. Tamer, A. Başoğlu, Y. Atalay, B .Zengin Kurt, and N. J. J. J. o. B. I. C. Dege, "A novel series of mixed-ligand M (II) complexes containing 2, 2′-bipyridyl as potent α-glucosidase inhibitor: synthesis, crystal structure, DFT calculations, and molecular docking," *JBIC Journal of Biological Inorganic Chemistry.*, vol. 24, pp. 747-764, 2019.

[55] P. Gurumoorthy, J. Ravichandran, and A. K. J. J. o. C. S. Rahiman, "Mixed-ligand binuclear copper (II) complex of 5-methylsalicylaldehyde and 2, 2′-bipyridyl: Synthesis, crystal structure, DNA binding and nuclease activity," *Chemical Sciences*, vol. 126, pp. 783-792, 2014.

[56] R.-Y. Li, H.-T. Liu, C.-C. Zhou, Z.-T. Chu, J. Lu, S.-N. Wang, J. Jin, and W.-F. J. I. C. F. Yan, "Ligand substitution induced single-crystal-to-single-crystal transformations in two Ni (II) coordination compounds displaying consequential changes in proton conductivity," *Inorganic Chemistry*, vol. 7, no. 9, pp. 1880-1891, 2020.

[57] R. Egbele, A. Ohwofosirai, U. Ugbune, B. Kpomah, and I. J. E. R. Yerima, "Synthesis and characterization of Mixed 2, 2-Bipyridine and penicillin G metal (II) complexes," *IJMCER*, vol. 3, no. 2, pp. 23-30, 2021.

[58] Y. Yamaguchi, H. Ichioka, A. Klein, W. W. Brennessel, and D. A. Vicic, "Linear Bis(perfluoroalkyl) Complexes of Nickel Bipyridine," *Organometallics*, vol. 31, no. 4, pp. 1477-1483, 2012.

[59] A. M.O, P. Ndifon, B. Ndosiri, P. A.G, D. Yufanyi, and A. Mohamadou, "Synthesis, characterisation and antimicrobial activities of cobalt(II), copper(II) and zinc(II) mixed-ligand complexes containing 1,10-phenanthroline and 2,2'-bipyridine," *Bulletin of the Chemical Society of Ethiopia*, vol. 24, 2010.

[60] N. A. Carmo dos Santos, M. Natali, E. Badetti, K. Wurst, G. Licini, and C. Zonta, "Cobalt, nickel, and iron complexes of 8-hydroxyquinoline-di(2-picolyl)amine for light-driven hydrogen evolution," *Dalton Transactions*, 10.1039/C7DT02666H vol. 46, no. 47, pp. 16455-16464, 2017.

[61] C. Deraeve, C. Boldron, A. Maraval, H. Mazarguil, H. Gornitzka, L. Vendier, M. Pitié, and B. Meunier, "Preparation and study of new poly-8-hydroxyquinoline chelators for an anti-Alzheimer strategy," (in eng), *Chemistry*, vol. 14, no. 2, pp. 682-96, 2008.

[62] H. A. Saadeh, K. A. Sweidan, and M. S. Mubarak, "Recent Advances in the Synthesis and Biological Activity of 8-Hydroxyquinolines," (in eng), *Molecules*, vol. 25, no. 18, 2020.

[63] T. M. Smit, A. K. Tomov, G. J. P. Britovsek, V. C. Gibson, A. J. P. White, and D. J. Williams, "The effect of imine-carbon substituents in bis(imino)pyridine-based ethylene polymerisation catalysts across the transition series," *Catalysis Science & Technology*, 10.1039/C2CY00448H vol. 2, no. 3, pp. 643-655, 2012.

[64] S. A. Ali, A. A. Soliman, A. H. Marei, and D. H. Nassar, "Synthesis and characterization of new chromium, molybdenum and tungsten complexes of 2-[2-(methylaminoethyl)] pyridine," (in eng), *Spectrochim Acta A Mol Biomol Spectrosc*, vol. 94, pp. 164-8, 2012.

[65] A. C. B. Yuoh, M. O. Agwara, D. M. Yufanyi, M. A. Conde, R. Jagan, and K. Oben Eyong, "Synthesis, Crystal Structure, and Antimicrobial Properties of a Novel 1-D Cobalt Coordination Polymer with Dicyanamide and 2-Aminopyridine," *International Journal of Inorganic Chemistry*, vol. 2015, p. 106838, 2015.

[66] C. Zhu, Y. Wang, Q. Mao, F. Li, Y. Li, and C. Chen, "Two 8-Hydroxyquinolinate Based Supramolecular Coordination Compounds: Synthesis, Structures and Spectral Properties," *Materials (Basel)*, vol. 10, no. 3, 2017.

[67] S. VanAtta, B. Duclos, and D. Green, "Microwave-Assisted Synthesis of Group 6 (Cr, Mo, W) Zerovalent Organometallic Carbonyl Compounds," *Organometallics*, vol. 19, 2000.

[68] M. Ardon, G. Hogarth, and D. Oscroft, "Organometallic chemistry in a conventional microwave oven: The facile synthesis of group 6 carbonyl complexes," *Journal of Organometallic Chemistry* ,vol. 689, pp. 2429-2435, 2004.

[69] R. M. Okasha, N. E. AL-Shaikh, F. S. Aljohani, A. Naqvi, and E. H. Ismail, "Design of Novel Oligomeric Mixed Ligand Complexes: Preparation, Biological Applications and the First Example of Their Nanosized Scale," *International journal of molecular sciences*, vol. 20, no. 3, p. 743, 2019.

[70] W. Morris, B. Volosskiy, S. Demir, F. Gándara, P. L. McGrier, H. Furukawa, D. Cascio, J. F. Stoddart, and O. M. Yaghi, "Synthesis, structure, and metalation of two new highly porous zirconium metal-organic frameworks," (in eng), *Inorg Chem*, vol. 51, no. 12, pp. 6443-5, 2012.

[71] R. K. Sodhi, S. J. C. T. Paul, and O. I. Journal, "Metal complexes in medicine an overview and update from drug design perspective," *Cancer Therapy & Oncology International Journal*, vol. 14, no. 1, pp. 25-32, 2019.

[72] K. Strohfeldt-Venables, *Essentials of inorganic chemistry : for students of pharmacy, pharmaceutical sciences and medicinal chemistry*. Chichester, West Sussex: Wiley, 2015.

[73] H. Pfeiffer, "Synthesis and biological activity of molybdenum carbonyl complexes and their peptide conjugates," Universität Würzburg Fakultät für Chemie und Pharmazie. Institut für Anorganische Chemie, 2012.

[74] A. T. Odularu, P. A. Ajibade, and J. Z. Mbese, "Impact of Molybdenum Compounds as Anticancer Agents," (in eng), *Bioinorg Chem Appl*, vol. 2019, p. 6416198, 2019.

[75] A. A. Soliman, S. A. Ali, A. H. Marei, and D. H. Nassar, "Synthesis, characterization and biological activities of some new chromium molybdenum and tungsten complexes with 2,6-diaminopyridine," (in eng), *Spectrochim Acta A Mol Biomol Spectrosc*, vol. 89, pp. 329-32, 2012.

[76] G. D. Frey, K. Öfele, H. G. Krist, E. Herdtweck, and W. A. J. I. c. a. Herrmann, "Tetrazole and triazole carbene complexes of group 6 metal carbonyls," *Inorganica Chimica Acta*, vol. 359, no. 9, pp. 2622-2634, 2006.

[77] M. Henary, C. Kananda, L. Rotolo, B. Savino, E. A. Owens, and G. J. R. a. Cravotto, "Benefits and applications of microwave-assisted synthesis of nitrogen containing heterocycles in medicinal chemistry," *RSC advances*, vol. 10, no. 24, pp. 14170-14197, 2020.

[78] Y.-J. Zhu and F. J. C. r. Chen, "Microwave-assisted preparation of inorganic nanostructures in liquid phase," *Chemical reviews*, vol. 114, no. 12 ,pp. 6462-6555, 2014.

[79] B. L. Hayes, *Microwave synthesis : chemistry at the speed of light*. Matthews, N.C: CEM Publishing, 2002.

[80] D. Dallinger and C. O. J. C. r. Kappe, "Microwave-assisted synthesis in water as solvent," *Chemical reviews*, vol. 107 ,no. 6, pp. 2563-2591, 2007.

[81] B. M. Zeglis, V. C. Pierre, and J. K. J. C. C. Barton, "Metallo-intercalators and metallo-insertors," *Chemical Communications*, no. 44, pp. 4565-4579, 2007.

[82] J. Carlos Lima and L. J. A.-C. A. i. M. C. Rodriguez, "Phosphine-gold (I) compounds as anticancer agents: general description and mechanisms of action," *Anti-Cancer Agents in Medicinal Chemistry (Formerly Current Medicinal Chemistry-Anti-Cancer Agents)*, vol. 11, no. 10, pp. 921-928, 2011.

[83] D. W. Bennett, T. A .Siddiquee, D. T. Haworth, S. E. Kabir, and F. K. Camellia, "The crystal and molecular structure of trans-tetracarbonylbis(triphenyl-phosphine)chromium(0) in a new unit cell: Is the trans conformer more stable than the cis?," *Chemical Crystallography*, vol ,34 .no. 6, pp. 353-359, 2004.

[84] G. Jaouen, W. Beck, and M. J. J. B. B. McGlinchey, Labeling, Medicine, "A novel field of research: bioorganometallic chemistry, origins, and founding principles," *Bioorganometallics: Biomolecules, Labeling, Medicine,* 2006.

[85] C. G. Hartinger and P. J. J. C. S. R. Dyson, "Bioorganometallic chemistry—from teaching paradigms to medicinal applications," *Chemical Society Reviews*, vol. 38, no. 2, pp. 391-401, 2009.

[86] M. A. Jakupec, M. S. Galanski, V. B. Arion, C. G. Hartinger, and B. K. J. D. t. Keppler, "Antitumour metal compounds: more than theme and variations," *Dalton Transactions*, no. 2, pp. 183-194, 2008.

[87] A. F. Peacock and P. J. J. C. A. A. J. Sadler, "Medicinal organometallic chemistry: designing metal arene complexes as anticancer agents," *Chemistry–An Asian Journal,* vol. 3, no. 11, pp. 1890-1899, 2008.

[88] K. Meister, J. Niesel, U. Schatzschneider, N. Metzler-Nolte, D. A. Schmidt, and M. J. A. C. I. E. Havenith, "Label-Free Imaging of Metal–Carbonyl Complexes in Live Cells by Raman Microspectroscopy," *Angewandte Chemie International Edition*, vol. 49, no. 19, pp. 3310-3312, 2010.

[89] I. Ott, B. Kircher, C. P. Bagowski, D. H. Vlecken, E. B. Ott, J. Will, K. Bensdorf, W. S. Sheldrick, and R. J. A. C. Gust , "Modulierung der biologischen Eigenschaften von Aspirin durch Bildung eines Bioorganometallderivats," *Angewandte Chemie*, vol. 121, no. 6, pp. 1180-1184, 2009.

[90] D. Schlawe, A. Majdalani, J. Velcicky, E. Heßler, T. Wieder, A. Prokop, and H. G. J. A. C. Schmalz, "Eisenhaltige Nucleosidanaloga mit apoptoseinduzierender Wirksamkeit," *Angewandte Chemie,*, vol. 116, no. 13, pp. 1763-1766, 2004.

[91] S. X. Lee, C. H. Tan, W. L. Mah, R. C. S. Wong, Y. L. Cheow, K. S. Sim, and K. W. Tan, "Synthesis of group 6 (chromium, molybdenum, and tungsten) photoCORMs as potential antimicrobial and anticancer agents," *Inorganica Chimica Acta*, vol. 525, p. 120491, 2021.

[92] L. H. Abdel-Rahman, A. A. Abdelghani, A. A. AlObaid, D. A. El-ezz, I. Warad, M. R. Shehata, and E. M .J. S. r. Abdalla, "Novel Bromo and methoxy substituted Schiff base complexes of Mn (II), Fe (III), and Cr (III) for anticancer, antimicrobial, docking, and ADMET studies," *Scientific Reports*, vol. 13, no. 1, p. 3199, 2023.

[93] S. Hosny, M. S. Ragab, and R. F. Abd El-Baki, "Synthesis of a new sulfadimidine Schiff base and their nano complexes as potential anti-COVID-19 and anti-cancer activity," *Scientific Reports*, vol. 13, no. 1, p. 1502, 2023.

[94] A. T. Odularu, P. A. Ajibade, J. Z. J. B. c. Mbese, and applications, "Impact of molybdenum compounds as anticancer agents," *Bioinorg Chem Appl*, vol. 2019, 2019.

[95] M. Freyss, "Density functional theory," Nuclear Energy Agency of the OECD (NEA)2015.

[96] F. Giustino, *Materials modelling using density functional theory: properties and predictions*. Oxford University Press, 2014.

[97] J. A. Steckel and D. Sholl, *Density Functional Theory*. John Wiley & Sons, Ltd, Hoboken, 2009.

[98] N. Harrison, "An introduction to density functional theory," *Nato Science Series Sub Series III Computer and Systems Sciences*, vol. 187, pp. 45-70, 2003.

[99] P. Skehan, R. Storeng, D. Scudiero, A. Monks, J. McMahon, D. Vistica, J. T. Warren, H. Bokesch, S. Kenney, and M. R. Boyd, "New colorimetric cytotoxicity assay for anticancer-drug screening," (in eng), *J Natl Cancer Inst,* vol. 82, no. 13, pp. 1107-12, 1990.

[100] B. M. Trost, M. Vaultier, and M. L. J. J. A. C. S. Santiago, "Synthesis of 2, 2'-Bis (dipheny1phosphino)-1, l'-binaphthyl," *Am. Chem. Soc,* vol. 102, no. 27, pp. 7932-7934. 1980.

[101] J. E. House, *Inorganic Chemistry* (Academic press). 2008.

[102] E. R. Davidson, K. L. Kunze, F. B. Machado, and S. J. J. A. o. c. r. Chakravorty, "The transition metal-carbonyl bond," *Acc. Chem. Res,* vol. 26, no. 12, pp. 628-635, 1993.

[103] A. L. Bogado, R. M. Carlos, C. Daólio, A. G. Ferreira, M. G. Neumann, F. Rominger, S. P. Machado, J. P. da Silva, M. P. de Araujo, and A. A. J. J. o. O. C. Batista, "Observation of vinylidene emission in mixed phosphine/diimine complexes of Ru (II) at room temperature in solution," *Organometallic Chemistry,* vol. 696, no. 26, pp. 4184-4190, 2012.

[104] Z. Abedin-Siddique, T. Ohno, K. Nozaki, and T. J. I. c. Tsubomura, "Intense Fluorescence of Metal-to-Ligand Charge Transfer in [Pt (0)(binap) 2][binap-' 2 ,2 =Bis (diphenylphosphino)-1, 1 '-binaphthyl]," *Inorg. Chem,* vol. 43, no. 2, pp. 663-673, 2004.

[105] M. Dalal, *A Textbook of Inorganic Chemistry–Volume 1*. Dalal Institute, 2017.

[106] B. Anupama, C. G. J. I. J. o. R. i. C. Kumari, and Environment , "Cobalt (II) complexes of ONO donor Schiff bases and N, N donor ligands: synthesis, characterization, antimicrobial and DNA binding study," *International Journal of Research in Chemistry and Environment,* vol. 3, no. 2, pp. 172-180, 2013.

[107] N. Sundaraganesan, C. Meganathan, and M. J. J. o. M. S. Kurt, "Molecular structure and vibrational spectra of 2-amino-5-methyl pyridine and 2-amino-6-methyl pyridine by density functional methods," *Journal of Molecular Structure,* vol. 891, no. 1-3, pp. 284-291, 2008.

[108] R. M. Silverstein, G. C. Bassler, and T. C. Morrill, *Spectrometric identification of organic compounds*, 4th edition ed. New York: Wiley, 1981.

[109] V. Krishnakumar, V. Balachandran, and T. Chithambarathanu, "Density functional theory study of the FT-IR spectra of phthalimide and N-bromophthalimide," *Spectrochimica Acta Part A: Molecular and Biomolecular Spectroscopy,* vol. 62, no. 4, pp. 918-925, 2005.

[110] Acol, W. O. George, P. S. McIntyre, and D. J. Mowthorpe, *Infrared spectroscopy* (Analytical chemistry by open learning). J. Wiley for ACOL, 1987.

[111] J. Coates, "Interpretation of infrared spectra, a practical approach," ed, 2000.

[112] S. Ramalingam, S. Periandy, S. J. S. A. P. A. M. Mohan, and B. Spectroscopy, "Vibrational spectroscopy (FTIR and FTRaman) investigation using ab initio (HF) and DFT (B3LYP and B3PW91) analysis on the structure of 2-amino pyridine," *Spectrochim. Acta Part A Mol. Biomol. Spectrosc.*, vol. 77, no. 1, pp. 73-81, 2010.

[113] B. S. Al-Farhan, M. T. Basha, L. H. Abdel Rahman, A. M. M. El-Saghier, D. Abou El-Ezz, A. A. Marzouk, M. R. Shehata, and E. M. Abdalla, "Synthesis, DFT Calculations, Antiproliferative, Bactericidal Activity and Molecular Docking of Novel Mixed-Ligand Salen/8-Hydroxyquinoline Metal Complexes," *Molecules*, vol. 26, no. 16, 2021.

[114] S. M. El-Megharbel and M. S. Refat, "Ligational behavior of clioquinol antifungal drug towards Ag(I), Hg(II), Cr(III) and

Fe(III) metal ions: Synthesis, spectroscopic, thermal, morphological and antimicrobial studies ",*Journal of Molecular Structure*, vol. 1085, pp. 222-234, 2015.

[115] S. Hosny, G. A. Gouda, and S. M. J. A. O. C. Abu-El-Wafa, "Novel nano copper complexes of a new Schiff base: green synthesis, a new series of solid Cr (II), Co (II), Cu (II), Pd (II) and Cd (II) chelates, characterization, DFT, DNA, antitumor and molecular docking studies," *Applied Organometallic Chemistry*, vol. 36, no. 5, p. e6627, 2022.

[116] D. Nama, D. Schott, P. S. Pregosin, L. Veiros, and M. J. J. O. Calhorda, "Diffusion and overhauser NMR studies on dicationic palladium complexes of BINAP," *Organometallics*, vol. 25, no. 19, pp. 4596-4604, 2006.

[117] P. Dotta, P. A. Kumar, P. S. Pregosin, A. Albinati, and S. J. O. Rizzato, "3, 5-Dialkyl effect on enantioselectivity in Pd chemistry : Applications involving both bidentate and monodentate auxiliaries," *Organometallics*, vol. 23, no. 10, pp. 2295-2304, 2004.

[118] G. Trabesinger, A. Albinati, N. Feiken, R. W. Kunz, P. S. Pregosin, and M. J. J. o. t. A. C. S. Tschoerner, "Enantioselective Homogeneous Catalysis and the “3, 5-Dialkyl Meta-Effect”. MeO− BIPHEP Complexes Related to Heck, Allylic Alkylation, and Hydrogenation Chemistry," *J. Am. Chem. Soc*, vol. 119, no. 27, pp. 6315-6323, 1997.

[119] B. C. Baker and D. T. J. A. C. Sawyer, "Proton nuclear magnetic resonance studies of 8-quinolinol and several of its metal complexes," *Analytical Chemistry*, vol. 40, no. 13, pp. 1945-1951, 1968.

[120] J. Kidrič, D. Hadži, D. Kocjan, and V. J. O. M. R. Rutar, "1H and 13C NMR study of 8-hydroxyquinoline and some of its 5-substituted analogues," *Organic Magnetic Resonance*, vol. 15, no. 3, pp. 280-284, 1981.

[121] D. J. Spielvogel, W. M. Davis, and S. L. Buchwald, "Preparation, Crystal Structure Analysis, and Catalytic Application of [(S)-BINAP]Ni(COD (and [(S)-BINAP]NiBr2," *Organometallics*, vol. 21, no. 18, pp. 3833-3836, 2002.

[122] I. Müller, C. Schneider, C. Pietzonka, F. Kraus, and C. G. J. I. Werncke, "Reduction of 2, 2′-Bipyridine by Quasi-Linear 3d-Metal (I) Silylamides—A Structural and Spectroscopic Study," *Inorganics*, vol. 7, no. 10, p. 117, 2019.

[123] F. M. Mück, D. Kloß, J. A. Baus, C. Burschka, and R. J. C. A. E. J. Tacke, "Novel Transition-Metal (M= Cr, Mo, W, Fe) Carbonyl Complexes with Bis (guanidinato) silicon (ii) Ligands," *Chemistry–A European Journal*, vol. 20, no. 31, pp. 9620-9626, 2014.

[124] W. Beck, "K. Nakamoto: Infrared and Raman Spectra of Inorganic and Coordination Compounds, 4. Auflage, John Wiley & Sons, New York, Chichester, Brisbane, Toronto, Singapore 1986. 484 Seiten ", .ed: Wiley Online Library, 1988.

[125] K. A. Leonova, O. V. Klimov, D. I. Kochubey, Y. A. Chesalov, I. P. Prosvirin, T. V. Larina, and A. S. J. P. Noskov, "Synthesis and characterisation of Co–Mo complexes containing the [Co (C2H8N2) 3] 2+ cation and [Mo2O7L] 4− anion, where L is an oxalic, tartaric, citric or nitrilotriacetic acid residue," *Polyhedron*, vol. 47, no. 1, pp. 65-72, 2012.

[126] S. A. Ali, T. A. Youssef, and L. H. J. J. o. C. C. Abdel-Rahman, "Structural studies of new group 6 complexes of salicylidene-2-aminopyridine," *Coordination Chemistry*, vol. 62, no. 4, pp. 577-582, 2009.

[127] M. y. Li, P. z. Hu, K. x. Xu, L. h. J. S. Cai, M.-O. Reactivity in Inorganic, and N.-M. Chemistry, "Synthesis and characterization of transition metal complexes of multidentate ligands containing a pyridine ring," *synthesis and Reactivity in Inorganic, Metal-*

Organic, and Nano-Metal Chemistry, vol. 35, no. 4, pp. 333-338, 2005.

[128] L. Mei, T. H. Ming, L. Q. Rong, S. Jie, Y. S. Zhong, and L. X. J. J. o. c. s .Liang, "The synthesis of N-Zn, N-Cu complexes involving 2-amino pyridine and ethylenediamine ligands and application to the Henry reaction," *chemical sciences,* vol. 121, pp. 435-440, 2009.

Appendix.

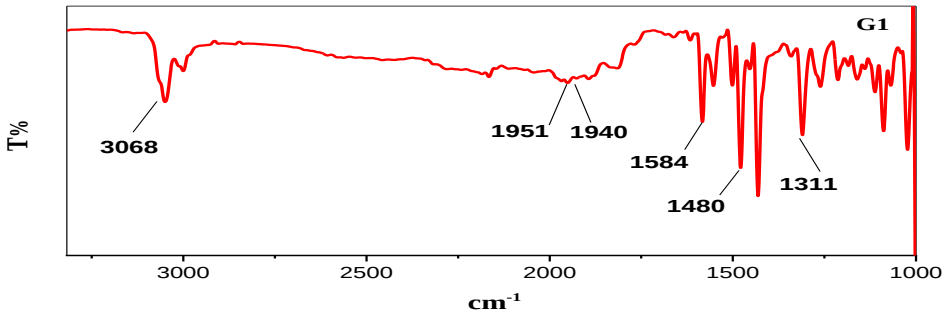

Figure 1. FTIR spectrum of $[Cr(CO)_2(BINAP)(bipy)]$.

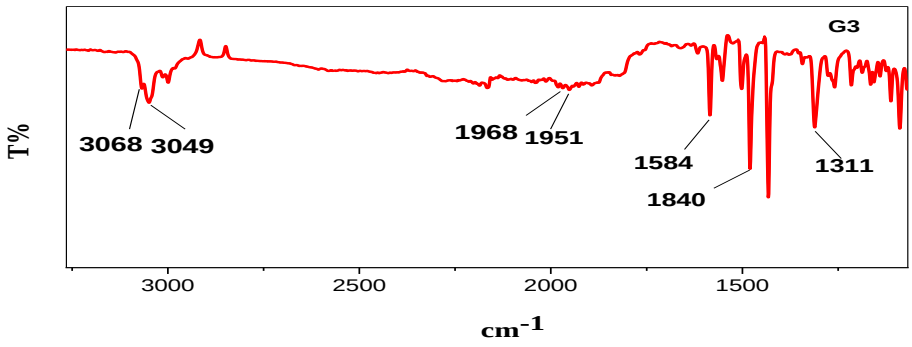

Figure 2. FTIR spectrum of $[Cr(CO)_2(BINAP)(2\text{-}AP)]$.

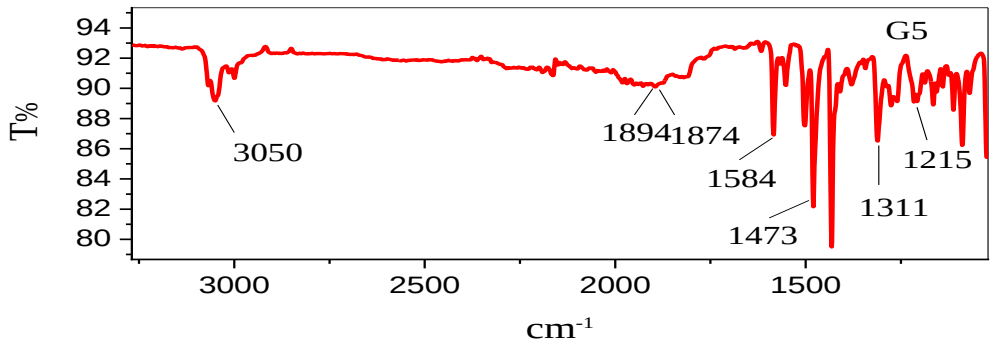

Figure 3. FTIR spectrum of [Cr(CO)$_2$(BINAP)(8-HQ)].

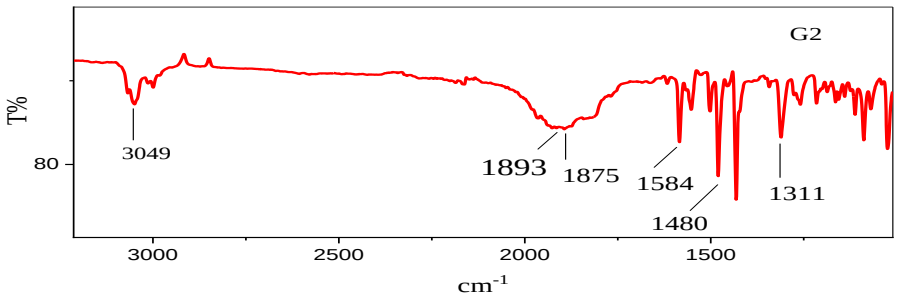

Figure 4. FTIR spectrum of [Mo(CO)$_2$(BINAP)(bipy)].

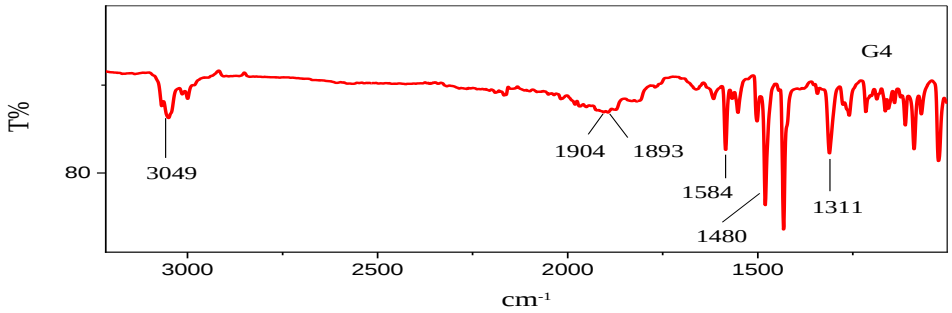

Figure 5. FTIR spectrum of [Mo(CO)$_2$(BINAP)(2-AP)].

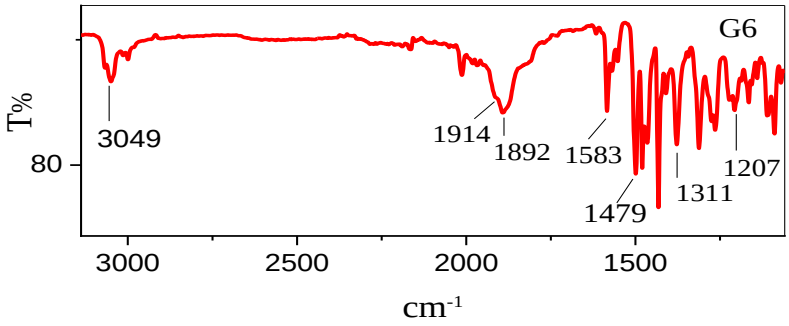

Figure 6. FTIR spectrum of [Mo(CO)$_2$(BINAP)(8-HQ)].